# MULTI-USER RELAYING SYSTEMS FOR ENHANCED PERFORMANCE AND SECRECY

BY YUPENG LIU

**A dissertation submitted to the**

**Graduate School—New Brunswick**

**Rutgers, The State University of New Jersey**

**in partial fulfillment of the requirements**

**for the degree of**

**Doctor of Philosophy**

**Graduate Program in Electrical and Computer Engineering**

**Written under the direction of**

**Athina P. Petropulu**

**and approved by**

_____

_____

_____

_____

_____

**New Brunswick, New Jersey**

**October, 2012**

## ABSTRACT OF THE DISSERTATION

# Multi-user relaying systems for Enhanced Performance and Secrecy

**by Yupeng Liu**

**Dissertation Director: Athina P. Petropulu**

High data rate, reliability and secrecy are fundamental pursuits in wireless communications systems. A multi-user wireless environment is particularly challenging because of interference and potential information wiretap. This dissertation proposes to utilize relay techniques to achieve high data rate, high reliability and absolute secrecy in multi-user wireless communications systems.

First, a communication system with multiple source-destination pairs needing to communicate simultaneously is investigated. A relay beamforming scheme is proposed, in which a multi-antenna relay assists the communication. The proposed scheme enjoys spatial multiplexing gain and has a significant data rate advantage over widely studied orthogonal transmission schemes, e.g., Time Division Multiple Access (TDMA) and Code Division Multiple Access (CDMA). The relay beamforming scheme also overcomes the difficulties of recently introduced interference alignment approaches by not requiring full cross-node Channel State Information (CSI). Beamforming schemes that maximize the system throughput and meet user Quality of Service (QoS) requirements are investigated, and both

optimal and low-complexity suboptimal schemes are proposed. The system performance in terms of sumrate is analyzed and the rate limit is derived. The impact of imperfect CSI is analyzed and various approaches are proposed for mitigating the imperfect CSI effects in a practical system. Relay antenna selection is proposed to use in conjunction with the relay beamforming for more reliable communications.

Second, physical layer secrecy in a two-slot communications system with one source, one destination, one eavesdropper and multiple relays is investigated. The goal is to achieve high secrecy rate without leaking any information to the eavesdropper. Different from the widely studied approaches in which the destination combines the listened signals in the first and second slots, we propose that the destination acts as a jammer in the first slot. This novel design effectively reduces the signal quality at the eavesdropper, and allows the secrecy rate to improve with higher power budget. Under this framework, a cooperative relaying scheme is proposed that targets at maximizing the secrecy rate. A set of novel approaches are proposed to realize this goal, namely, relay selection and optimal power allocation among the first/second slot data and jamming signals. Analysis of the scaling law of secrecy rate is conducted showing the secrecy rate trend at large transmit power and number of relays.

# Acknowledgements

First of all, I would like to express my sincere gratitude to my advisor, Dr. Athina P. Petropulu, for her tremendous time and effort spent in leading, supporting and encouraging me during the last four years. It would be impossible for me to finish this work without her constant help and invaluable guidance throughout my Ph.D. study. I will always look up to her as an inspiration to my professional career.

I would express my gratitude to the members of my Ph.D. thesis committee, Professors Waheed U. Bajwa, Hongbin Li, Predrag Spasojevic and Wade Trappe for their precious time and their valuable suggestions.

I am also deeply indebted to Professor H. Vincent Poor at Princeton University his valuable guidance, suggestions and comments during our collaborative research. My thanks also goes Professor John M. Walsh for his help in my graduate study.

Many thanks to my colleagues in the Communications and Signal Processing Laboratory (CSPL): Lun Dong, Jiangyuan Li, Xin Liu, Shuangyu Luo, Sagar Shah, Shunqiao Sun and Yao Yu for their many forms of help and their friendship during the time we spent together.

Finally but most importantly, I would like to express my special thanks to my parents and beloved wife, Tingyu He, for their continuous understanding, supporting, encouraging and inspiring in my research and life.

# Table of Contents

# List of Tables

# List of Figures

# Chapter 1
# Introduction

Wireless communications, especially cellular technologies, have received explosive growth over the recent few of decades. The steady evolution of wireless communications is attributed to the technological advances such as wideband signal processing, novel and complicated transreceiver designs, low-power and high-speed silicon processors with small footprint. On the other hand, the development of wireless communications is driven by ever growing users' demands on wireless services. The wireless services have shifted from the dominant voice calls to high speed data connections with various Quality of Service (QoS) requirements, e.g., web-browsing, realtime multi-media, cloudy storage and social networking. Future wireless systems should provide the same fast and reliable user experiences as in wireline systems.

One fundamental characteristic differentiating wireless systems from wireline systems is the broadcast nature of the wireless channels, which results in interference when multiple signal streams are transmitted over the same channel. To avoid interference, traditional systems separate different data streams or communications pairs into orthogonal channels. The orthogonality can be achieved by time division, frequency division, code division, etc. Naturally, the scarcity of wireless resources such as spectrum and power make it hard to provide a high data rate to a large number of users. The recently introduced multiple-input multiple-output (MIMO) technology creates one more dimension, i.e., the space dimension. Using multiple antennas at the transmitter and receiver, MIMO technology [1, 2] can improve the capacity of wireless systems significantly without

consuming additional time, frequency or code dimensions.

However, size limitations of transmitters and receivers, and also the cost of radio front ends, may limit the number of antennas a node can employ. This prevents the implementation of MIMO technology in systems with multiple sources and destinations equipped with only single antenna at each node. Also, allowing multiple sources to transmit over the same channel in a non-orthogonal fashion can result in higher data rates, as long as there is a way to control the inter-user interference introduced by the coexistence of the multiple signal streams. The background overview on on multi-user communications is provided in Section 1.1.

Ensuring secrecy is the other critical issue that a wireless system is facing. An untrusted, or unfriendly node can wiretap the transmitted signals, thus compromising the secrecy of the communications links. Considering the information secrecy, the design goal is to deliver information to the legitimate destination with a data rate as high as possible while preventing untrusted nodes from hearing the useful information. The secrecy requirement has been primarily handled with cryptographic approaches that involve public and private keys [3, 4, 5]. Key-based cryptographic approaches have been widely implemented in commercial communications systems on various layers, e.g., SSL and WEP [6, 7]. However, the key-based cryptographic methods are challenged by possible key leakage and/or surprise attacks [8, 4]. Recently, physical layer secrecy approach approaches have become popular because they provide a more fundamental way to achieve the secrecy goal regardless of the decoding ability and key availability at the untrusted node. Therefore, physical layer secrecy approaches can provide absolute secrecy. We introduce the background of the physical layer secrecy concept in Section 1.2.

Cooperative relaying technology has the potential to play a significant role in both the suppression of interference in multi-user systems and also in participating in the design of systems that can prevent untrusted users from accessing information.

## 1.1 Multiple user communications

For a point-to-point single antenna Gaussian channel, Shannon showed the channel capacity is $C = \log(1 + SNR)$ *bits per channel use* [9]. The degree of freedom (DoF) is defined as $DoF = \frac{C}{\log(SNR)}$ which measures the power efficiency of a communication system. The DoF is 1 in a point-to-point Gaussian channel. Multiple-input-multiple-output (MIMO) technology can significantly improve the DoF of wireless communications. In a system with $M$ and $N$ antennas at the receiver and receiver, respectively, the DoF is improved to $\min\{M, N\}$ which yields linearly increased capacity. The same slope of capacity increment can be achieved in multi-antenna broadcast (BC) and multiple access (MAC) channels, even when each receiver in BC or transmitter in MAC has one antenna only[10].

Another common communications environment is a multi-point to multi-point channel, in which each source node is distinctly paired with a destination node and transmits signal to the corresponding destination node simultaneously with all the other sources. This channel is commonly referred to as interference channel. For the $2 \times 2$ case, i.e., two sources and two destinations, the authors of [11] propose a scheme which can achieve the capacity within one bit. For generalized interference channels, the central task of transceiver design is interference control for achieving high throughput. One could classify the interference control approaches in the literature as follows.

- Treating the interference as noise. In this approach, each destination directly decodes the received signals as if the interference is not present in the system. Although this approach has been used in practical systems for years, e.g., cellular networks with intercell interference, it does not work well when the interference level is high.

- Strong interference cancelation (IC). When the interfering signal is strong, the destination may be able to decode the interference signal correctly and

subsequently subtract it from the received signal thus improve the receive quality of the desired but weak signal. However, the strong interference assumption in fact limits the desired signal's strength and results in throughput loss. In the 2x2 special case, [12, 13, 14] show that the IC scheme achieves capacity in the existence of very strong interference.

- Orthogonal multiple access. This is the most widely used scheme in practice. Each source-destination pair is allocated a part of the radio resource, which is not shared with other source-destination pairs. Examples include Time Division Multiple Access (TDMA), Code Division Multiple Access (CDMA) [15], and Orthogonal Frequency Division Multiplexing (OFDM). However, the degree of freedom of the schemes with orthogonal multiple access is one.

- Interference alignment. In [16], the upper bound of the degree of freedom of a generalized $K \times K$ interference channel is shown to be $\frac{K}{2}$. This $\frac{K}{2}$ freedom of degree is further shown to be achievable through the technique of interference alignment [17]. The interference alignment divides the received signal space into two identical parts. The beamforming vectors over symbols at each source are carefully selected based on the channel state information (CSI) of the other sources. This design guarantees that the interferences at one destination from all undesired sources fall in the same half vector space, which is orthogonal to the half vector space of the desired signals. By using interference alignment, each user can achieve degree of freedom of $\frac{1}{2}$. At any source, however, the interference alignment requires the exact CSI of other source and destinations, which is usually not easy to obtain in a practical system.

Another approach to manage the interferences at destinations is adding one or more relay nodes between the sources and destinations. Through properly designed beamforming matrices, the relays can deliver interference-free signals to

the destinations. The basics of relay techniques are covered in section 1.3.

## 1.2 Physical Layer Secrecy Communications

We are in a significant transition decade of wireless communication technologies and services. In the consumer market, people are increasingly spending a large amount of time on wireless devices for the commerce and social needs. A lot of actions performed on wireless networks have high secrecy requirements, e.g., sensitive emails, private user profile and wireless transactions. From the military point of view, sensitive data, e.g., battle field realtime video and control information of missiles, is now routinely transmitted over wireless networks.

The changes in the wireless network utility and the broadcast nature of wireless signals, raise crucial security concerns. The state-of-art technologies to deal with the secrecy issue typically involve the upper newtwork layers (above physical layer). Usually, these secrecy approaches are based on symmetric-key and asymmetric-key protocols. For the symmetric-key approach, the sender and the legitimate receiver must share the key securely before communications. For the asymmetric-key protocols, the public-key is widely distributed and the private-key is available only to the legitimate receiver. Both the symmetric and asymmetric key approaches are based on the assumptions that high complexity prevents decryption without knowledge of the shared key (symmetric) or private key (asymmetric). However, the secrecy is not always guaranteed in these two approaches due to two problems, 1) leakage of the shared or private key to the eavesdropper and 2) the unproven complexity assumption is always challenged by the fast increasing processing speed of super computers.

On the contrary, physical-layer secrecy approaches, whereby the legitimate destinations can reliably receive the communicated information, prevent untrusted nodes from being able to decode the electromagnetic signal even if they knew

the encoding/decoding schemes. This type of secrecy is immune to key leakages and strong capability of decoding at the eavesdropper. The absolute secrecy in noisy wireless channels is first investigated by Wyner [18]. It is shown that if the channel of the eavesdropper is a degraded version of the legitimate receiver, a non-zero secret rate is achievable without sharing a key, while the eavesdropper can decode almost no information. The physical layer secrecy results are extended to the general Gaussian channel in [19]. It is shown that a positive secrecy rate is possible provided that the legitimate destination link is stronger than the eavesdropper link. The secrecy rate over fading channels is investigated in [20]. The secrecy capacity of the broadcast channel [21] wireless channel has subsequently been characterized.

MIMO technologies can mitigate the dependence of the positive secrecy rate on the condition of better channel of the legitimate destination than the eavesdropper, due to the additional degree of freedom provided by MIMO. However, due to hardware cost and size limitations, nodes may not be equipped with multiple antennas (nodes may be too small to guarantee the required antenna separation). Node cooperation, however, can overcome this difficulty since multiple cooperative nodes can form a virtual multi-antenna transmitter. As a typical implementation of cooperation, relay techniques are proposed to use to improve the physical layer secrecy [22, 23, 24].

## 1.3 Relay Technology in Multiuser and physical layer secrecy communications

In order to guarantee the increasing QoS requirements in the high speed cellular networks, various types of diversity are utilized for improving the link reliability in wireless systems. These techniques include channel coding technologies, time or frequency diversity, spatial diversity and multiuser diversity. All types of diversity

may not be very effective if the destinations are far from the sources, or in case of deep fading due to shadowing.

In addition to the above mentioned methods on improving the link reliability and throughput, cooperation diversity which takes advantage of partners' antennas, can greatly help the sources reach the destinations even when the direct links between sources and destinations are very weak. Therefore, the link reliability in terms of outage probability and bit error rate (BER) can be reduced and the coverage of the cellular network can be improved. A pioneer work on cooperative networks [25] established that the capacity upper bound of a relay system with one source, one relay and one destination is characterized by max-flow min-cut theory. The advantage of relay systems for improving the capacity region and extending the wireless coverage is shown in [26, 27] by deploying two sources as the partners of each other to relay cross information. To realize the advantages of the relay concept, several relay protocols have been developed, such as AF, DF and CF. All these schemes have been shown to be able to provide diversity in AF, DF and CF schemes [28, 29, 30, 31, 32, 33].

Because of these advantages, relay technologies also find their place in multiple user communications. The MIMO relay broadcast channel and MIMO relay multiple access channel are shown to have a very elegant duality property. Capacity bounds and QoS guarantee problems in MIMO relay broadcast systems are investigated in [34, 35]. Employing relays in multi-point to multi-point systems is particularly of interest because it can enable simultaneous transmission rather than separating the signals from all sources in orthogonal channels. Two types of implementation of relays have been considered in literature. The first is that one or more relays with multiple antennas can be deployed between sources and destinations. These schemes enable independent processing of mixed signals from the sources at each relay [36]. The second is that multiple single antenna relays corporately help to forward the signals to the destinations [37, 38]. Both schemes

have shown to be able to deliver interference-free signal at each destination, with certain assumptions of channel state information availability at the relay.

Relay technologies also play an important role in physical layer secrecy communications. Consider an unfavorable channel condition in which the source-destination link is weaker than the source-eavesdropper link. Typically, in this scenario positive secrecy rate is not achievable. Adding one or more friendly relays can solve this problem by either cooperative beamforming or cooperative jamming. In cooperative beamforming, multiple relays cooperatively focus the forwarded signal to the destination while steering the signal away from the eavesdropper. In cooperative jamming, multiple friendly relays cooperatively transmit a jamming signal, e.g., white noise, along the null space of the channel from the relays to the legitimate destination. The jamming signal only causes interference to the eavesdropper and is harmless to the legitimate destination. Both cooperative beamforming and jamming schemes may achieve higher positive secrecy rate than that in a non-relay system.

## 1.4 Contributions of the Dissertation

This thesis investigates relay application in multi-user communications systems. Three important aspects in wireless communications are focused on, i.e., throughput maximization, Quality of Service (QoS) guarantee and communications with physical layer secrecy. The throughput maximization and QoS guarantee are investigated in a multiple source-destination system with one relay equipped with multiple antennas. The physical layer secrecy is investigated in a system with one source, one destination and one eavesdropper with single-antenna relays.

### 1.4.1 Sumrate in relay assisted multi-point to multi-point communications systems.

A wireless system with multiple source-destination pairs is considered. Each source is uniquely paired with one destination. All sources transmit independent signal streams to the destinations. Unlike dealing with this system with orthogonal transmission or interference alignment, one AF relay with multiple antennas is used to receive, process and forward signals to the destinations by using a ZeroForceing BeamForming (ZFBF) matrix. Under this system model, we focus on three important but open problems. The first one is to design the relay beamforming matrix to maximize the system sumrate. The second one is the analysis of the sumrate limit. The last one is analysis of system behavior under imperfect CSI. The contributions through addressing these problems are summarized as follows

- We propose a ZFBF matrix design in a way that the sumrate of all S-D pairs is maximized.

- We analytically show that with high source and/or relay power, ZFBF with sumrate maximization achieves an ergodic sumrate that maintains a constant gap from the maximum possible ergodic sumrate. This implies that the proposed approaches is optimal in terms of multiplexing gain.

- We investigate the impact of imperfect CSI on the sumrate of ZFBF relaying and derive an upper bound of the sumrate loss caused by CSI errors. The bound reveals that the ratio of the source and relay power plays an important role in the sumrate penalty. The bound also suggests that the system becomes interference limited in the high signal-to-noise ratio (SNR) regime unless the CSI accuracy improves at the relay with source/relay power increasing.

This part of work has been published in:

- Y. Liu and A.P. Petropulu, "On the sumrate of AF relaying Systems with multiple source-destination pairs," *IEEE Trans. on Wireless Comm.*, vol. 10, no. 11, pp. 37323742, Oct, 2011.
- Y. Liu and A.P. Petropulu, "On amplify-and-forward relay networks with multiple source-destination pairs," *IEEE Global Telecom. Conf. (Globecom)*, Dec. 2010, pp. 1-5.

### 1.4.2 QoS Guarantee in multiple-point to multi-point systems with relay assistance

In a system with multiple source destination pairs, each destination has its own QoS requirement. One important problem is how the system can meet the QoS requirements with minimal system resources. Again, one AF relay with multiple antennas is used to precode the signal before forwarding with the precoding enabling signal separation at the destinations. This part of the thesis targets at minimizing the relay transmit power while keeping the signal-to-noise-plus-interference (SINR) higher than the required thresholds. The novelty of our contribution as compared to the existing literature is optimal beamforming design in both cases of multiantenna relay and distributed relays, low complexity relay beamforming design, and implementation of relay antenna selection. The design of relay beamforming under imperfect CSI does not involve any numerical optimization thus has low complexity. Relay antenna selection is shown to be able to further improve the outage performance. The contributions of this part are as follows:

- We solve the power minimization problem with destination SINR constraints via Semi-definite Programming (SDP). A cooperative beamforming design

based on distributed relays is also proposed for supporting the simultaneous SINR destination requirements. Both designs require perfect CSI.

- An iterative relay weights design is proposed to meet the SINR requirements and control interference in a scenario of imperfect relay CSI. The design is based on meeting the worse case SINR requirements. The design does not involve any numerical optimization and has low complexity. The proof of convergence is provided.

- Antenna selection is shown to be a good tool for further decreasing the outage probability. Several antennas selection methods are proposed according to the criterion of minimizing the interference or the outage probability.

This part of work is included in:

- Y. Liu and A.P. Petropulu, "QoS Satisfaction in amplify-and-forward relay networks with multiple source-destination pairs," *submitted to IEEE Trans. on Wireless Comm.*, 2012.

- Y. Liu and A.P. Petropulu, "Cooperative beamforming in multi-source Multi-destination relay systems with SINR constraints," *in IEEE International Conference on Acoustics Speech and Signal Processing (ICASSP)*, March 2010, pp. 2870-2873.

- Y. Liu and A.P. Petropulu, "Robust AF relay transmission with multiple source-destination pairs under channel uncertainty," *in IEEE Asilomar Conf. on Signals, Systems and Computers*, Nov. 2010, pp. 126-130.

- Y. Liu and A.P. Petropulu, "QoS guarantees in relay networks with multiple source-destination pairs and imperfect CSI," *in IEEE 7th Sensor Array and Multichannel Signal Processing Workshop (SAM)*, June 2012, pp. 101-104.

- Y. Liu and A.P. Petropulu, "Antenna selection in relay networks with multiple source-destination pairs in the presence of imperfect CSI," *in the 46th Annual Conference on Information Sciences and Systems (CISS)*, Mar. 2012.

### 1.4.3 Destination assisted cooperative jamming in physical layer secrecy systems

In a physical layer secrecy system assisted by multiple DF relays, each relay participating in the signal forwarding in the second slot must decode the message correctly and securely. This requires adequate source transmission power in the first slot which may result in high signal quality at the eavesdropper. So the system secrecy rate is limited. With a large decoding set of the relay nodes, the first slot secrecy rate is limited by the relay with the lowest first-hop secrecy rate. This causes that the system does not benefit from a large number of relays.

To overcome the aforementioned two difficulties, a destination assisted jamming scheme is proposed. Note that destination assisted jamming is a natural choice in a system with a disconnected source-destination link [39, 40]. In the system investigated in this paper, although the destination can hear from the source, the destination chooses to act as a jammer rather than receive the signal. It will be shown that, although the destinations useful signal in the first slot is discarded, the overall secrecy of the system is improved as compared with the methods in literature.

The contributions are summarized as follows:

- We propose a destination-assisted jamming scheme in which the destination does not listen in the first slot, but rather cooperates with the source in transmitting noise. Due to the cooperative jamming, the eavesdropper Signal-to-Interference-plus-Noise-Ratio (SINR) in the first slot is limited

when the transmission power increases. The secrecy rate is therefore improved significantly.

- The optimal power allocation is determined among source, relay and destination signal and jamming noise, to maximize the system secrecy rate. We show that this non-convex optimal power allocation problem can be converted into a one dimensional line search plus a bi-sectional search problem.

- We extend the proposed jamming scheme to the environment with multiple relays. Two relay selection schemes are proposed to choose the best relay to decode-and-forward the signal. The selections filter out bad relays which result the tight first slot secrecy constraints and limit the secrecy rate. The optimal method is based on the computation of the optimal power allocation through all possible relays to be selected. The suboptimal method is purely based on the CSI of each relay and has low computation requirements.

- The scaling law of the secrecy rate is analyzed in the region of high transmit power and large number. The scaling law of secrecy rate takes the form of $\frac{1}{2}\log_2(1+\frac{P_0}{8}\log K)-1.6$ bits/s/Hz under Rayleigh channel.

- We designe a limited feedback approach to acquire CSI which enables distributed calculation of jamming weight vectors and power allocation at each relay.

This part of work is included in:

- Y. Liu and A.P. Petropulu, "Destination assisted cooperative jamming for wireless physical layer security," *submitted to IEEE Trans. on Info. Forensics and Security,* 2012.

- Y. Liu and A.P. Petropulu, and H. Vecent Poor, "Joint decode-and-forward and jamming for wireless physical layer security with destination assistance," *IEEE Asilomar Conf. on Signals, Systems and Computers*, 2011,

pp. 109-113.

- Y. Liu and A.P. Petropulu, and H. Vecent Poor, "Relay selection and scaling law in destination assisted physical layer secrecy systems," *IEEE Statistical Signal Processing Workshop (SSP)*, Aug. 2012.

## 1.5 Outline of the thesis

This dissertation is organized as follows.

In Chapter 2, we present the proposed the relay beamforming design in multi-point-to-multi-point systems to maximize the sumrate. Sumrate results are analyzed under perfect and imperfect relay CSI.

In Chapter 3, the QoS meeting problem in multi-point-to-multi-point systems is considered. Relay beamforming design and antenna selection are proposed to combat the relay CSI errors.

In Chapter 4, a destination assisted cooperative jamming/beamforming scheme is proposed in physical layer security systems. Chapter 5 contains concluding remarks and possible directions for future work.

## 1.6 Notations

Notation - Boldface uppercase letters denote matrices and boldface lowercase letters denote vectors. $(\cdot)^T$ and $(\cdot)^{\mathcal{H}}$ denote transpose and conjugate transpose operators, respectively. $[\mathbf{X}]_{i,j}$, $[\mathbf{X}]_{:,j}$ and $[\mathbf{X}]_{i,:}$ denote the i-j element, $j$th column and $i$th row of the matrix $\mathbf{X}$, respectively. $\texttt{vec}(\mathbf{X}) = [[\mathbf{X}]_{:,1}^T, [\mathbf{X}]_{:,2}^T, ...]^T$. For a vector $\mathbf{x}$, $[\mathbf{x}]_i$ denotes the $i$th element and $\texttt{diag}\{\mathbf{x}\}$ denotes a diagonal matrix in which the $i$th diagonal element is $[\mathbf{x}]_i$. $I(\cdot;\cdot)$ denotes mutual information. $\mathcal{CN}(\mu, \sigma^2)$ and $\mathcal{N}(\mu, \sigma^2)$ denote respectively complex and real Gaussian variables

with mean equal to $\mu$ and variance equal to $\sigma^2$. $\mathcal{X}(n, \sigma^2)$ denotes a $n$-degrees chi-square distribution, with zero mean and variance $\sigma^2$ in each degree. $\mathbb{E}$ denotes expectation operation.

# Chapter 2

# On the Sumrate of Amplify-and-Forward Relay Networks with Multiple Source-Destination Pairs

The Chapter considers a network scenario in which multiple Source-Destination (S-D) node pairs need to communicate simultaneously. Each source and destination is equipped with a single antenna and the communication is assisted by a multi-antenna relay operating in an Amplify-and-Forward fashion. The communication is completed in two slots; 1) the sources transmit simultaneously and 2) the relay retransmits the signals which were received at its antennas after linearly processing them via a zeroforcing beamforming (ZFBF) matrix. Two different designs for ZFBF matrix are proposed. The first design allocates the total relay power so that all data streams have the same power. The second design allocates the total relay power in a way that maximizes the sumrate of all S-D pairs. We show analytically that, when the source or relay power is high, the proposed sumrate maximization has the same ergodic sumrate as the cut-set bound with two identical slots and a ZF precoder in the broadcast hop, or a ZF equalizer in the multiple access hop or maintains a constant gap from the cute-set bound when a ZF precoder is employed in the broadcast hop. Although initially full relay channel state information (CSI) is assumed, an upper bound of the sumrate loss caused by relay CSI errors is derived.

Relaying approaches are strong candidates for delivering high performance in next generation wireless communication systems. Indeed, they have the potential to achieve extended coverage, throughput enhancement and energy savings [26]

by combating a weak direct link between the source and destination, caused by large pathloss or shadowing. Among various relaying protocols, e.g. Amplify-and-Forward (AF), Decode-and-Forward (DF) and Compress-and-Forward (CF) [28], AF relaying is popular for its low complexity and implementation cost.

Recently, relay techniques has been exploited with Multiple input multiple output (MIMO) [1, 2]. In [41, 36], point-to-point MIMO techniques were proposed and capacity bounds were analyzed.

The optimal relay BF structure for maximizing the throughput in antenna AF relay systems was proposed in [42], for the case in which the relay serves one source and one destination and in [43], for the case in which the relay forwards the signal that it receives from two simultaneously transmitting nodes. Both schemes require that sources and destinations have multiple antennas. MIMO relay systems with one source and multiple destinations have been investigated in [44, 34]. Apart from these prior works, there is another potentially high throughput application of MIMO relaying, i.e., using multiple antenna relay(s) for supporting simultaneous communication between multiple S-D pairs. For example, [36] employs a large group of relays to support each independent S-D antenna pair. The transmit signals from the relays belonging to the same group add coherently at the destination antennas. [45] proposed a BF design for minimizing the mean square error of received data at all destinations. In [46, 47], the authors implemented ZFBF and channel triangulating BF at a number of relays for separating data streams. The ZFBF matrix at each relay was generated so that a relay power constraint is satisfied [46]. However, the constraint on the BF matrix is so strict that the relay power may not be used up, which as a result limits the sumrate. One shared assumption in the aforementioned works is the availability of perfect CSI at the relay. To the best of our knowledge, no works have quantified the impact on performance of CSI errors at the relay.

A similar setup is considered in this section as in [46, 47], i.e., a system with

multiple single antenna S-D pairs. We focus on the model with one AF relay equipped with multiple antennas. This model can be employed in a network has one device with adequate space for equipping with multiple antennas, e.g., a base station with remote antennas, which are wired together. This scheme has advantages over the scheme using multiple relays with single antenna, i.e., it does not requires timing and phase synchronization and information changing among relay nodes, which are hard to be satisfied in a practical wireless system.

In the first slot the sources transmit simultaneously over the sources-relay (S-R) link, which is referred as Multiple Access (MAC) Link , while in the second slot, the relay retransmits signals which are received at its antennas after linearly processing them via a ZFBF [48, 49] matrix over the relay-destinations (R-D) channel which is called Broadcast (BC) link. The contribution of this work can be summarized as follows.

- We propose two different designs of the ZFBF matrix. The first design allocates the total relay power so that all data streams have the same useful signal power. The second design allocates the total relay power in a way that maximizes the sumrate of all S-D pairs.

- We show analytically that with high source and/or relay power, the ZFBF with the sumrate maximization design achieves an ergodic sumrate that maintains a constant gap from the maximal possible ergodic sumrate. The latter is determined by the cut-set theory [50] with two identical slots and a ZF precoder in the BC hop, or a ZF equalizer in the MAC hop. This confirms the optimality of the proposed approaches in terms of multiplexing gain.

- We investigate the impact of imperfect CSI on the sumrate of ZFBF relaying.

  A tight upper bound is derived quantifying the sumrate loss caused by the

relay CSI errors. The bound shows that the ratio of the source and relay power plays an important role in the sumrate penalty. It also demonstrates that with static CSI accuracy at the relay, the system becomes interference limited in the high SNR region and also that with improved CSI accuracy at the relay, the system sumrate can always benefits from increasing source and relay power.

## 2.1 System Model

A system with $M$ single antenna sources and $M$ single antenna destinations is considered. One relay, equipped with $K$ antennas assists the sources in sending data to their distinct destinations. The system model is depicted in Fig.2.1. The direct links between sources and destinations are assumed to be negligible due to large pathloss or shadowing. The source signal vector $\mathbf{s} \in \mathbb{C}^{M\times 1}$ contains the baseband signals of the $M$ sources. $[\mathbf{s}]_i, i = 1, ..., M$, are assumed to be statistically independent and identically distributed (i.i.d.) $\mathcal{CN}(0, 1)$. The transmit power of source $i$ and the relay is $P_i$ and $P_0$, respectively. Frequency flat fading in all channels is assumed and initially, all channels are assumed to be known at the relay. Communications occur in a half-duplex fashion.

In the first slot, the sources transmit $\mathbf{s}$ over the S-R channel $\mathbf{F} \in \mathbb{C}^{K\times M}$ and the relay receives $\mathbf{r} = \mathbf{F}\mathbf{\Lambda_s}\mathbf{s} + \mathbf{n}$, where $\mathbf{r} \in \mathbb{C}^{K\times 1}$; $\mathbf{\Lambda_s} = \mathtt{diag}\{\sqrt{P_1}, ..., \sqrt{P_M}\}$; $\mathbf{n} \in \mathbb{C}^{K\times 1}$ represents additive noise at the relay, with $\mathbf{n}_i \sim \mathcal{CN}(0, 1)$. In the second slot, the relay applies a BF matrix $\mathbf{W} \in \mathbb{C}^{K\times K}$ on $\mathbf{r}$ and transmits the vector

$$\mathbf{t} \triangleq \mathbf{W}\mathbf{r} = \mathbf{W}\mathbf{F}\mathbf{\Lambda_s}\mathbf{s} + \mathbf{W}\mathbf{n},\ \mathbf{t} \in \mathbb{C}^{K\times 1}. \tag{2.1}$$

Let $\mathbf{G} \in \mathbb{C}^{K\times M}$ denote the R-D channel. The received signal vector at the

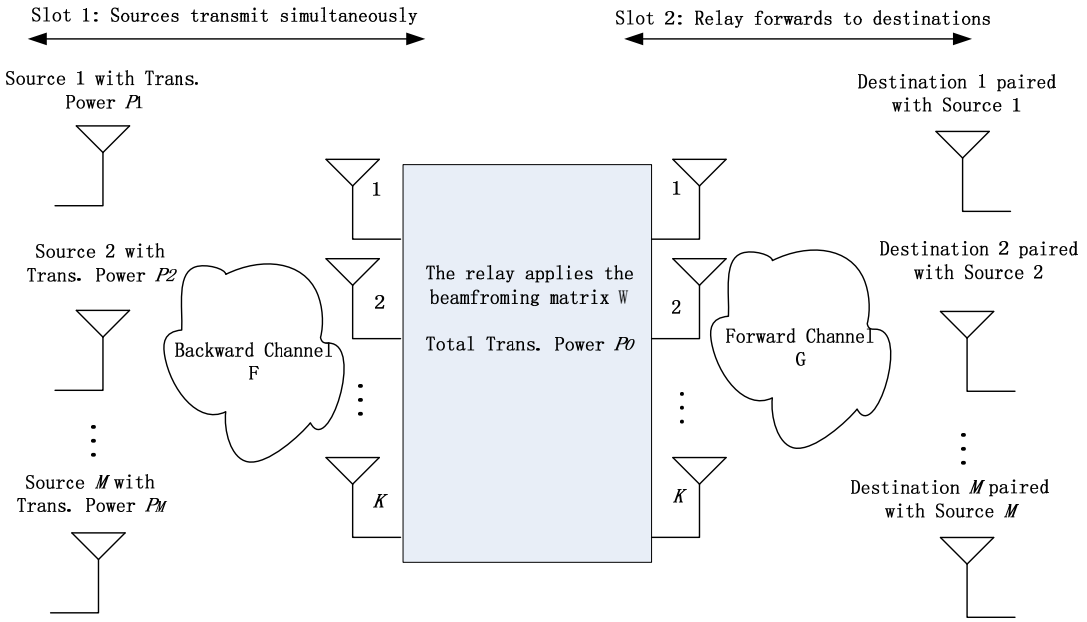


Figure 2.1: A relay system with multiple source-destination pairs

destinations is

$$\mathbf{y} = \mathbf{GWF\Lambda_s s} + \mathbf{GWn} + \mathbf{z}, \tag{2.2}$$

where $\mathbf{z}$ represents the noise vector at the destination. It is assumed that $[\mathbf{z}]_i \sim \mathcal{CN}(0,1)$. The relay transmit power and the SINR at the $i$th destination can be expressed as follows, respectively:

$$P_R = \mathbb{E}||\mathbf{t}||^2 = \mathtt{Tr}(\mathbf{WF\Lambda_s^2 F}^{\mathcal{H}}\mathbf{W}^{\mathcal{H}}) + \mathtt{Tr}(\mathbf{WW}^{\mathcal{H}}) \tag{2.3}$$

$$\mathtt{SINR}_i = \frac{P_i|\mathbf{g}_i^T\mathbf{W}\mathbf{f}_i|^2}{\sum_{j=1,\ldots M}^{j\neq i} P_j|\mathbf{g}_i^T\mathbf{W}\mathbf{f}_j|^2 + ||\mathbf{g}_i^T\mathbf{W}||^2 + 1} \tag{2.4}$$

The goal of this chapter is to maximize the system sumrate, $R = \frac{1}{2}\sum_{i=1}^{M}\log_2(1+\mathtt{SINR}_i)$, subject to a relay total power constraint $P_R \leq P_0$. If (3.2) and (3.3) are directly used for this goal, the formulated problem is non-convex and complicated, which is hard to solve [51].

### 2.1.1 Cut-set upper bound of sumrate

For the system under investigation, an upper bound of the sumrate can be obtained using cut-set theory [50]. Since the direct links from the sources to the destinations are ignored, the half-duplex cut-set bound with two identical slots can be readily expressed as

$$C \leq \frac{1}{2}\min\{\max_{p(\mathbf{s})} I(\mathbf{s};\mathbf{r}), \max_{p(\mathbf{t})} I(\mathbf{t};\mathbf{y})\}. \tag{2.5}$$

The term $\max_{p(\mathbf{s})} I(\mathbf{s};\mathbf{r})$ in (2.5) denote the capacity of the MAC-cut, for which it holds that $\max_{p(\mathbf{s})} I(\mathbf{s};\mathbf{r}) = \log_2 \det(\mathbf{I} + \mathbf{F}{\mathbf{\Lambda_s}}^2\mathbf{F}^{\mathcal{H}}) \triangleq C_{MAC}$. The term $\max_{p(\mathbf{t})} I(\mathbf{t};\mathbf{y})$ in (2.5) denotes the capacity of BC-cut and is further upper bounded as $\max_{p(\mathbf{t})} I(\mathbf{t};\mathbf{y}) \leq \max_{\mathbf{Q_t}=\mathbb{E}\mathbf{t}\mathbf{t}^{\mathcal{H}},\ trace(\mathbf{Q_t}\leq P_0)} \log\det(\mathbf{I} + \mathbf{G}\mathbf{Q_t}\mathbf{G}^{\mathcal{H}}) \triangleq C_{BC,Coop}$. The achievable throughput is upper bounded by the smaller one of the capacity of the MAC-cut and BC-cut. Since ZFBF is employed for relay signal forwarding in this chapter, we analyze the sumrate difference between the proposed approaches and the cut-set bound (2.5) with a ZF precoder in the BC hop and/or a ZF equalizer in the MAC hop. The value $\max\{C_{MAC}, C_{BC,Coop}\}$ is used in simulations for evaluating how the sumrate of the proposed approaches are close to the maximal possible throughput.

## 2.2 Sumrate of ZFBF Relaying with Multiple S-D Pairs

Since the optimal BF matrix that maximizes the sumrate is hard to obtain, we use the ZF criterion to simplify the BF matrix design problem. To guarantee that there is no interference among S-D pairs, i.e., the $i$th destination only receives the signal from $i$th source, the BF matrix $\mathbf{W}$ must satisfy $[\mathbf{G}]_{i,:}\mathbf{W}[\mathbf{F}]_{:,j} = 0, i, j = 1, ..., M, i \neq j$, which implies that $\mathbf{GWF}$ is diagonal. One way to enforce these

conditions is to employ the following structure to $\mathbf{W}$ [38],

$$\mathbf{W} = \underbrace{\mathbf{G}^{\mathcal{H}}[\mathbf{G}\mathbf{G}^{\mathcal{H}}]^{-1}}_{\mathbf{W_G}} \mathbf{\Lambda}_R \underbrace{[\mathbf{F}\mathbf{F}^{\mathcal{H}}]^{-1}\mathbf{F}^{\mathcal{H}}}_{\mathbf{W_F}}, \tag{2.6}$$

where $\mathbf{\Lambda}_R = \mathtt{diag}\{\rho_1, ..., \rho_M\}$. Eq.(3.5) requires that $\mathtt{rank}(\mathbf{F}),\ \mathtt{rank}(\mathbf{G}) = M$.

By substituting (3.5) into (3.1), (3.2) and (3.3), the received signal at the $i$th destination becomes $[\mathbf{y}]_i = \rho_i\sqrt{P_i}[\mathbf{s}]_i + \rho_i[\mathbf{W_F}]_{i,:}\mathbf{n} + [\mathbf{z}]_i$ and $\mathtt{SINR}_i$ and relay transmit power expressions become

$$\mathtt{SINR}_i^{ZF} = \frac{P_i|\rho_i|^2}{|\rho_i|^2\sigma_{\mathbf{f}_i}^2 + 1}, \tag{2.7}$$

$$P_R^{ZF} = \sum_{i=1}^{M} \sigma_{\mathbf{g}_i}^2 P_i|\rho_i|^2 + \mathbf{x}^{\mathcal{H}}\mathbf{\Gamma}\mathbf{x}, \tag{2.8}$$

where $\mathbf{\Gamma} \triangleq \sum_{i=1}^{M} \mathtt{diag}\{[\mathbf{W_F}]_{i,:}\}^{\mathcal{H}}\mathbf{W_G}^{\mathcal{H}}\mathbf{W_G}\mathtt{diag}\{[\mathbf{W_F}]_{i,:}\}$, $\sigma_{\mathbf{f}_i}^2 \triangleq ||[\mathbf{W_F}]_{i,:}||^2$, $\sigma_{\mathbf{g}_i}^2 \triangleq ||[\mathbf{W_G}]_{:,i}||^2$ and $\mathbf{x} \triangleq [\rho_1, ..., \rho_M]^T$. The first and second term of the denominator of RHS of (2.7) represents forwarded noise level and additive noise level at the $i$th destination, respectively. Similarly, the first and second term of the RHS of (2.8) represents forwarded signal power and signal power in relay transmission power, respectively.

$\{\rho_1, ..., \rho_M\}$ in $\mathbf{\Lambda}_R$ can be adjusted to achieve the goal of maximizing the system sumrate and are our design variables. Note that not only the amplitude of $\rho_i$ affects the system throughput, but also the phase of $\rho_i$, which controls the forwarded noise power from the relay. We propose two different designs for $\{\rho_1, ..., \rho_M\}$ – a) equal power allocation and b) sumrate maximization. The two designs are discussed next.

### 2.2.1 Design 1: Equal power allocation

The relay assigns to each S-D pair the same useful signal power, i.e., $|\rho_i|^2\sigma^2_{\mathbf{g}_i}P_i = c, i = 1, ..., M$. By defining $\mathbf{x}_0 = [(\sigma^2_{\mathbf{g}_1}P_1)^{-\frac{1}{2}}, ..., (\sigma^2_{\mathbf{g}_M}P_M)^{-\frac{1}{2}}]^T$ and applying the total power constaints (2.8), $c$ should satisfy $c^2\mathbf{x}_0^{\mathcal{H}}\left[\mathtt{diag}\{[\sigma^2_{\mathbf{g}_1}P_1, ..., \sigma^2_{\mathbf{g}_M}P_M] + \mathbf{\Gamma}\}\right]\mathbf{x}_0 = P_0$. So we obtain:

$$\rho_i = \sqrt{\frac{P_0}{\mathbf{x}_0^{\mathcal{H}}\left[\mathtt{diag}\{[\sigma^2_{\mathbf{g}_1}P_1, ..., \sigma^2_{\mathbf{g}_M}P_M] + \mathbf{\Gamma}\}\right]\mathbf{x}_0\sigma^2_{\mathbf{g}_i}P_i}}. \tag{2.9}$$

### 2.2.2 Design 2: Sumrate maximization

The equal power allocation method is simple but it does not achieve the maximal system throughput. For scenarios in which different users face different channel conditions, there are better ways to adjust $\rho_i, i = 1, ..., M$. In this section, we allocate the weights $\{\rho_1, ..., \rho_M\}$, so that the sumrate is maximized. This problem is formulated as

$$\max_{\rho_i, i=1,...,M} C_{ZF} \triangleq \frac{1}{2}\sum_{i=1}^{M}\log_2\left(1 + \mathtt{SINR}_i^{ZF}\right), \quad s.t. \;\; P_R^{ZF} \leq P_0. \tag{2.10}$$

The problem of (2.10) is still non-convex. The constraint in (2.10) is the sum of two parts, i.e., the signal power $\sum_{i=1}^{M}\sigma^2_{\mathbf{g}_i}P_i|\rho_i|^2$ part and the forwarded noise power $\mathbf{x}^{\mathcal{H}}\mathbf{\Gamma}\mathbf{x}$. The idea is to first solve a relaxed version of (2.10) by discarding the contribution of the forwarded noise in the constraint. The effects of ignoring the forwarded noise are the following: 1) the power constraint at the relay is violated and 2) only the magnitudes of $\rho_1, ..., \rho_M$ can be computed. To address these two effects, the phases of $\rho_1, ..., \rho_M$ are optimized to minimize the power of the forwarded noise from the relay and then $|\rho_1|, ..., |\rho_M|$ are decreased accordingly to restore the power constraint. This idea leads to the following two-step suboptimal algorithm.

**Step 1:** Solve the following problem by ignoring the forwarded noise power, $\mathbf{x}^{\mathcal{H}}\mathbf{\Gamma}\mathbf{x}$, in (2.10),

$$\max_{|\rho_i|^2,\ i=1,...,M} C_{ZF}, \quad s.t. \sum_{i=1}^{M} \sigma_{\mathbf{g}_i}^2 P_i |\rho_i|^2 \leq P_0. \tag{2.11}$$

Using Lagrangian multipliers, this results in a water-filling-like solution, i.e.,

$$|\rho_i|^2 = f^+(q_i a_i b_i, b_i(q_i + a_i), b_i - \lambda),\ \sum_{i=1}^{M} |\rho_i|^2 b_i = P_0, \tag{2.12}$$

where $f^+(a,b,c) = \begin{cases} 0, & \texttt{if } b^2 - 4ac < 0 \\ \max\left\{\frac{-b+\sqrt{b^2-4ac}}{2a}, 0\right\}, & \texttt{else} \end{cases}$ and $a_i = \sigma_{\mathbf{f}_i}^2$, $b_i = P_i\sigma_{\mathbf{g}_i}^2$ and $q_i = P_i + a_i$. The derivation of (2.12) is given as follows:

The sumrate optimization problem ignoring the forwarded noise is written as

$$\max_{\mathbf{x}\in\mathbb{C}^{M\times 1}} \sum_{1}^{M} \log\left(1 + \frac{P_i|\rho_i|^2}{|\rho_i|^2\sigma_{\mathbf{f}_i}^2 + 1}\right) \quad s.\ t. \sum_{i=1}^{M} \sigma_{\mathbf{g}_i}^2 P_i |\rho_i|^2 \leq P_0.$$

Let us define $a_i = \sigma_{\mathbf{f}_i}^2$, $b_i = P_i\sigma_{\mathbf{g}_i}^2$, $q_i = P_i + a_i$ and $x_i = |\rho_i|^2$. By introducing the Lagrangian multiplier $\lambda$, we obtain the Lagrangian function as follows:

$$L(x_i, \lambda) = \sum_{i=1}^{M} \log(a_i x_i + 1) - \sum_{i=1}^{M} \log(q_i x_i + 1) + \lambda(\sum_{i=1}^{M} b_i x_i - P_0)).$$

Since $x_i > 0$, it must hold that $\frac{\partial L(x_i,\lambda)}{\partial x_i} = 0$, which yields

$$b_i a_i q_i x_i^2 + b_i(a_i + q_i)x_i = \frac{P_i}{\lambda} - b_i. \tag{2.13}$$

Eq.(2.13) has at most one positive root, since $b_i a_i q_i > 0$ and $b_i(a_i + q_i) > 0$. Therefore, by defining $\mu = \frac{P_i}{\lambda}$ and solving (2.13), we can obtain the expressions of the $|\rho_i|^2$ as in (2.12).

**Step 2:** Let the obtained $|\rho_i|,\ i = 1, ..., M$ form a real valued power control

vector $\mathbf{x}_{tmp} \triangleq [|\rho_1|, ..., |\rho_M|]^T$. $\mathbf{x}_{tmp}$ results $P_R^{ZF} \geq P_0$. So, in this step we first adjust the phase of each $\rho_i$ to minimize the forwarded noise power (this does not affect $\mathtt{SINR}_i,\ i = 1, ..., M$) and then scale $\rho_i$ to restore the relay power constraint. The problem of adjusting the phase is formulated as

$$\min_{\mathbf{v} \in \mathbb{C}^{M \times 1}} \mathbf{v}^{\mathcal{H}} \mathtt{diag}\{\mathbf{x}_{tmp}\}^{\mathcal{H}} \mathbf{\Gamma} \mathtt{diag}\{\mathbf{x}_{tmp}\} \mathbf{v}; \quad s.\ t.\ \ |[\mathbf{v}]_i| = 1, \tag{2.14}$$

where the $i$th element of $\mathbf{v}$ captures the phase of $|\rho_i|$, i.e., $\rho_i \triangleq |\rho_i|[\mathbf{v}]_i$. Let $\mathbf{Q} \triangleq \mathtt{diag}\{\mathbf{x}_{tmp}\}^{\mathcal{H}} \mathbf{\Gamma} \mathtt{diag}\{\mathbf{x}_{tmp}\}$, $\mathbf{\Psi} \triangleq \mathbf{v}\mathbf{v}^{\mathcal{H}}$, and $\mathbf{q}_i \in \mathbb{C}^{M \times M}$ with all zero elements except an 1 at the $i$-th diagonal element. Then, the problem of (2.14) is equivalent to

$$\min_{\mathbf{\Psi} \in \mathbb{C}^{M \times M}} Tr\{\mathbf{Q}\mathbf{\Psi}\}; \quad s.\ t.\ \ \mathtt{Tr}\{\mathbf{q}_i \mathbf{\Psi}\} = 1;\ \mathbf{\Psi} \succ 0;\ \mathtt{rank}\{\mathbf{\Psi}\} = 1, \tag{2.15}$$

which can be converted to convex using semi-definite relaxation by dropping the rank 1 condition, and can then be solved using semi-definite programming tools (e.g. Sedumi [52]) and randomization techniques [53]. The solution of (2.15) gives a phase vector $\mathbf{v}_{opt}$ which results in reduced noise forwarding power $P_n^{min} = \mathbf{v}_{opt}^{\mathcal{H}} \mathtt{diag}\{\mathbf{x}_{tmp}\}^{\mathcal{H}} \mathbf{\Gamma} \mathtt{diag}\{\mathbf{x}_{tmp}\} \mathbf{v}_{opt}$. So the total relay transmit power with $[\rho_1, ..., \rho_M] = \mathtt{diag}\{\mathbf{x}_{tmp}\}\mathbf{v}_{opt}$ would be to $P_0 + P_n^{min}$, by noting that the phase vector $\mathbf{v}_{opt}$ does not change the relay useful signal power. To restore the relay power from $P_0 + P_n^{min}$ back to $P_0$, we only need properly decrease the amplitude of $\mathbf{x}_{tmp}$:

$$\mathbf{x}_{opt} = \mathtt{diag}\{\mathbf{v}_{opt}\}\mathbf{x}_{tmp} \sqrt{\frac{P_0}{P_0 + P_n^{min}}}, \tag{2.16}$$

$\rho_i^{opt} = [\mathbf{x}_{opt}]_i$ and the corresponding ZFBF matrix equals $\mathbf{W}_{opt} = \mathbf{W}_{\mathbf{G}} \mathtt{diag}\{\mathbf{x}_{opt}\} \mathbf{W}_{\mathbf{F}}$.

**Remarks:** *A simpler, but not optimal, method without numerical optimization exists.* $\mathbf{Q}$ *has a Singular Value Decomposition* $\mathbf{Q} = \mathbf{V}\mathbf{D}\mathbf{V}^{\mathcal{H}}$. *If the phase*

*vector* $\mathbf{v}$ *can be along* $\mathbf{V}(:, M)$*, which corresponds to the smallest singular value of* $\mathbf{Q}$*, the forwarded noise power is minimized. So a good criterion is selecting* $\mathbf{v}$ *which has the largest inner product with* $\mathbf{V}(:, M)$*, i.e.,* $\max_{\mathbf{v}\in\mathbb{C}^{M\times 1}} |\mathbf{v}^{\mathcal{H}}\mathbf{V}(:, M)|$*; s. t.* $|[\mathbf{v}]_{ii}| = 1$*. The solution is* $\mathbf{v}_{subopt}$*,* $[\mathbf{v}_{subopt}]_i = \frac{\mathbf{V}(i,M)}{|\mathbf{V}(i,M)|}$.

The proposed methods can be extended to the multiple relay case. By letting each relay apply the proposed methods, the useful signals will add up together at each destination. So the throughput can be improved. In terms of sumrate maximization, however, direct applying the proposed sumrate maximization method maybe not be optimal since the power allocation of one relay may be affected by another one.

## 2.3 Ergodic Sumrate Analysis in High SNR Regime

In this section, the ergodic sumrate of the proposed ZFBF sumrate maximization approach is analyzed in the high SNR regime by comparing it to the maximum possible ergodic sumrate as given by the cut-set theory, with a ZF precoder in the BC-hop and/or ZF equalizer in the MAC-hop. Via this comparison, we get a sense of how much throughput is lost due to the AF operation at the relay. In the analysis we assume that the elements of the channel matrices **F, G** are i.i.d., $\mathcal{CN}(0, 1)$.

In the high SNR regime (high source power and/or relay power), the gap between the ergodic sumrate of the ZFBF AF relaying and the cut-set bound with ZF precoder in the BC hop and/or ZF equalizer per S-D pair in the MAC hop is upper bounded by a positive constant, which is related to $K - M$ only.

For the cut-set bound, the power allocation in the BC-cut with a ZF precoder that maximizes the sumrate is a standard waterfilling solution $\{P_i^{StdWF}, i = 1, ..., M\}$ based on a total power constraint $P_0$ and channel gains $\sigma_{\mathbf{g}_i}^{-2}, i = 1, ..., M$. We will prove Theorem 1 for the following three high SNR cases:

- **Case I**- The source power and relay power are both very large and increase at the same rate, so that $P_i \to \infty$ and $\frac{P_0}{P_i} = c_i$, where $c_i$ is a positive finite constant.

In this case, the ratio of the forwarded signal power to the forwarded noise power in the relay transmit power tends to infinity so that the effect of the forwarded noise on $\rho_i, i = 1, ..., M$ can be ignored. In that case, the amplitudes of $\rho_i, i = 1, ..., M$ can be determined based on the forwarded signal power only. Then, if the relay still allocates $\{P_i^{StdWF}, i = 1, ..., M\}$, it holds

$$\lim_{P_i \to \infty,\ P_0/P_i = c_i} |\rho_i^{StdWF}|^2 = \frac{P_i^{StdWF}}{\sigma_{\mathbf{g}_i}^2 P_i}, \tag{2.17}$$

Since the proposed design is obtained to maximize the sumrate, the weights $\{|\rho_i^{opt}|^2, i = 1, ..., M\}$, obtained based on (2.12) must outperform the standard waterfilling solution $\{|\rho_i^{StdWF}|^2, i = 1, ..., M\}$. Thus we have the following relation:

$$C_{AF,ZF}^{opt} \geq \frac{1}{2} \sum_{i=1}^{M} \log_2 \left( 1 + \frac{P_i^{StdWF} P_i}{P_i^{StdWF} \sigma_{\mathbf{f}_i}^2 + P_i \sigma_{\mathbf{g}_i}^2} \right). \tag{2.18}$$

where the RHS of (2.18) comes from substituting (2.17) into (2.7). The upper bound of the expectation of the difference of $C_{AF,ZF}^{opt}$ and the ergodic sumrate of

the BC-hop with a ZF precoder is shown in (2.19)-(2.23) at the top of next page,

$$\mathbb{E}C_{Cut,BCZF} - \mathbb{E}C_{AF,ZF}^{opt} \leq \mathbb{E}C_{BC,ZF} - \mathbb{E}C_{AF,ZF}^{opt} \tag{2.19}$$

$$\overset{P_i\to\infty}{\leq} \frac{1}{2}\mathbb{E}\sum_{i=1}^{M}\left[\log_2\left(1+\frac{P_i^{StdWF}}{\sigma_{\mathbf{g}_i}^2}\right) - \log_2\left(1+\frac{P_i^{StdWF}}{\frac{P_i^{StdWF}}{P_i}\sigma_{\mathbf{f}_i}^2+\sigma_{\mathbf{g}_i}^2}\right)\right]$$

$$\leq \frac{1}{2}\mathbb{E}\sum_{i=1}^{M}\log_2\left(1+c_i\frac{\sigma_{\mathbf{f}_i}^2}{\sigma_{\mathbf{g}_i}^2}\right) \tag{2.20}$$

$$\leq \frac{1}{2}\mathbb{E}_{\sigma_{\mathbf{f}_i}^2}\sum_{i=1}^{M}\log_2\left(1+c_i(K-M+1)\sigma_{\mathbf{f}_i}^2\right) \tag{2.21}$$

$$= \frac{1}{2}\mathbb{E}_{\sigma_{\mathbf{f}_i}^2}\sum_{i=1}^{M}\log_2\left(\frac{2}{\sigma_{\mathbf{f}_i}^2}+2c_i(K-M+1)\right) - \frac{1}{2}\mathbb{E}_{\sigma_{\mathbf{f}_i}^2}\sum_{i=1}^{M}\log_2\left(\frac{2}{\sigma_{\mathbf{f}_i}^2}\right) \tag{2.22}$$

$$\leq \frac{M}{2}\log_2[2(c_i+1)(K-M+1)] + \frac{M}{2}1.4427(\gamma - \sum_{j=1}^{K-M}\frac{1}{j}), \tag{2.23}$$

where $C_{Cut,BCZF}$ stands for the cut-set bound in the BC-hop with a ZF precoder and, $C_{BC,ZF}$ denotes the ergodic sumrate of the BC-hop with a ZF precoder; $\gamma = 0.577$ in (2.23) is the Euler's constant; $1.4427 = \log_2 e$ in (2.23) is due to the log base change; (2.19) is based on the fact $\mathbb{E}\min(x_1, x_2) \leq \mathbb{E}x_1$; (19) is because that $\frac{P_i^{StdWF}}{P_i} \leq c_i$; (2.21) is based on Jensen's inequality and the facts $1/\sigma_{\mathbf{g}_i}^2 \sim \mathcal{X}^2(2(K-M+1), \frac{1}{2})$[54]; (2.23) is based on Jensen's inequality and (4.352-1) in [55].

When $K-M+1$ is very large, it is well-known that $\sum_{j=1}^{K-M}\frac{1}{j} \to \log(K-M)+\gamma$, so the RHS of (2.23) becomes:

$$\texttt{RHS of (2.23)} = \frac{M}{2}\log_2[2(c_i+1)]$$

This indicates that the throughput loss of the proposed ZFBF approach with AF operation is bounded by a constant compared with any other two-hop systems with two identical slots and a ZF precoder in the BC hop; this constant is only related to the ratio of the relay and source power with large relay antenna number.

In Fig. 2.2, we plot the value of RHS of (2.23) divided by $M$, i.e., the sumrate gap upper bound per S-D pair, at different values of $K - M$. One can see that the sumrate gap upper bound per S-D pair is only related to $K - M$ based on (2.23). Also, Fig. 2.2 shows that as $K - M$ increases, the sumrate gap upper bound per S-D pair decreases.

- **Case II**- Large source power, $P_i \to \infty$ and small relay power, i.e., $P_i \gg P_0$.

In this case too, the effect of the forwarded noise on the relay transmit power can be ignored. Further, since $|\rho_i| \to 0$, it holds that $|\rho_i|^2 \sigma_{\mathbf{f}_i}^2 \ll 1$, thus, the forwarded noise in the SINR (2.7) is much smaller than the additive noise and can be ignored. The proposed sumrate maximization method degenerates to the standard waterfilling, i.e., $|\rho_i^{opt}|^2 \to |\rho_i^{StdWF}|^2$. Then, it holds

$$C_{AF,ZF}^{opt} \overset{P_i \gg P_0}{\to} \frac{1}{2} \sum_{i=1}^{M} \log_2 \left( 1 + \frac{P_i^{StdWF}}{\sigma_{\mathbf{g}_i}^2} \right) = C_{Cut,BCZF}$$

which means that the sumrate $C_{AF,ZF}^{opt}$ is the same as the cut-set bound with a ZF BC-hop.

- **Case III**- Large relay power, i.e., $P_0 \to \infty$ and small source power, i.e., $P_0 \gg P_i$.

When $P_0 \gg P_i$, the cut-set bound is dominated by the MAC-hop, thus we only consider the comparison of $C_{AF,ZF}^{opt}$ and $C_{Cut,MACZF}$, which is the sumrate of the MAC-hop when the relay employs a ZF equalizer. Since $P_0 \to \infty$, it also holds that $|\rho_i|^2 \to \infty$. By applying $|\rho_i|^2 \to \infty$ to (2.7), we obtain

$$C_{AF,ZF}^{opt} \overset{|\rho_i|^2 \to \infty}{\to} \frac{1}{2} \sum_{i=1}^{M} \log_2 \left\{ 1 + \frac{P_i}{\sigma_{\mathbf{f}_i}^2} \right\} \triangleq C_{Cut,MACZF}.$$

Therefore, the ergodic sumrate of the ZFBF AF relaying system approaches the cut-set bound with a ZF equalizer in the MAC-hop.

Combining the above three cases, we conclude that in the high SNR regime, the ZFBF AF relay system either has the same ergodic sumrate as the cut-set bound with ZF precoder and/or receiver, or maintains a constant gap from the cut-set bound with a ZF precoder. The ZF equalizer in MIMO MAC and the ZF precoder in MIMO BC can both achieve multiplexing gain $M$ [56][54]. Considering that ZFBF relaying uses two slots for one symbol transmission, the proposed sumrate maximization approach achieves spatial multiplexing gain of $\frac{M}{2}$, thus is optimal.

*Remarks:* Note that the ergodic sumrate difference between the ZFBF and ZF-Dirty-Paper-Coding (ZF-DPC) tends to be a constant [57], and also that the sumrate gap between ZF-DPC and the system with cooperation receive antennas vanishes [54] in high SNR regime. As a result, Theorem 1 can also apply to the case of an optimal receiver in the MAC-hop and ZF-DPC precoder in the BC-hop. Note that by replacing $P_i^{StdWF}$ in the sumrate maximization method with $\frac{P_0}{M}$ in the equal power allocation method Theorem 1 can be easily shown to be also valid for the equal power allocation case.

## 2.4 Impact of the CSI errors on the sumrate

In order to calculate the ZFBF matrix, the relay must have CSI on both the MAC and BC hops. However, in a real scenario, the CSI obtained by the relay usually contains errors. In this section, we investigate the effect of CSI error on the ergodic sumrate of the proposed equal power allocation approach. The reason we analyze the equal power allocation is that this method has close form expressions for $\rho_i,\ i = 1, ..., M$, but the proposed sumrate maximization method does not. In the following, the elements of $\mathbf{F}$, $\mathbf{G}$ are assumed to be i.i.d. $\mathcal{CN}(0, 1)$. We also assume that each source has the same transmit power, i.e., $P_i = P_T,\ i = 1, ..., M$ for simplicity.

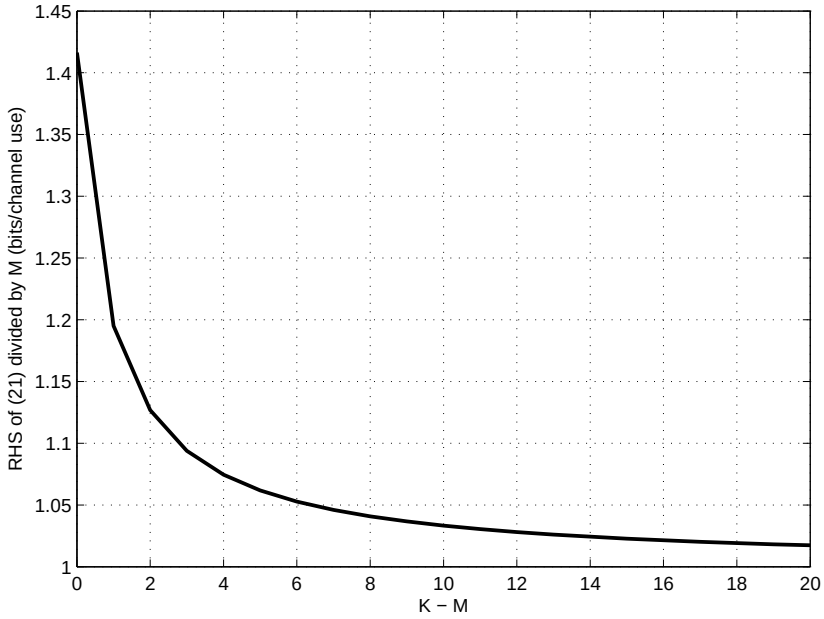


Figure 2.2: Value of (2.23) over $M$ at different $K - M$.

Let the true channel matrices, $\mathbf{F}$ and $\mathbf{G}$, be related to the estimates avaialbe at the relay, i.e., $\hat{\mathbf{F}}$ and $\hat{\mathbf{G}}$, through the following equations [58]:

$$\mathbf{F} = \sqrt{1-\alpha^2}\hat{\mathbf{F}} + \alpha\mathbf{E}_{\mathbf{F}}; \quad \mathbf{G} = \sqrt{1-\beta^2}\hat{\mathbf{G}} + \beta\mathbf{E}_{\mathbf{G}} \quad (0 \leq \alpha, \beta \leq 1). \tag{2.24}$$

In the above equation, $\hat{\mathbf{F}}$ and $\hat{\mathbf{G}}$ can be viewed as scaled versions of the MMSE estimates of $\mathbf{F}$ and $\mathbf{G}$, respectively, where the estimates and true channels have the same variances; $\mathbf{E}_{\mathbf{F}}$ and $\mathbf{E}_{\mathbf{G}}$ are CSI error matrices, which are statistically uncorrelated with $\mathbf{F}$ and $\mathbf{G}$ and their elements are assumed i.i.d., $\mathcal{CN}(0,1)$. The parameters $\alpha$ and $\beta$ quantify the CSI errors the MAC and BC links, respectively. We assume that the relay has the same CSI errors levels for all S-D pairs, however, the results also apply to the case that there are different errors between different links.

Suppose that the relay uses $\hat{\mathbf{F}}$ and $\hat{\mathbf{G}}$ for forming the BF matrice, i.e., $\mathbf{W}_{\mathbf{G}} =$

$\hat{\mathbf{G}}^{\mathcal{H}}[\hat{\mathbf{G}}\hat{\mathbf{G}}^{\mathcal{H}}]^{-1}$ and $\mathbf{W_F} = \hat{\mathbf{F}}^{\mathcal{H}}[\hat{\mathbf{F}}\hat{\mathbf{F}}^{\mathcal{H}}]^{-1}$. For presentation convenience, let us normalize each column of $\mathbf{W_G}$ and each row of $\mathbf{W_F}$ as

$$\tilde{\mathbf{W}}_{\mathbf{G}} = \mathtt{diag}\{|||[\mathbf{W_G}]_{:,i}||\}^{-1}\mathbf{W_G}; \quad \hat{\mathbf{W}}_{\mathbf{F}} = \mathtt{diag}\{|||[\mathbf{W_F}]_{i,:}||\}^{-1}\mathbf{W_F}.$$

In order to derive the sumrate loss, we will make the following assumptions:

- **AS3.1**: the proposed approach works in the moderate to high source power region so that $\rho_1, ..., \rho_M$ can be approximated by ignoring the forwarded noise, i.e., $\rho_i \simeq \sqrt{\frac{P_{fw}}{P_T|\hat{a}_i^{\mathbf{f}}|^2}}$, where $\hat{a}_i^{\mathbf{f}} = [\hat{\mathbf{W}}_{\mathbf{F}}]_i\hat{\mathbf{F}}_{:,i}$ and $P_{fw}$ is the relay power per S-D pair with $P_{fw} = \frac{P_0}{M}$.

- **AS3.2**: $\alpha,\ \beta << 1$ so that the variation of the received useful signal power at each destination caused by CSI errors can be ignored, i.e., $\eta_i \simeq \hat{\eta}_i$, where $\eta_i$ and $\hat{\eta}_i$ are the received useful signal power at the $i$th destination without and with CSI errors, respectively.

- **AS3.3**: The change on the forwarded noise level at each destination, caused by the CSI errors, is ignored, i.e. $n_i^{fw} \simeq \hat{n}_i^{fw}$, where $n_i^{fw}$ and $\hat{n}_i^{fw}$ are the received forwarded noise power at the $i$th destination without and with CSI errors, respectively. This is becaused that the forwarded noise levels are much smaller than the interference among S-D pairs.

On denoting the interference power at the $i$th destination from $j$th ($j \neq i$)

source by $I_j^{(i)}$, the ergodic sumrate penalty resulting from the CSI errors is expressed as

$$\begin{aligned}\Delta R &= \mathbb{E}\log\left(1+\frac{\eta_i}{n_i^{fw}+1}\right) - \mathbb{E}\log\left(1+\frac{\hat{\eta}_i}{\sum_{j=1,\ldots,M}^{j\neq i} I_j^{(i)} + \hat{n}_i^{fw}+1}\right) \\ &= \mathbb{E}\log\left(\frac{\eta_i + n_i^{fw}+1}{\hat{\eta}_i + \hat{n}_i^{fw}+1+\sum_{j=1,\ldots,M}^{j\neq i} I_j^{(i)}}\right) + \mathbb{E}\log\left(\frac{\hat{n}_i^{fw}+1+\sum_{j=1,\ldots,M}^{j\neq i} I_j^{(i)}}{n_i^{fw}+1}\right) \\ &\leq \mathbb{E}\log\left(1+\frac{\sum_{j=1,\ldots,M}^{j\neq i} I_j^{(i)}}{\hat{n}_i^{fw}+1}\right), \end{aligned} \tag{2.25}$$

where the last step is due to AS3.2 and AS3.3. The throughput loss (2.25) depends on the interference and the forwarded noise. Because the interference term have dominant effect on the sumrate penalty, we approximate $\hat{n}_i^{fw}$ by ignoring the effect of the small CSI errors as

$$\begin{aligned}\hat{n}_i^{fw} &= \mathbb{E}|[\mathbf{G}]_{i,:}\tilde{\mathbf{W}}_{\mathbf{G}}\mathbf{\Lambda}_R\hat{\mathbf{W}}_{\mathbf{F}}\mathbf{n}|^2 \simeq \mathbb{E}|[\hat{\mathbf{G}}]_{i,:}\hat{\mathbf{W}}_{\mathbf{G}}\mathbf{\Lambda}_R\hat{\mathbf{W}}_{\mathbf{F}}\mathbf{n}|^2 \\ &= |\rho_i\hat{a}_i^{\mathbf{g}}|^2 = \frac{P_{fw}|\hat{a}_i^{\mathbf{g}}|^2}{P_T|\hat{a}_i^{\mathbf{f}}|^2}, \end{aligned} \tag{2.26}$$

where $\hat{a}_i^{\mathbf{g}} = [\hat{\mathbf{G}}]_{i,:}[\hat{\mathbf{W}}_{\mathbf{G}}]_{:,i}$. The interference from the $j$th source at the $i$th destination is written as

$$\begin{aligned} r_j^{(i)} &= (\sqrt{1-\beta^2}[\hat{\mathbf{G}}]_{i,:} + \beta[\mathbf{E}_{\mathbf{G}}]_{i,:})\hat{\mathbf{W}}_{\mathbf{G}}\mathbf{\Lambda}_R\hat{\mathbf{W}}_{\mathbf{F}}(\sqrt{1-\alpha^2}[\hat{\mathbf{F}}]_{:,j} + \alpha[\mathbf{E}_{\mathbf{F}}]_{:,j})s_j \\ &\overset{(a)}{\simeq} \beta[\mathbf{E}_{\mathbf{G}}]_{i,:}\hat{\mathbf{W}}_{\mathbf{G}}\mathbf{\Lambda}_R\hat{\mathbf{W}}_{\mathbf{F}}\sqrt{1-\alpha^2}[\hat{\mathbf{F}}]_{:,j}s_j + \sqrt{1-\beta^2}[\hat{\mathbf{G}}]_{i,:}\hat{\mathbf{W}}_{\mathbf{G}}\mathbf{\Lambda}_R\hat{\mathbf{W}}_{\mathbf{F}}\alpha[\mathbf{E}_{\mathbf{F}}]_{:,j}s_j \\ &= \beta x_{\mathbf{g}}^{(i,j)}\rho_j\sqrt{1-\alpha^2}\hat{a}_j^{\mathbf{f}}s_j + \sqrt{1-\beta^2}\hat{a}_i^{\mathbf{g}}\beta x_{\mathbf{g}}^{(i,j)}\rho_i s_j, \end{aligned} \tag{2.27}$$

where step (a) is based on the fact that $[\hat{\mathbf{G}}]_{i,:}\hat{\mathbf{W}}_{\mathbf{G}}\mathbf{\Lambda}_R\hat{\mathbf{W}}_{\mathbf{F}}[\hat{\mathbf{F}}]_{:,j} = 0$ and also the fact that the term $\alpha\beta[\mathbf{E}_{\mathbf{G}}]_{i,:}\hat{\mathbf{W}}_{\mathbf{G}}\mathbf{\Lambda}_R\hat{\mathbf{W}}_{\mathbf{F}}[\mathbf{E}_{\mathbf{F}}]_{:,j}$ can be ignored due to the assumption

of small $\alpha$ and $\beta$. Therefore, the interference power $I_j^{(i)}$ can be expressed as

$$\begin{aligned} I_j^{(i)} &= \mathbb{E}_{s_j}|r_i^{(j)}|^2 = \mathbb{E}_{s_j}|\beta x_{\mathbf{g}}^{(i,j)}\rho_j\sqrt{1-\alpha^2}\hat{a}_j^{\mathbf{f}}s_j|^2 + \mathbb{E}|\sqrt{1-\beta^2}\hat{a}_i^{\mathbf{g}}\alpha x_{\mathbf{f}}^{(i,j)}\rho_i s_j|^2 + \epsilon_j^{(i)} \\ &= \beta^2(1-\alpha^2)\rho_j^2|\hat{a}_j^{\mathbf{f}}|^2|x_{\mathbf{g}}^{(i,j)}|^2P_T + \alpha^2(1-\beta^2)\rho_i^2|\hat{a}_i^{\mathbf{g}}|^2|x_{\mathbf{f}}^{(i,j)}|^2P_T + \epsilon_j^{(i)} \\ &= \underbrace{\beta^2(1-\alpha^2)P_{fw}|x_{\mathbf{g}}^{(i,j)}|^2}_{I_j^{(i),\mathbf{G}}} + \underbrace{\alpha^2(1-\beta^2)P_{fw}\frac{|\hat{a}_i^{\mathbf{g}}|^2}{|\hat{a}_i^{\mathbf{f}}|^2}|x_{\mathbf{f}}^{(i,j)}|^2}_{I_j^{(i),\mathbf{F}}} + \epsilon_j^{(i)}, \end{aligned} \tag{2.28}$$

where $x_{\mathbf{f}}^{(i,j)} = [\hat{\mathbf{W}}_{\mathbf{F}}]_{i,:}[\mathbf{E}_{\mathbf{F}}]_{:,j}$ and $x_{\mathbf{g}}^{(i,j)} = [\mathbf{E}_{\mathbf{G}}]_{i,:}[\hat{\mathbf{W}}_{\mathbf{G}}]_{:,j}$; $\epsilon_j^{(i)} = \beta\sqrt{1-\beta^2}\alpha\sqrt{1-\alpha^2}$ $\rho_j\rho_i P_T[x_{\mathbf{g}}^{(i,j)}\hat{a}_j^{\mathbf{f}}(\hat{a}_i^{\mathbf{g}}x_{\mathbf{f}}^{(i,j)})^{\mathcal{H}} + (x_{\mathbf{g}}^{(i,j)}\hat{a}_j^{\mathbf{f}})^{\mathcal{H}}\hat{a}_i^{\mathbf{g}}x_{\mathbf{f}}^{(i,j)}]$. Later we will show that $\epsilon_j^{(i)}$ does not contribute to the sumrate loss upper bound. Note that $I_j^{(i),\mathbf{F}}$ and $I_j^{(i),\mathbf{G}}$ are related to the CSI errors of $\mathbf{F}$ and $\mathbf{G}$, respectively. Based on the quantities of $\hat{n}_i^{fw}$ and $I_j^{(i)}$ derived in this section, an upper bound of sumrate loss caused by CSI errors is given in the following theorem.

**Theorem 2:** *The sumrate loss is upper bounded as*

$$\begin{aligned} \Delta R \leq \frac{M}{2}\log\Bigg(1 &+ \beta^2(1-\alpha^2)P_{fw}(M-1)h_{K-M+1}(\frac{P_{fw}}{P_T}) \\ &+ \alpha^2(1-\beta^2)P_T(M-1)h_{K-M+1}(\frac{P_T}{P_{fw}})\Bigg) \triangleq \Delta R_{ub}, \end{aligned} \tag{2.29}$$

*where* $h_n(x) = \mathbb{E}\left[x\frac{|g_1|^2}{|g_2|^2}+1\right]^{-1}$ *with* $g_1, g_2 \sim \mathcal{X}(2n, \frac{1}{2})$.

**Proof:** The sumrate penalty of (2.25) is further written as:

$$\begin{aligned} \Delta R &\overset{(a)}{\leq} \log\left(1 + \mathbb{E}\left\{\frac{\sum_{j=1,\ldots,M}^{j\neq i} I_j^{(i),\mathbf{G}}}{\hat{n}_i^{fw}+1}\right\} + \mathbb{E}\left\{\frac{\sum_{j=1,\ldots,M}^{j\neq i} I_j^{(i),\mathbf{F}}}{\hat{n}_i^{fw}+1}\right\} + \mathbb{E}\left\{\frac{\sum_{j=1,\ldots,M}^{j\neq i} \epsilon_j^{(i)}}{\hat{n}_i^{fw}+1}\right\}\right) \\ &\overset{(b)}{=} \log\left(1 + \mathbb{E}\left\{\frac{\sum_{j=1,\ldots,M}^{j\neq i} I_j^{(i),\mathbf{G}}}{\hat{n}_i^{fw}+1}\right\} + \mathbb{E}\left\{\frac{\sum_{j=1,\ldots,M}^{j\neq i} I_j^{(i),\mathbf{F}}}{\hat{n}_i^{fw}+1}\right\}\right) \end{aligned} \tag{2.30}$$

where step (a) is based on the Jensen's inequality; step (b) uses the fact that that $x_{\mathbf{g}}^{i,j},\ x_{\mathbf{f}}^{i,j} \sim \mathcal{CN}(0,1)$[58], independent of $\hat{a}_i^{\mathbf{f}}$ and $\hat{a}_i^{\mathbf{g}}$. We first evaluate

$\mathbb{E}\left\{\frac{\sum_{j=1,\ldots,M}^{j\neq i} I_j^{(i),\mathbf{F}}}{\hat{n}_i^{fw}+1}\right\}$.

$$\mathbb{E}\left\{\frac{\sum_{j=1,\ldots,M}^{j\neq i} I_j^{(i),\mathbf{F}}}{\hat{n}_i^{fw}+1}\right\} = \mathbb{E}\left\{\frac{\beta^2(1-\alpha^2)P_{fw}\sum_{j=1,\ldots,M}^{j\neq i}|x_{\mathbf{g}}^{(i,j)}|^2}{\frac{P_{fw}|\hat{a}_i^{\mathbf{g}}|^2}{P_T|\hat{a}_i^{\mathbf{f}}|^2}+1}\right\}$$
$$\overset{(a)}{=} \beta^2(1-\alpha^2)P_{fw}(M-1)\mathbb{E}\left\{\left[\frac{P_{fw}|\hat{a}_i^{\mathbf{g}}|^2}{P_T|\hat{a}_i^{\mathbf{f}}|^2}+1\right]^{-1}\right\} \quad (2.31)$$

where (a) was obtained by noting that $x_{\mathbf{g}}^{(i,j)} \sim \mathcal{CN}(0,1), j\neq i$ so that $\sum_{j=1,\ldots,M}^{j\neq i}$ $|x_{\mathbf{g}}^{(i,j)}|^2 = M-1$ and $x_{\mathbf{g}}^{(i,j)}, j\neq i$ are independent with $\hat{a}_i^{\mathbf{g}},\ \hat{a}_i^{\mathbf{f}}$. Similarly, $\mathbb{E}\left\{\frac{\sum_{j=1,\ldots,M}^{j\neq i} I_j^{(i),\mathbf{F}}}{\hat{n}_i^{fw}+1}\right\}$ is computed as follows:

$$\mathbb{E}\left\{\frac{\sum_{j=1,\ldots,M}^{j\neq i} I_j^{(i),\mathbf{F}}}{\hat{n}_i^{fw}+1}\right\} = \mathbb{E}\left\{\frac{\alpha^2(1-\beta^2)P_{fw}\frac{|\hat{a}_i^{\mathbf{g}}|^2}{|\hat{a}_i^{\mathbf{f}}|^2}\sum_{j=1,\ldots,M}^{j\neq i}|x_{\mathbf{f}}^{(i,j)}|^2}{\frac{P_{fw}|\hat{a}_i^{\mathbf{g}}|^2}{P_T|\hat{a}_i^{\mathbf{f}}|^2}+1}\right\}$$
$$= \mathbb{E}\left\{\frac{\alpha^2(1-\beta^2)P_T\sum_{j=1,\ldots,M}^{j\neq i}|x_{\mathbf{f}}^{(i,j)}|^2}{\frac{P_T|\hat{a}_i^{\mathbf{f}}|^2}{P_{fw}|\hat{a}_i^{\mathbf{g}}|^2}+1}\right\}$$
$$= \alpha^2(1-\beta^2)P_T(M-1)\mathbb{E}\left\{\left[\frac{P_T|\hat{a}_i^{\mathbf{f}}|^2}{P_{fw}|\hat{a}_i^{\mathbf{g}}|^2}+1\right]^{-1}\right\}. \quad (2.32)$$

where step (a) is by noting that $x_{\mathbf{f}}^{(i,j)}, j\neq i$ are i.i.d. zero mean unit variance complex Gaussian variables so that $\mathbb{E}\sum_{j=1,\ldots,M}^{j\neq i}|x_{\mathbf{f}}^{(i,j)}|^2 = M-1$ and $x_{\mathbf{f}}^{(i,j)}, j\neq i$ are independent of $\hat{a}_i^{\mathbf{g}}$ and $\hat{a}_i^{\mathbf{f}}$.

The remaining task is computing $\mathbb{E}\left[\frac{P_{fw}|\hat{a}_i^{\mathbf{g}}|^2}{P_T|\hat{a}_i^{\mathbf{f}}|^2}+1\right]^{-1}$ and $\mathbb{E}\left[\frac{P_T|\hat{a}_i^{\mathbf{f}}|^2}{P_{fw}|\hat{a}_i^{\mathbf{g}}|^2}+1\right]^{-1}$, where $|\hat{a}_i^{\mathbf{g}}|^2,\ |\hat{a}_i^{\mathbf{f}}|^2 \sim \mathcal{X}(2(K-M+1),\frac{1}{2})$ and are independent. Define $h_n(x) \triangleq \mathbb{E}\left[x\frac{|\hat{a}_i^{\mathbf{f}}|^2}{|\hat{a}_i^{\mathbf{g}}|^2}+1\right]^{-1}$ with $n=K-M+1$, so that $h$ function can be evaluated based on the pdf function of chi-square distribution:

$$h_n(x) = \frac{1}{n!^2}\int_{a_1=0}^{\infty}\int_{a_2=0}^{\infty}\left[x\frac{a_1}{a_2}\right](a_1a_2)^{n-1}e^{-a_1+a_2}da_1da_2.$$

**Remarks**: Eq. (2.29) shows that if $\alpha$ and $\beta$ are small, the bound can be

decoupled into two parts: $\Delta R_{ub} \approx \Delta R_{ub}^{\mathbf{G}} + \Delta R_{ub}^{\mathbf{F}}$, where $\Delta R_{ub}^{\mathbf{G}} \triangleq \frac{M}{2}\log\left(1+\beta^2(1-\alpha^2)P_{fw}(M-1)h_{K-M+1}(\frac{P_{fw}}{P_T})\right)$ and $\Delta R_{ub}^{\mathbf{F}} \triangleq \frac{M}{2}\log\left(1+\alpha^2(1-\beta^2)P_T(M-1)h_{K-M+1}(\frac{P_T}{P_{fw}})\right)$. This approximation can be justified by the fact $\log(1+x+y) \approx \log(1+x)+\log(1+y)$ with $x,\ y \ll 1$. $\Delta R_{ub}^{\mathbf{F}}$ and $\Delta R_{ub}^{\mathbf{G}}$ are from the contributions of the CSI errors of $\mathbf{F}$ and $\mathbf{G}$, respectively. Each contribution, however, is smaller than the bound in [58] since $h(\cdot) < 1$. $h_1(x)$ is plotted in Fig.2.3 for the case $K = M$. It can be seen that in the large difference region between relay and source power (i.e., $x$ is large), $\log(h_1(x))$ is linear with $x(dB)$, which indicates that (2.29) is bounded when among the relay and source power one is fixed and the other goes infinite.

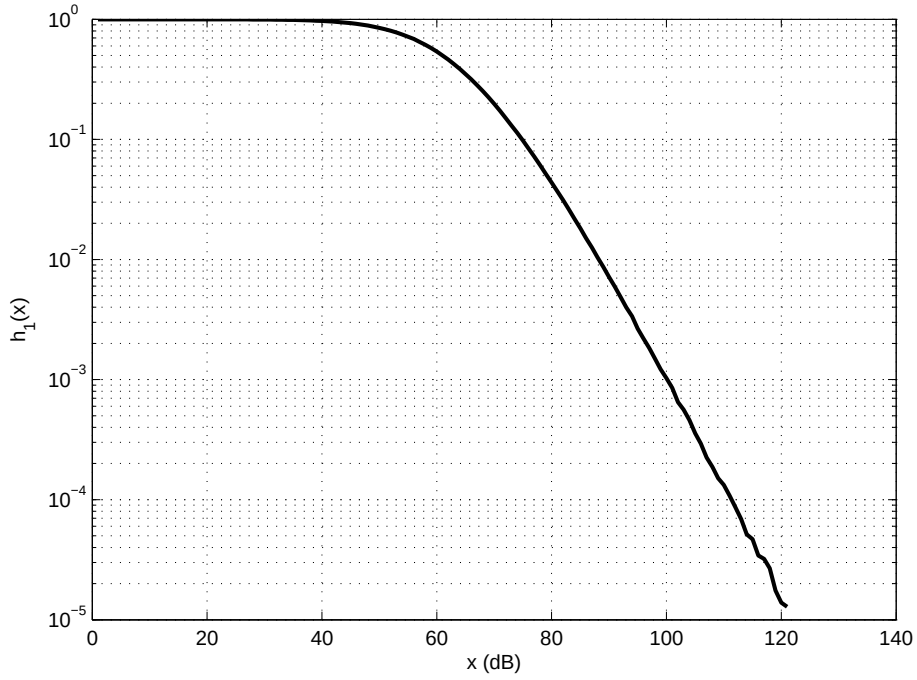


Figure 2.3: $h_1(x)$

Consider the case that $P_T, P_{fw} \to \infty$, $\frac{P_T}{P_{fw}} = c$. The interference of each destination also increase with the same rate based on (2.28). This means that if the CSI accuracy does not improve with increasing $P_T$ and $P_{fw}$, the system becomes interference limited and the sumrate cannot benefit from the power increasing.

To overcome this negative effects, we need to reduce the CSI errors indicators $\alpha^2$ and $\beta^2$. This can be realized for example by making the power of the pilots used for channel estimation increase at the same rate as the source and relay power increase. This yields $\alpha^2 P_{fw} \leq q_R, \;\; \beta^2 P_T \leq q_T$, in which $q_R$ and $q_T$ are two constants. Plugging in these two inequities in to (2.29), the bound becomes

$$\Delta R \leq \frac{M}{2} \log \left( 1 + q_R (M-1) h_{K-M+1}(\frac{P_{fw}}{P_T}) + q_T (M-1) h_{K-M+1}(\frac{P_T}{P_{fw}}) \right), \tag{2.33}$$

which is a constant for a fixed ratio $\frac{P_{fw}}{P_T}$. This indicates the ergodic sumrate of the ZFBF relay system maintains the power gain with improving CSI accuracy at the relay.

## 2.5 Simulation Results

Three distinct S-D pairs are simulated in this section. A 3-antenna relay assists the data transmission. Unless otherwise specify, the elements of $\mathbf{F}, \mathbf{G}$ are i.i.d., $\mathcal{CN}(0,1)$. All sources are assumed to have the same transmit power budget $P_T$. Each sumrate point is based on averaging over 5000 independent and random channel realizations.

In Fig.2.4, the sumrate performance of the proposed sumrate maximization and equal power allocation methods are illustrated. For comparison purposes, the sumrate of the power allocation scheme of [46] is also shown. In [46], a conservative power allocation was employed so that the relay transmit power is always less than the power constraint even in the extreme cases, e.g., when all sources' transmit signals are the same. This power allocation scheme does not always use all relay power. Simulations show that this comparison method consumes around $\frac{1}{3}$ of the total relay power, while the proposed sumrate maximization and equal power allocation methods utilize all relay power ($P_0$) at the relay. Fig.2.4 shows

that both proposed approaches outperform the method of [46] as they utilize all available relay power. One can observe a small advantage of the sumrate maximization method as compared to the equal power allocation, though the difference is rather small.

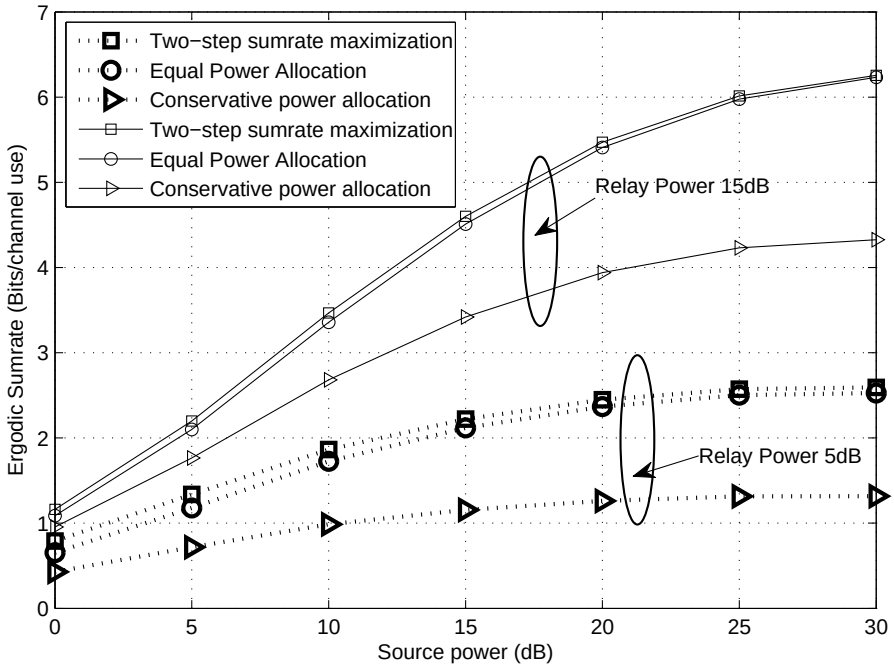


Figure 2.4: Sumrate comparison of sumrate maximization and equal power allocation methods (relay power at 5dB and 15dB; source power at $0 \sim 30dB$). The pathloss is the same for all channels.

In Fig.2.5, the path loss of the three source-relay links and relay-destinations links are set to be {-20dB, -10dB, 0dB}, i.e., they are different between different links. Unlike in Fig.2.4, one can see that in this case, the sumrate maximizing approach performs significantly better than the equal power allocation one. In the aspect of computational complexity, however, the equal power allocation method has lower load than that of the sumrate maximization method. For example, in 5000 channel realizations in Matlab using cvx tools [59] on the average, the sumrate maximization method costs 0.90s, i.e., 0.003s for waterfilling and 0.897s

for noise minimization (numerical optimization). The proposed equal power allocation costs 0.0017s. When the channel conditions of different S-D pairs diverse largely, the increase of the complexity might be tolerable due to the performance advantage of the sumrate maximization method over the equal power allocation. When the channel conditions of S-D pairs are similar or the system only has limit computation capability, the equal power allocation method might be a better choice. Alternatively, using the eigenvector method proposed at the end of Section III is another way to accomplish forwarded noise reduction with lower computational load.

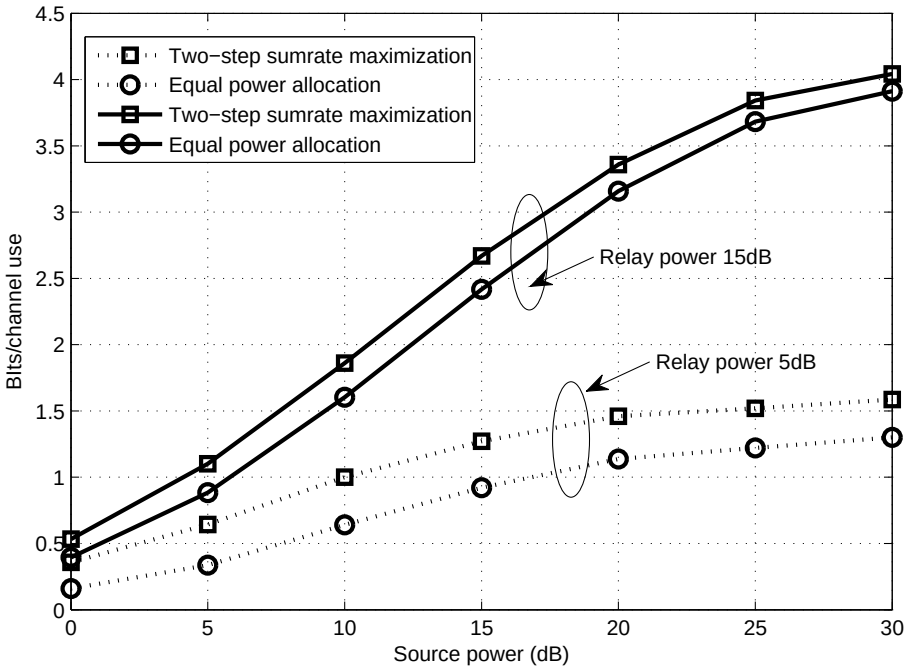


Figure 2.5: Sumrate comparison of sumrate maximization and equal power allocation methods (relay power at 5dB and 15dB; source power $0 \sim 30dB$). The pathloss is different between different channels.

The proposed sumrate maximizing method is suboptimal since the steps of amplitude and phase design of $\rho_1, ..., \rho_M$ are separated. Next we test how close the sumrate maximization method performs to the optimal solution. In particular, the optimal solution is obtained via an exhaustive search by randomly generating

40000 trials of directions of weight vector $[\rho_1, ..., \rho_M]$ on the unit complex sphere in every channel realization, and then assigned the maximal amplitude to each direction trial. Note that 40000 trials are very dense on a a three dimensional complex unit sphere. Then the one weight vector which achieved the maximal sumrate was selected. The sumrate comparison of the proposed sumrate maximization approach and the exhaustive search is shown in Fig.2.6 in the revised text, where one can see that the proposed maximization method performs almost equally well to the exhaustive search.

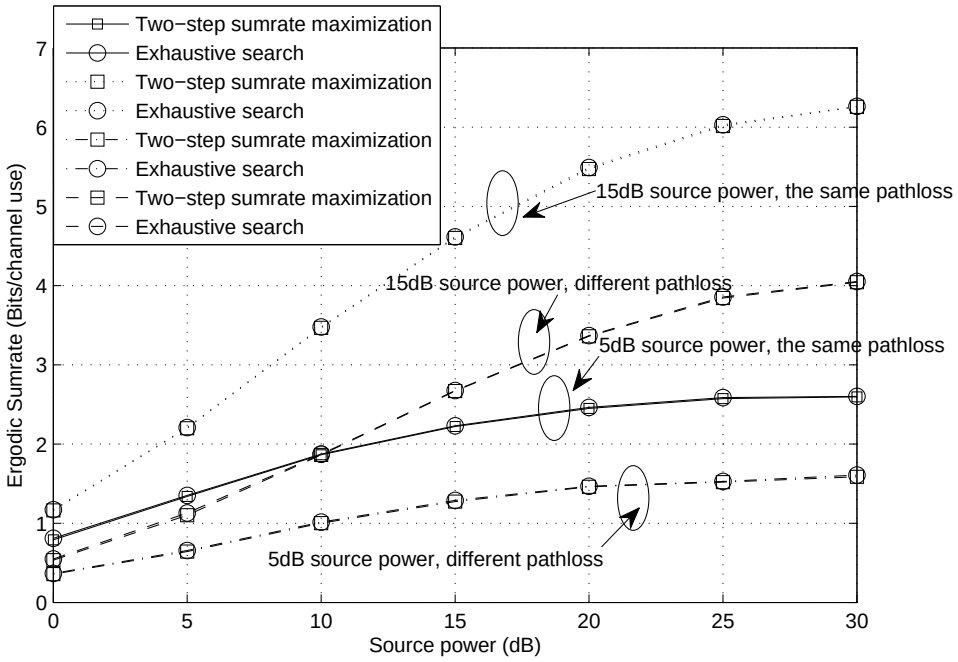


Figure 2.6: Sumrate comparison of sumrate maximization and exhaustive search methods (same pathloss and different pathloss on different channels are both considered).

Next, the ergodic sumrate of the sumrate maximization approach is tested in the high SNR region. The case of large relay power ($P_0 = 40dB$) and varying source power ($P_i$) between $0dB$ to $20dB$ is considered and the corresponding results are shown in Fig.2.7. As a benchmark, the upper bound of the cut-set bound, $\mathbb{E}\frac{1}{2}\max\{C_{MAC}, C_{BC,Coop}\}$, and the cut-set bounds with a relay ZF equalizer/precoder are also plotted. One can see that the sumrate of the proposed

sumrate maximization approach is almost the same as that of the cut-set bound with ZF equalizer/precoder. Fig.2.8 shows another high SNR case in which both the relay and source power increase with the same rate. The ergodic sumrate of the porposed sumrate maximization approach maintains a constant gap which is caused by the AF operation at the relay from the cut-set bound with ZF precoder in the BC hop. These observations are consistent with the analysis in Section 2.3. Also, the sumrate of the proposed sumrate maximization method in these three cases has the same slope as the cut-set sumrate bound with two identical slots.

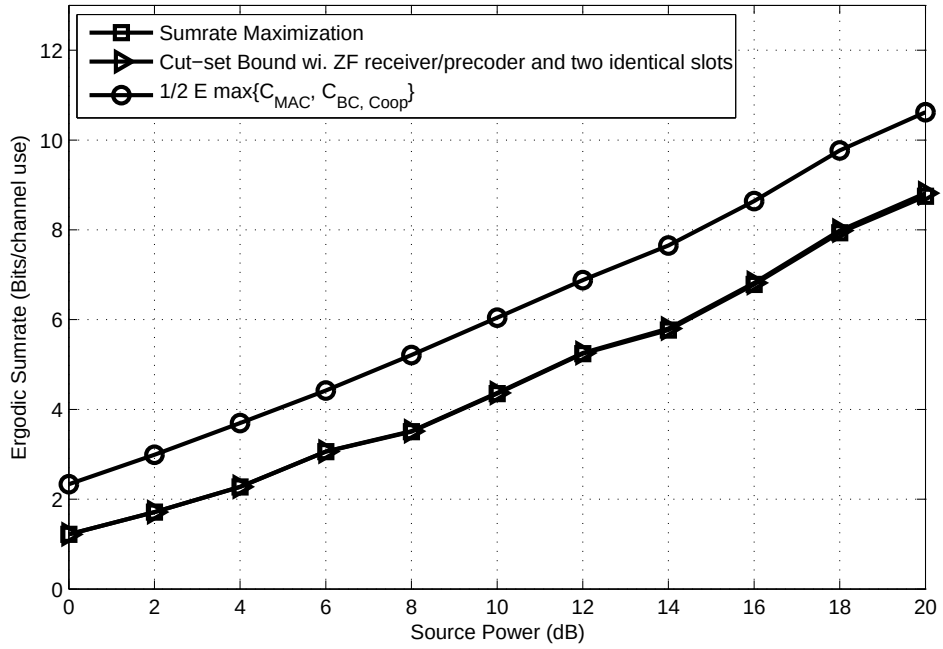


Figure 2.7: Sumrate comparison of the sumrate maximization approach and cut-set bound at high relay power (40dB) and small source power ($0 \sim 20$dB)

Next, we investigate the ergodic sumrate of the proposed sumrate maximization approach in the moderate SNR region. The curves in Fig.2.9 are based on fixed relay power ($P_0 = 20dB$) and varying source power ($P_i = 0 \sim 30dB$). It can be seen that the sumrate of the proposed sumrate maximization still has a similar trend with increasing SNR as that of the cut-set bound. Sumrate floors are also observed in this figure. This is because with increasing $P_i$, or $P_0$, the

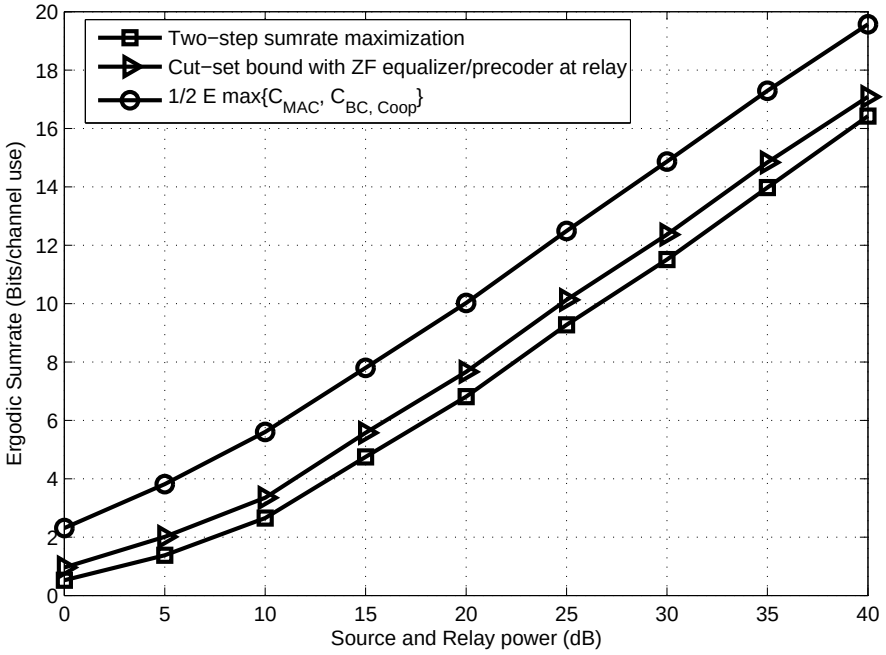


Figure 2.8: Sumrate comparison of the sumrate maximization approach and cut-set bound with relay and source power increasing at the same rate ($0 \sim 40$dB)

sumrate of ZFBF relay converges to the sumrate of the BC-hop or the MAC-hop, respectively. Similar curves can be obtained with fixed moderate source power and varying relay power.

The lower bound of the ergodic sumrate penalty caused by the CSI errors at the relay then is verified. For both channels of the MAC and Broadcast links, the CSI errors parameters are set to $\alpha = \beta = 0.045$ and $\alpha = \beta = 0.1$. The following cases are included: 1) the relay power is fixed and the sources power increases and 2) both the power of the sources and relay increase at the same time. Figs. 2.10, 2.11 show that the lower bound and the simulated sumrate loss are very close. The curves corresponding to the case of fixed sources power and increasing relay power will be similar to those in Fig.2.10. In Fig.2.12, we draw the sumrate curve under CSI errors when the relay and sources' power both increase. The sumrate floor observed in Fig.2.12 is consistent with the analysis in Section V which indicates that the fixed CSI errors makes the system interference-limited and the sumrate

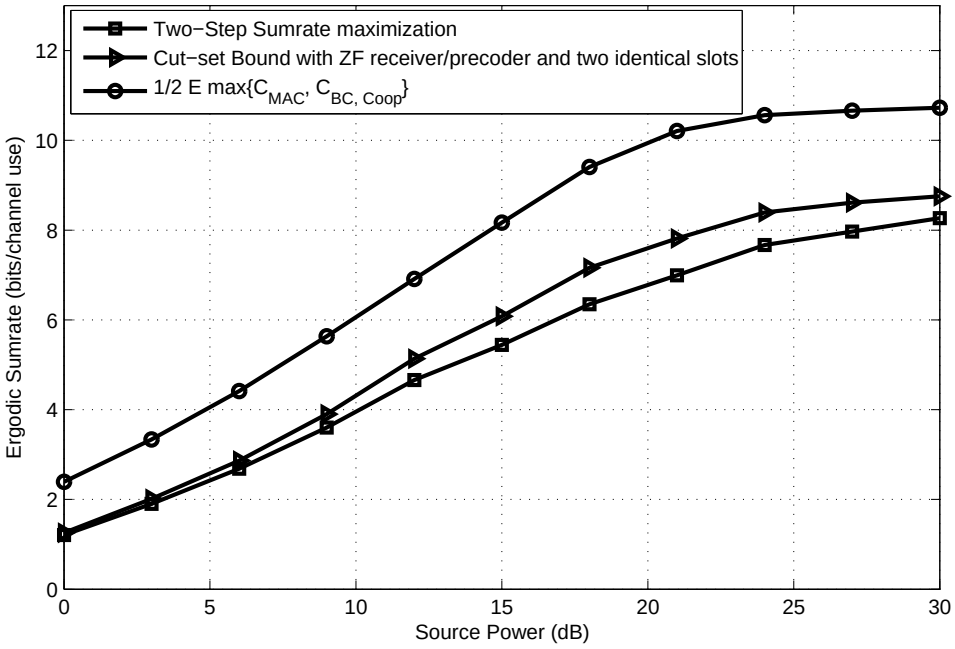


Figure 2.9: Sumrate comparison of the sumrate maximization approach and cut-set bound at moderate relay power (20dB) and varying source power ($0 \sim 30$dB)

does not benefit from power gain. We also draw the curves corresponding to decreasing CSI errors indicators $\alpha, \beta$ according to $\alpha\sqrt{P_T} = \beta\sqrt{P_0} = 0.045$ and $\alpha\sqrt{P_T} = \beta\sqrt{P_0} = 0.1$ for simulating a scenario in which the training power for channel estimation increases with the data transmission power. It can be seen that the ergodic sumrate under CSI errors has the same trend as that of the scheme with perfect CSI at the relay, with increasing relay and source power. This verifies the analysis in Section V.

## 2.6 Summary

In this Section, we investigate the AF relaying systems with multiple S-D pairs and a single relay with multiple antennas. We propose two designs of the ZFBF matrix of the relay for supporting simultaneous communications of all S-D pairs. The first one allocates the total relay power so that all data streams have the same

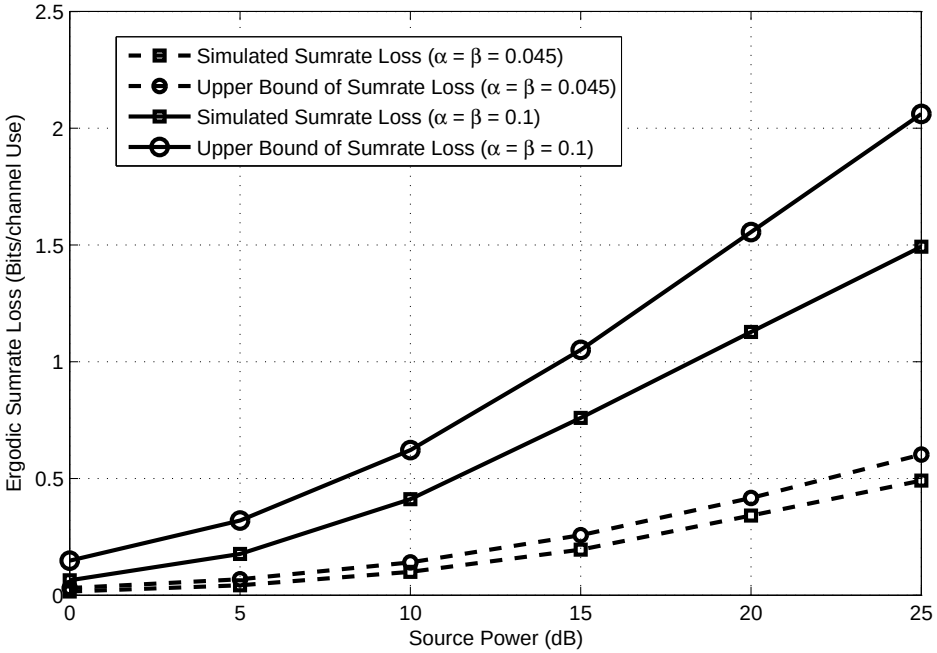


Figure 2.10: Comparison of proposed sumrate loss upper bound and simulated sumrate loss at fixed relay power (15dB) and varying source power ($0 \sim 25$dB)

power. The second one allocates the total relay power in a way that maximizes the sumrate of all S-D pairs. The sumrate maximization method has overall best sumrate while the equal power allocation method is simple yet shown to have good sumrate performance via simulations when S-D pairs have similar channel conditions. The proposed sumrate maximization approach is shown to achieve a multiplexing $\frac{M}{2}$ via comparison with the cut-set bound. The sumrate of the proposed equal power allocation approach is also investigated under relay CSI errors. An upper bound the ergodic sumrate loss caused by the CSI errors is derived, which shows that the power gain cannot be achieved under fixed relay CSI errors. However, it is shown that if the training power for the channel estimation increases as fast as data transmission power, the sumrate can benefit from the data transmission power.

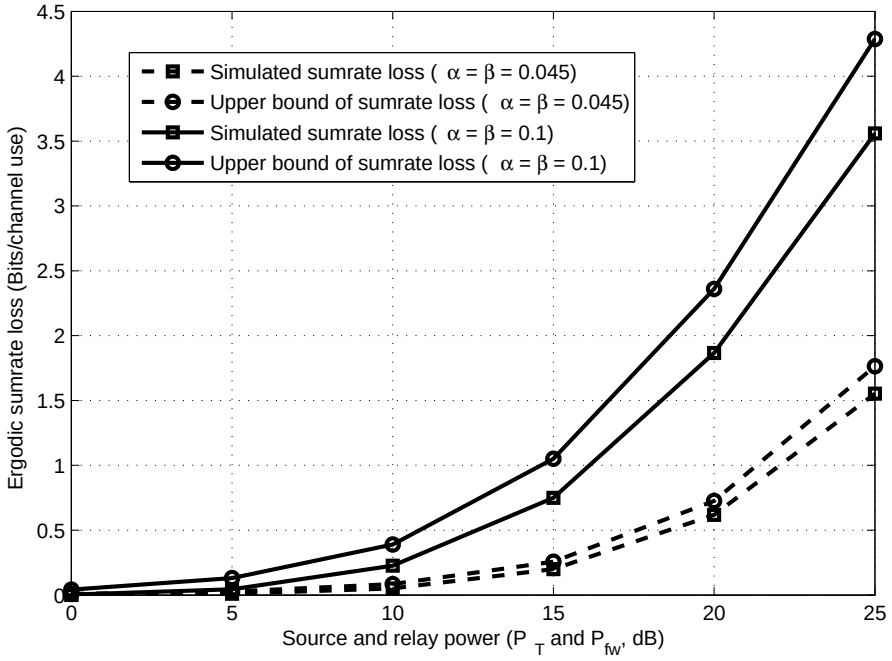


Figure 2.11: Comparison of proposed sumrate loss upper bound and simulated sumrate loss with relay and source power increasing at the same rate ($0 \sim 25$dB)

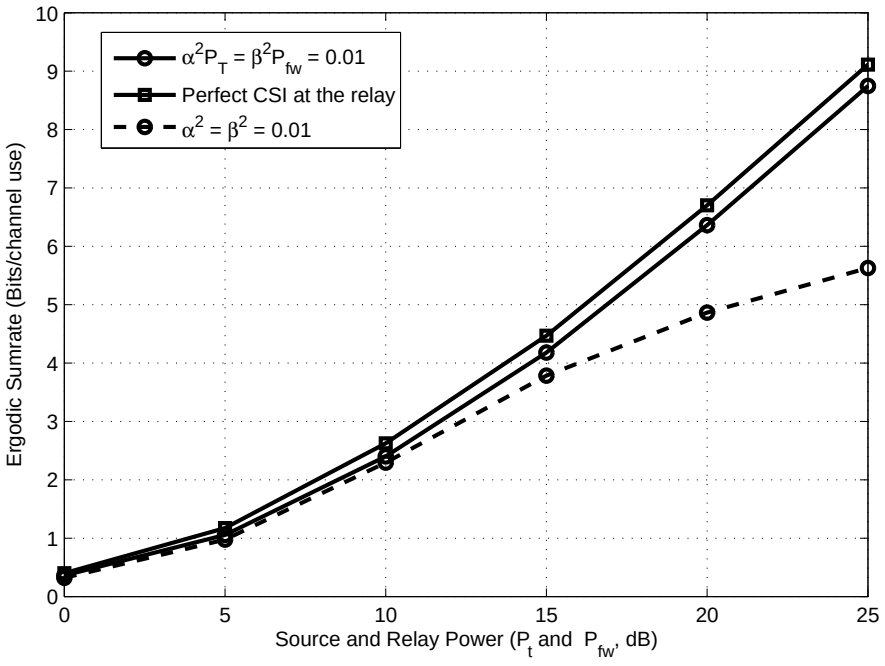


Figure 2.12: Sumrate comparison of three cases with relay and source power increasing at the same rate ($0 \sim 25$dB): a) imperfect relay CSI with fixed CSI accuracy, b) imperfect relay CSI with improving CSI accuracy, c) perfect relay CSI.

# Chapter 3

# QoS Guarantees in AF Relay Networks with Multiple Source-Destination Pairs in the Presence of Imperfect CSI

Wireless systems typically operate under limited resources, e.g. power and spectrum, thus, it is desirable to design relay systems that can support high data rate and meet the QoS requirements of the users while using as low power as possible. Such a QoS/power efficiency problem in MIMO relay systems has been investigated in the context of broadcast channels in [35]. In the context of communications between multiple source-destination (S-D) pairs, relay power minimization subject to the SINR requirement of each destination has been investigated in [60, 61]. For cases in which full CSI is available to the relay, [60] approaches the problem by using a generally structured beamforming (gBF) matrix at the relay. The case of imperfect CSI is addressed in [61] by incorporating the effect of CSI errors into the SINR expression of each source-destination (S-D) pair. Both [60] and [61] solve the underlying optimization problems numerically, which involves high complexity.

In this chapter, we investigate a system with multiple ($M$) S-D pairs and one AF relay with $K$ antennas ($K \geq M$). Each source has a distinct destination in each transmission period. The relay operates on a half duplex AF protocol; it hears the simultaneous transmission from all sources in the first slot, and broadcasts the linearly processed received data in the second slot. The relay is constrained to use a specially structured beamforming matrix, i.e., a Zeroforcing Beamforming (ZFBF) matrix [48, 49] so that each destination receives an

interference-free signal. The goal of this work is to design the ZFBF matrix so that the SINR requirements of each S-D pair are met and the transmit power at the relay is minimized. We show that, under perfect CSI at the relay, this problem can be solved by using a semi-definite relaxation approach. We also propose a suboptimal method, that is computationally very simple and achieves near optimal performance in terms of outage probability and minimal relay power.

Due to the size limitation, it is not always feasible for the relay to equip with multiple antennas. The simultaneous communications between the sources and destinations can be also supported by multiple distributed relays with single antenna. The beamforming matrix is a diagonal matrix as each relay can only forward an amplified version of the signal that it received. Such a proper designed diagonal beamforming matrix can also support communications between multiple sources and destinations given a large enough number of relays. It is shown that this QoS meeting problem can be solved by SDP with relaxation. A ZFBF based simplified design is also proposed to decrease the computational load.

We also study the case of single relay with multiple antennas with imperfect CSI at the relay. Imperfect CSI at the relay results in interference at the destinations. The interference lowers the destination SINR and increases the outage probability. We propose an adaptive beamforming weight design scheme to reduce the outage probability; the amplitude of the beamforming weight for each S-D pair is increased iteratively so that the worst case [62, 63, 64] SINR, i.e., the minimum possible SINR resulting due to the relay CSI errors, meets the SINR requirement at each destination. Assuming that the relay has access to multiple antennas, each one facing an independent channel, we propose an optimal or suboptimal antenna selection scheme, with the optimization criterion being the minimization of outage probability, or the minimization of the destination interference. In this way, the relay is able to activate the minimum number of antennas

required by the ZF conditions, i.e., $M$, in order to support low probability of outage, or low interference communications. Simulations show that the combination of adaptive weight design and antenna selection outperforms existing BF matrix design schemes.

*Relation to literature:* By enforcing the ZFBF structure to the BF matrix, the SINR requirements of destinations are decoupled, which allows for low-dimensional and low-complexity approaches for computing the BF matrix.

The complexity reduction is significant when compared to the methods of [60, 61] that use generally structured BF matrices. ZFBF also allows for low complexity antenna selection schemes in case of imperfect relay CSI. In general, using a suboptimal BF matrix may result in a performance penalty. However, simulation suggest that the proposed adaptive design based on ZFBF achieves very close outage performance as compared to gBF [61]. When both antenna selection and the proposed adaptive design are used, the resulting outage and power efficiency performances are superior to the gBF results.

The rest of this chapter is organized as follows. Section II provides the system model and the approach to solve the QoS guarantees problem under perfect relay CSI. Section III presents the relay antenna selection methods and the adaptive weight design method for combating the impact of imperfect CSI. Section IV presents simulation results, and Section V provides concluding remarks.

## 3.1 Relay beamforming with perfect CSI

## 3.2 System Model

A system with $M$ distinct source-destination pairs that need to communicate simultaneously is considered. The sources and destinations are assumed to well separated so that the direct links between them can be ignored. Each source or destination node has one antenna. The communications is facilitated by one

AF relay with $K$ antennas ($K \geq M$). Initially, we assume that the CSI of the source-relay and relay-destination links are perfectly known at the relay. The communications between the sources and destinations is divided into two slots. The first slot is for information sharing, in which the sources transmit the baseband signal $\mathbf{s} = [s_1, ..., s_M]^T$ intended for the destinations $\{1, ..., M\}$, using power $\{\sqrt{P_1}, ..., \sqrt{P_M}\}$. $s_i, i = 1, ..., M$, are i.i.d. $\mathcal{CN}(0, 1)$. In the second slot, the relay(s) use a beamforming matrix $\mathbf{W} \in \mathbb{C}^{K \times K}$ to linearly process the received signals $\mathbf{r}$, where $\mathbf{r} = \mathbf{F}\mathbf{\Lambda_s}\mathbf{s} + \mathbf{n}$, and subsequently broadcast $\mathbf{Wr}$ it to the destinations. Here $\mathbf{F} \in \mathbb{C}^{K \times M}$ denotes the channel between sources and relay, $\mathbf{\Lambda_s} = \mathtt{diag}\{\sqrt{P_1}, ..., \sqrt{P_M}\}$ is the source power matrix and $\mathbf{n} = [n_1, ..., n_K]^T$ represents additive noise, with $n_i \sim \mathcal{CN}(0, 1)$.

On denoting the relay-destination channel matrix by $\mathbf{G}$ from the relays to the destination, received signals at the destinations, put in a vector $\mathbf{y}$, can be expressed as:

$$\mathbf{y} = \mathbf{GWF\Lambda_s s} + \mathbf{GWn} + \mathbf{z} \tag{3.1}$$

where $\mathbf{z}$ represents noise at the destinations and $[\mathbf{z}]_i \sim \mathcal{CN}(0, 1)$.

Note that in case of distributed relays with single antennas, $\mathbf{W}$ is a diagonal matrix.

The sum transmit power at the relays is expressed as

$$P_T = \mathtt{Tr}(P_0 \mathbf{WFF}^{\mathcal{H}}\mathbf{W}^{\mathcal{H}}) + \mathtt{Tr}(\mathbf{WW}^{\mathcal{H}}) \tag{3.2}$$

where $\mathbb{E}$ and $(\cdot)^{\mathcal{H}}$ represents the operation of expectation and conjugation transpose.

The SINR at the destination $i$ equals

$$\mathtt{SINR}_i = \frac{P_0|\mathbf{g}_i^T\mathbf{W}\mathbf{f}_i|^2}{\sum_{j=1,...M}^{j\neq i} P_0|\mathbf{g}_i^T\mathbf{W}\mathbf{f}_j|^2 + ||\mathbf{g}_i^T\mathbf{W}||^2 + 1} \tag{3.3}$$

Our goal is to design $\mathbf{W}$ that meets a certain SINR at each destination, i.e., $\mathtt{SINR}_i \geq \gamma_i$, while minimizing the sum transmit power at the relays, i.e.,

$$\min_{\mathbf{W}\in\mathbb{C}^{K\times K}} P_T, \quad s.t. \ \mathtt{SINR}_i \geq \gamma_i \tag{3.4}$$

### 3.2.1 Single relay with multiple antennas

With a relay with multiple antennas, the beamforming matrix $\mathbf{W}$ can take arbitrary structure. The interference among the S-D pairs can be eliminated by using a beamforming matrix with the following structure [46]:

$$\mathbf{W} = \underbrace{\mathbf{G}^{\mathcal{H}}[\mathbf{G}\mathbf{G}^{\mathcal{H}}]^{-1}}_{\mathbf{W_G}} \mathbf{\Lambda}_R \underbrace{[\mathbf{F}^{\mathcal{H}}\mathbf{F}]^{-1}\mathbf{F}^{\mathcal{H}}}_{\mathbf{W_F}} \tag{3.5}$$

where $\mathbf{\Lambda}_R = \mathtt{diag}\{\rho_1, ..., \rho_M\}$, in which $\rho_i$ is a complex scalar. Eq.(3.5) requires that $\mathtt{rank}(\mathbf{F}) = M$ and $\mathtt{rank}(\mathbf{G}) = M$. By substituting (3.5) in (3.1), we obtain $\mathbf{y} = \mathbf{\Lambda}_R\mathbf{\Lambda}_s\mathbf{s} + \mathbf{\Lambda}_R\mathbf{W_F}\mathbf{n} + \mathbf{z}$. Note that a similar model was considered in our previous work [65] for the study of capacity. Let $\sigma^2_{\mathbf{f}_i} \triangleq ||[\mathbf{W_F}]_{i,:}||^2$, $\sigma^2_{\mathbf{g}_i} \triangleq ||[\mathbf{W_G}]_{:,i}||^2$; $\mathbf{\Gamma} = \sum_{i=1}^{K} \mathtt{diag}\{[\mathbf{W_F}]_{:,i}\}^{\mathcal{H}}\mathbf{W}_{\mathbf{G}}^{\mathcal{H}}\mathbf{W_G}\mathtt{diag}\{[\mathbf{W_F}]_{:,i}\}$. Then, the SINR at the ith destination and the relay transmit power are, respectively,

$$\mathtt{SINR}_i = \frac{P_i|\rho_i|^2}{|\rho_i|^2\sigma^2_{\mathbf{f}_i} + 1} \tag{3.6}$$

$$P_R = \sum_{i=1}^{M} \sigma^2_{\mathbf{g}_i} P_i|\rho_i|^2 + \mathbf{x}^{\mathcal{H}}\mathbf{\Gamma}\mathbf{x} \tag{3.7}$$

where $\mathbf{x} = [\rho_1, ..., \rho_M]^T$. The problem of interest is formulated as follows:

$$\min P_R \quad s.t.\ \mathtt{SINR}_i \geq \gamma_i,\ \ i = 1, ..., M \tag{3.8}$$

where $\gamma_i, i = 1, ..., M$ is the SINR requirement of the $i$th S-D pair.

Based on (3.6), the constraints of (3.8) are equivalent to $|[\mathbf{x}]_i|^2 \geq \gamma_i(P_i - \gamma_i|\sigma_{\mathbf{f}_i}|^2)^{-1},\ \ i = 1, ..., M$. By defining $\mathbf{Q} \triangleq \mathtt{diag}\{[\sigma^2_{\mathbf{g}_1} P_1, ..., \sigma^2_{\mathbf{g}_M} P_M]\} + \mathbf{\Gamma}$, we can write $P_R = \mathbf{x}^{\mathcal{H}}\mathbf{Q}\mathbf{x}$, and the problem of (3.8) becomes:

$$\min_{\mathbf{x} \in \mathbb{C}^{M \times 1}} \mathbf{x}^{\mathcal{H}}\mathbf{Q}\mathbf{x},\ \ s.t. |[\mathbf{x}]_i|^2 \geq \psi_i^2,\ \ i = 1, ..., M \tag{3.9}$$

where $\psi_i = \sqrt{\gamma_i(P_i - \gamma_i|\sigma_{\mathbf{f}_i}|^2)^{-1}}$.

For the problem of (3.9) to be feasible, it is required that $P_i > \gamma_i|\sigma_{\mathbf{f}_i}|^2$. However, the feasible set is non-convex if $[\mathbf{x}]_i$ takes complex values. To address this issue, we first transform (3.9) into the following equivalent formulation:

$$\begin{aligned} &\min_{\in \mathbb{C}^{M \times M}} Tr\{\mathbf{Q}\mathbf{X}\} \\ &s.t.\ \ Tr\{\Theta_i \mathbf{X}\} \geq \psi_i^2;\ \mathbf{X} \succ 0;\ rank\{\mathbf{X}\} = 1 \end{aligned} \tag{3.10}$$

which can be further converted into a convex problem using semi-definite relaxation by dropping the rank 1 condition [53, 66]. Then, the problem can be solved using semi-definite programming tools (e.g. Sedumi [52]) and randomization techniques [53].

**A suboptimal solution:** A suboptimal solution not involving numerical optimization for calculating the weight vector $\mathbf{x}$ can be obtained (see also [67]) as follows:

$$\mathbf{x}_{subopt} = \mathbf{\Psi} \tag{3.11}$$

where $[\mathbf{\Psi}]_i = \sqrt{\gamma_i(P_i - \gamma_i|\sigma_{\mathbf{f}_i}|^2)^{-1}}$. This suboptimal solution simply sets each weight to the smallest value that meets the QoS requirements. In the medium to high source transmit power region, the signal part, i.e., the first term of the RHS of (3.7), dominates the sum transmit power of the relay and the suboptimal solution, is expected to be near optimal in terms of minimizing the relay transmission power. This is confirmed via simulations in Section 3.3.5. This simple solution also reduces the computational complexity of the BF matrix design, as compared to (3.10), because no numerical optimization is involved. As we will later show via simulations, this suboptimal solution is comparable to the optimal solution of Eq.(3.10) in terms of power efficiency.

### 3.2.2 Distributed relays with single antenna

In the case that all relays are distributed so that the beamforming matrix $\mathbf{W}$ is diagonal.

#### Optimal Beamforming

Using this diagonal property, the sum transmit power in (3.2) at the relays is written as

$$P_T = \mathbf{w}^{\mathcal{H}}\mathbf{R}_T\mathbf{w} \tag{3.12}$$

where $\mathbf{w} = [[\mathbf{W}]_{11}, ..., [\mathbf{W}]_{KK}]^T$ with $[\mathbf{W}]_{pp}, p = 1, ..., K$ denotes the forwarding weight of relay $j$ in the second slot and $\mathbf{R}_T = \texttt{diag}\Big\{1 + P_0 \sum_{i=1,...,M} |f_{1i}|^2, ..., 1 + P_0 \sum_{i=1,...,M} |f_{Ki}|^2\Big\}$.

Denoting $\mathbf{a} \odot \mathbf{b}$ by the pointwise product of two matrices(vectors), we can

rewrite the SINR expressions (3.3) as

$$\mathtt{SINR}_i = \frac{P_0 \mathbf{w}^{\mathcal{H}} \mathbf{R}_{\mathbf{s}}^{(i)} \mathbf{w}}{P_0 \mathbf{w}^{\mathcal{H}} \mathbf{R}_{\mathbf{I}}^{(i)} \mathbf{w} + \mathbf{w}^{\mathcal{H}} \mathbf{R}_{\mathbf{n}}^{(i)} \mathbf{w} + 1} \tag{3.13}$$

where $\mathbf{R}_{\mathbf{s}}^{(i)} = (\mathbf{g}_i^T \odot \mathbf{f}_i^T)^{\mathcal{H}} (\mathbf{g}_i^T \odot \mathbf{f}_i^T)$, $\mathbf{R}_{\mathbf{I}}^{(i)} = \sum_{j=1,...M}^{j \neq i} (\mathbf{g}_j^T \odot \mathbf{f}_i^T)^{\mathcal{H}} (\mathbf{g}_j^T \odot \mathbf{f}_i^T)$ and $\mathbf{R}_{\mathbf{n}}^{(i)} = \mathtt{diag}\{|[\mathbf{G}]_{1i}|^2, ..., |[\mathbf{G}]_{Mi}|^2\}$. Note that $\mathbf{G} = [\mathbf{g}_1, ..., \mathbf{g}_M]^T$ with $\mathbf{g}_i = [g_{1i}, ..., g_{Ki}]^T$. Under these conditions, the problem of meeting QoS constraints with minimal relay transmit power is rewritten as

$$\min_{\mathbf{w}} \mathbf{w}^{\mathcal{H}} \mathbf{R}_T \mathbf{w}, \quad s.t. \quad \mathbf{w}^{\mathcal{H}} \mathbf{Q}^{(i)} \mathbf{w} \geq 1, i = 1, ..., M \tag{3.14}$$

where $\mathbf{Q}^{(i)} = \gamma_i^{-1} [P_0 \mathbf{R}_{\mathbf{s}}^{(i)} - \gamma_i P_0 \mathbf{R}_{\mathbf{I}}^{(i)} - \gamma_i \mathbf{R}_{\mathbf{n}}^{(i)}]$.

Let $\mathbf{X} \triangleq \mathbf{w}\mathbf{w}^{\mathcal{H}}$. The above optimization problem is equivalent to:

$$\begin{aligned} &\min_{\mathbf{X}} \mathtt{Tr}(\mathbf{X}\mathbf{R}_T) \\ s.t.\ &\mathtt{Tr}(\mathbf{X}\mathbf{Q}^{(i)}) \geq 1, i = 1, ..., M; \mathbf{X} \succeq 0; \mathtt{rank}(\mathbf{X}) = 1 \end{aligned}$$

Here $\mathbf{X} \succeq 0$ means that $\mathbf{X}$ is semi-positive definite. The feasible set of the above problem is not convex because the rank constraint. Therefore, we switch to consider a relaxed problem by dropping the rank constraint [53, 66]:

$$\begin{aligned} &\min_{\mathbf{X}} \mathtt{Tr}(\mathbf{X}\mathbf{R}_T) \\ s.t.\ &\mathtt{Tr}(\mathbf{X}\mathbf{Q}^{(i)}) \geq 1, i = 1, ..., M, \ \ \mathbf{X} \succeq 0 \end{aligned} \tag{3.15}$$

which can be solved by SDP tools like SeDuMi [52]. If the rank of the solution $\mathbf{X}^*$ of the above problem is not equal to one, some randomization algorithms can be used to obtain a suboptimal rank one solution (see [53] and references therein).

**Zero-forcing Beamforming with distributed relays**

When the number of relays ($K$) is large, we have to process the optimization over a long vector $\mathbf{w} \in \mathbb{C}^{K\times 1}$ which yields high complexity. Next we apply the ZF concept into the beamforming matrix design to completely cancel IDI. The ZF operation also projects the beamforming vector to a low dimensional subspace so that the number of variables for optimization is smaller, thus lowering complexity.

To completely cancel the interference at each destination, the weight vector needs to satisfy [37, 68]

$$(\mathbf{g}_j^T \odot \mathbf{f}_i^T)\mathbf{w} = 0, i, j = 1, ..., M, i \neq j \tag{3.16}$$

Note that $K > M(M-1)$ is needed to guarantee non-zero solution. Denoting $\mathbf{C_{fg}} = [\mathbf{e}_1, ..., \mathbf{e}_M]^T$ with $\mathbf{e}_i = [\mathbf{f}_i \odot \mathbf{g}_1, ..., \mathbf{f}_i \odot \mathbf{g}_{i-1}, \mathbf{f}_i \odot \mathbf{g}_{i+1}, ..., \mathbf{f}_i \odot \mathbf{g}_M]$, the SVD of $\mathbf{C_{fg}}$ is expressed as

$$\mathbf{C_{fg}} = \mathbf{U}\Sigma\mathbf{V}^{\mathcal{H}} \tag{3.17}$$

where $\mathbf{V} = [\mathbf{V}_s, \mathbf{V}_{null}]$, in which $\mathbf{V}_s \in \mathbb{C}^{K\times M(M-1)}$ and $\mathbf{V}_{null} \in \mathbb{C}^{K\times(K-M(M-1))}$. To satisfy (3.16), it is sufficient and necessary for $\mathbf{w}$ to have the following structure:

$$\mathbf{w} = \mathbf{V}_{null}\tilde{\mathbf{w}} \tag{3.18}$$

where $\tilde{\mathbf{w}} \in \mathbb{C}^{K-M(M-1)\times 1}$. Substituting (3.16) and (3.18) into (3.14), the transmit power minimization problem under ZF conditions in the distributed relay case is formulated as

$$\min_{\tilde{\mathbf{w}}} \tilde{\mathbf{w}}^{\mathcal{H}}\tilde{\mathbf{R}}_T\tilde{\mathbf{w}}, \;\; s.t. \;\; \tilde{\mathbf{w}}^{\mathcal{H}}\tilde{\mathbf{Q}}^{(i)}\tilde{\mathbf{w}} \geq 1, i = 1, ..., M \tag{3.19}$$

where $\tilde{\mathbf{Q}}^{(i)} = \gamma_i^{-1}\mathbf{V}_{null}^{\mathcal{H}}[P_0\mathbf{R}_{\mathbf{s}}^{(i)} - \gamma_i\mathbf{R}_{\mathbf{n}}^{(i)}]\mathbf{V}_{null}$ and $\tilde{\mathbf{R}}_T = \mathbf{V}_{null}^{\mathcal{H}}\mathbf{R}_T\mathbf{V}_{null}$. This problem can also be solved by SDP with relaxation similarly as in the optimal beamforming case.

### 3.2.3 Simulation Results

A three-source three-destination system is considered. The channel coefficients of source-relay-antenna pairs or relay-antenna-destination pair are i.i.d. zero mean complex Gaussian random variables with unit variance. Three schemes are evaluated in the simulations: the ZFBF with single multi-antenna relay, as given in (3.10), the optimal beamforming with distributed relays as given in (3.14), and ZFBF with distributed relays as in (3.19). Both outage probability and transmit power are tested. An outage for the $i$th S-D pair occurs in the following situations: 1) no matter how large $|\rho_i|^2$ the relay uses, the SINR requirement at that link cannot be fulfilled, i.e., $P_i \leq \gamma_i|\sigma_{\mathbf{f}_i}|^2$, and 2) the relay's required transmit power exceeds 35dB. Each point in a figure is based on average over $5,000$ channel realizations.

Fig.3.1 shows the outage probability of the three cases. Outage occurs when the relay(s) fail to meet the SINR requirement of at least one destination, no matter how large power the relays consume. With larger source power $P_0$, the outage probabilities decrease in all cases, while the ZFBF approach with a single multi-antenna relay outperforms the other two approaches. With increasing source power the gaps among the three outage probabilities decrease.

Fig.3.2 demonstrates the average relay power needed to meet the SINR requirement of each destination over all their non-outage transmission periods. However, if one scheme's outage probability in simulation exceeds 10%, the power consumed at relays will be set to $+\infty$ which indicates that the source-relay-destination link cannot support reliable communications. Again, the ZFBF in the single multi-antenna relay case yields the smallest required transmit power at the

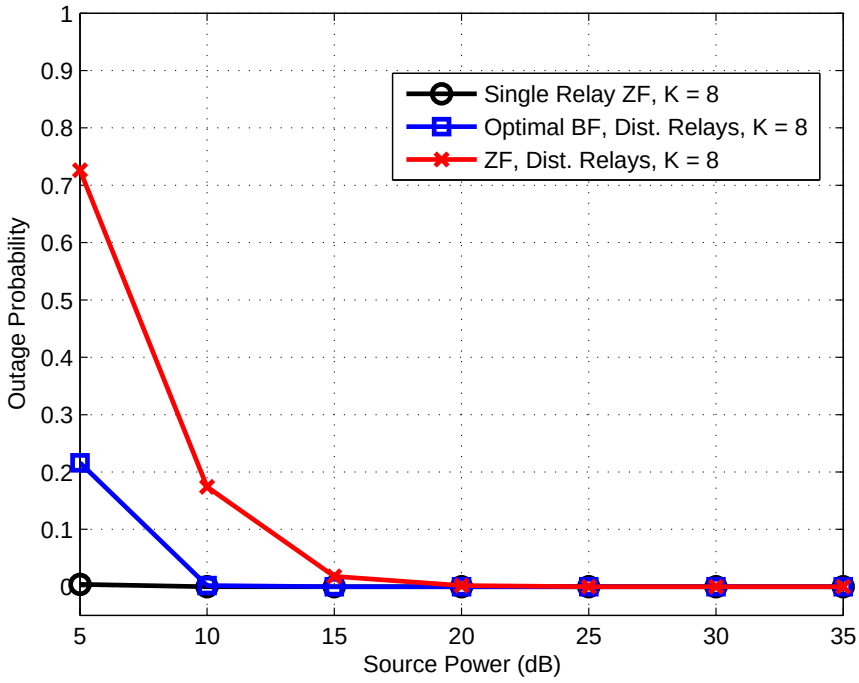


Figure 3.1: Outage probability comparison of single relay BF and distributed relay BF at different source transmit Power, Target SINR = 5dB, Perfect CSI

relays. Also, the performance differences among the three methods are smaller with higher source power.

The effect of the relay number on the optimal transmit power at the relays is shown in Fig.3.3. With $K < M(M-1)+1 = 7$, the ZFBF in distributed relay case does not work because the ZF conditions cannot be satisfied. With more relays, all three schemes need less power to satisfy the SINR requirements at the destinations. With fewer relay antennas, the ZFBF in the distributed relay case lacks enough dimensions to process the optimization ($\mathbf{w} \in \mathbb{C}^{K-M(M-1)\times 1}$), and that causes the required sum transmit power at the relays to be very high. With more relays, the minimized required power in the ZF scheme is very close to that of the optimal beamforming with distributed relays. One can also see that in Fig.3.3, the sum transmit power of relays is all under $25dB$ for providing at least $10dB$ SINR at the destinations. This affordable power consumption shows the ability of the multiuser relaying system to support parallel data streams.

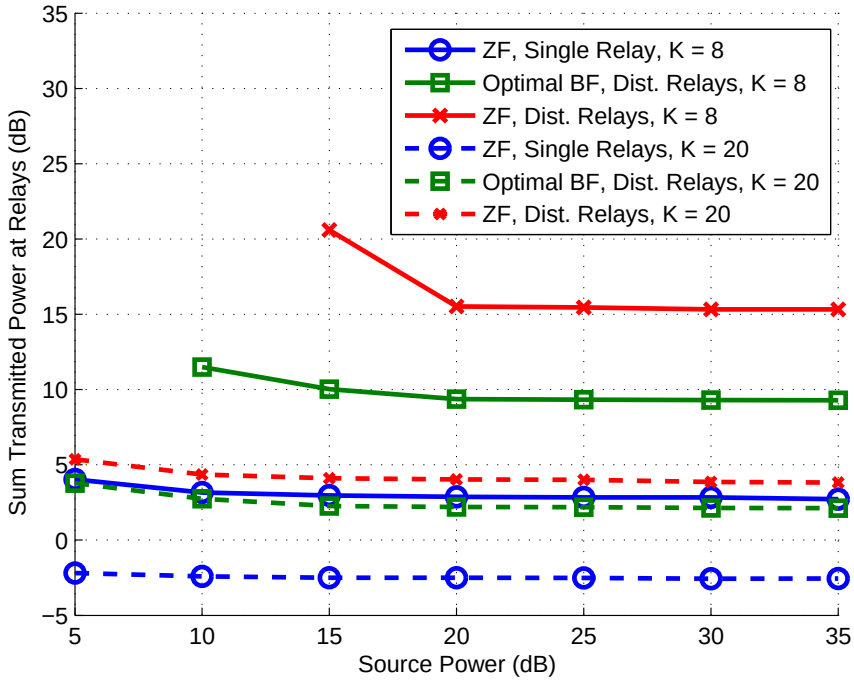


Figure 3.2: Relay transmit power comparison of single relay BF and distributed relay BF at different source transmit Power, Target SINR = 5dB, Perfect CSI

Based on the simulations, the ZFBF in the single multi-antenna relay case has the best power efficiency and outage performance. Also the optimal beamforming matrix computation is very simple at high source power region. However, this method is invalid in the system with distributed relays. The ZFBF in the case of distributed relays gains closed performance compare to that in optimal beamforming with distributed relays when the number of relays is large. What is good is that the ZFBF also reduces the complexity of the SDP optimization by lowering the dimension of the subspace of $\mathbf{w}$. Therefore, ZFBF is good for a system with a large number of distributed relays. If the number of relays is small and the relays are distributed, the optimal beamforming as (3.14) should be used. It is noted that accurate synchronization of transmission timing among distributed relays and perfect CSI at the relay nodes are required in the proposed schemes. The impact of such errors on multi-source multi-destination relaying networks will be considered in future work.

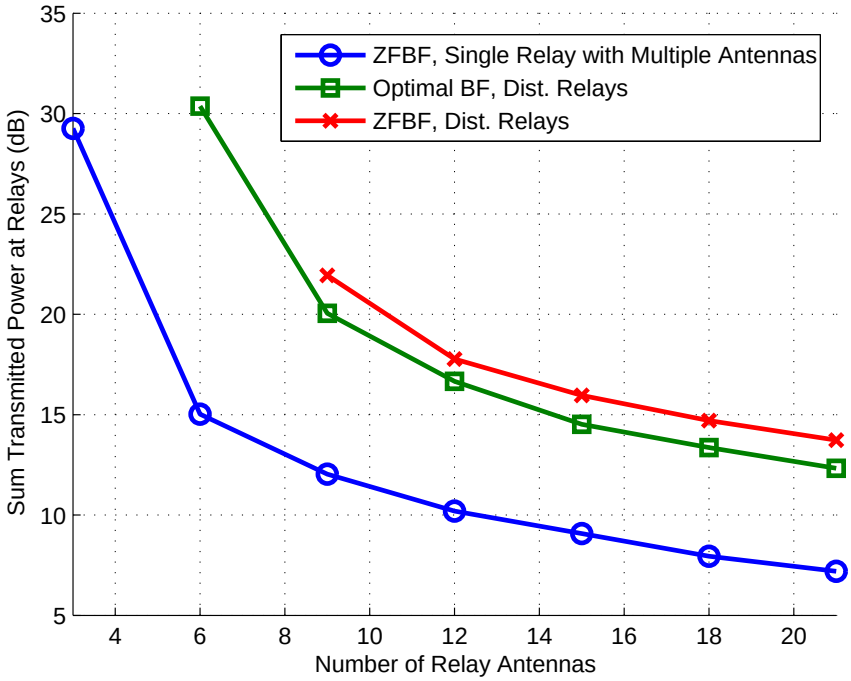


Figure 3.3: Relay transmit power comparison of single relay BF and distributed relay BF at different numbers of relay antennas, Target SINR = 5dB, Perfect CSI

Then the proposed ZFBF design in case of single relay with multiple antennas is compared with the methods in literature. The optimal method, based on (3.10) and the simplified one based on (3.11), are tested. Both methods are compared to the method proposed in [60], which does not employ zero-forcing but rather optimizes the BF matrix numerically over generally structured matrices. We refer to the optimization over general BF matrices in [60] as *gBF under perfect CSI*. The outage probability and relay transmit power performance are shown in Figs.3.4 and 3.5, respectively. Compared to gBF under perfect CSI, the proposed methods have comparable outage probability performance. In the low destination SINR range, the proposed methods consume more power, while in the medium SINR range (larger than 5dB), the proposed methods have very similar power requirements as the gBF with perfect CSI.

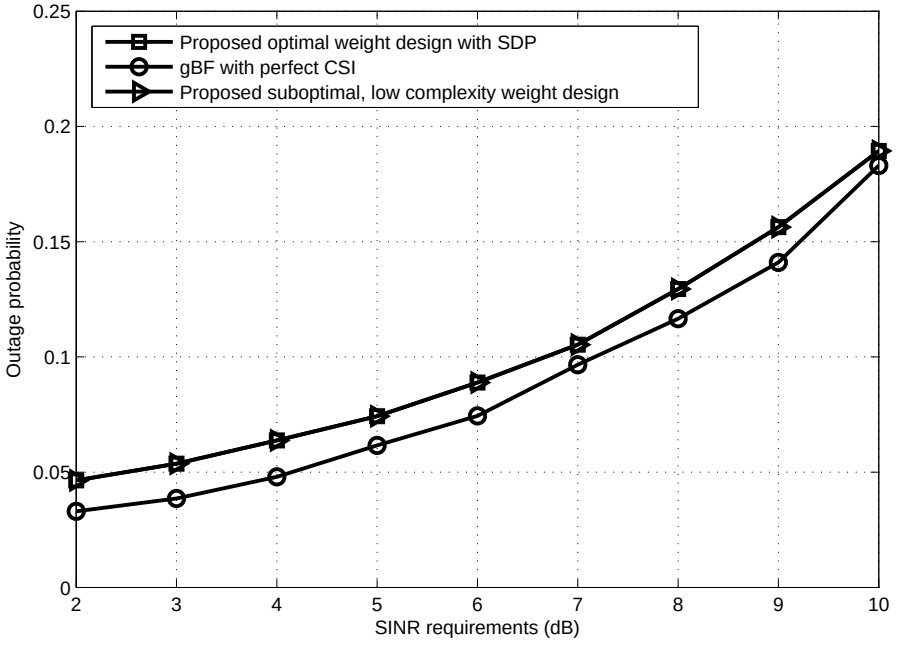


Figure 3.4: Outage probability comparison of 1) optimal ZFBF 2) suboptimal ZFBF and 3) optimal gBF in single relay ZF at different targeted SINRs, source transmit power = 20dB, perfect CSI

## 3.3 Meeting QoS constraints with imperfect CSI and single relay

In a realistic scenario, the relay always obtains the CSI with errors, e.g., through channel estimation and limited rate feedback. These CSI errors introduce inter-S-D-pair interference, which reduces the SINR at the destinations and increases the outage probability. If the above described method were to be used in such realistic scenario, the performance would degrade. In this section we propose two methods to mitigate the negative effects of imperfect CSI.

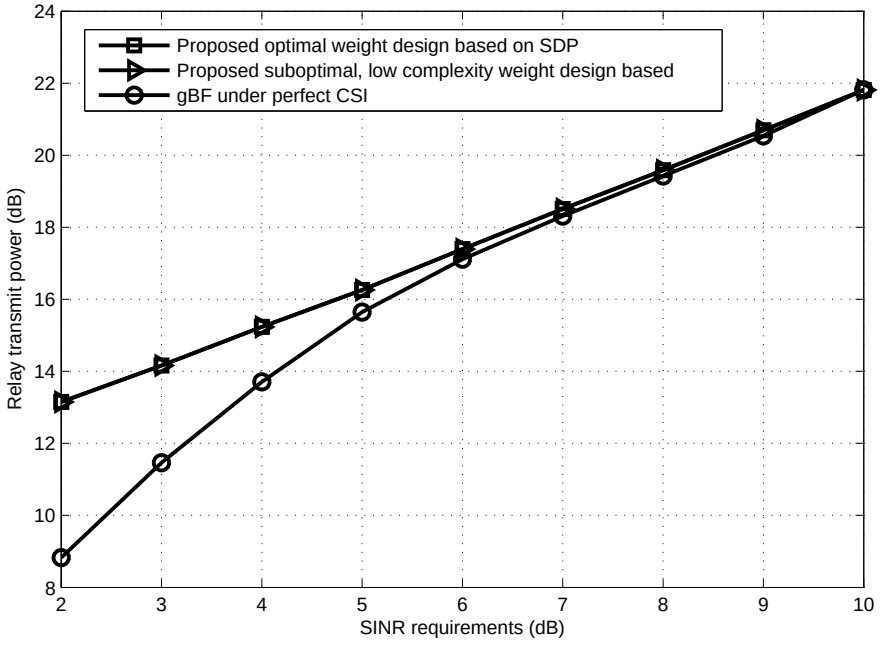


Figure 3.5: Relay transmit power comparison of 1) optimal ZFBF 2) suboptimal ZFBF and 3) optimal gBF in single relay ZF at different targeted SINRs, source transmit power = 20dB, perfect CSI

### 3.3.1 Models of CSI errors and destination signal

Let us model the relation of the true channels $\mathbf{F}$, $\mathbf{G}$ and their estimates $\hat{\mathbf{F}}$, $\hat{\mathbf{G}}$ observed at the relay, as follows [69, 70, 58]:

$$\mathbf{F} = \hat{\mathbf{F}} + \mathbf{E_F}; \quad \mathbf{G} = \hat{\mathbf{G}} + \mathbf{E_G}. \tag{3.20}$$

where the CSI error matrices, $\mathbf{E_F}$ and $\mathbf{E_G}$, are statistically uncorrelated with $\hat{\mathbf{F}}$ and $\hat{\mathbf{G}}$, and have elements which are i.i.d., $\mathcal{CN}(0, \alpha^2)$ and $\mathcal{CN}(0, \beta^2)$ respectively. Thus, the elements of $\hat{\mathbf{F}}$ and $\hat{\mathbf{G}}$ follow i.i.d. $\mathcal{CN}(0, 1-\alpha^2)$ and $\mathcal{CN}(0, 1-\beta^2)$, respectively. The accuracy of the estimates is reflected by the parameters $0 < \alpha,\ \beta < 1$, i.e., larger $\alpha$ and $\beta$ mean a less accurate CSI estimate. We assume that $\alpha,\ \beta << 1$.

The relay calculates the ZFBF matrix as $\hat{\mathbf{W}} = \hat{\mathbf{W}}_{\mathbf{G}} \mathbf{\Lambda}_R \hat{\mathbf{W}}_{\mathbf{F}}$, where $\hat{\mathbf{W}}_{\mathbf{G}} =$

$\hat{\mathbf{G}}^{\mathcal{H}}[\hat{\mathbf{G}}\hat{\mathbf{G}}^{\mathcal{H}}]^{-1}$, $\hat{\mathbf{W}}_{\mathbf{F}} = [\hat{\mathbf{F}}^{\mathcal{H}}\hat{\mathbf{F}}]^{-1}\hat{\mathbf{F}}^{\mathcal{H}}$. The design of $\mathbf{\Lambda}_R$ will be discussed in Sec.3.3.3.

The received signal at the $i$th destination, considering the multiple user interference caused by the CSI errors, is written as

$$y_i = \underbrace{[\mathbf{G}]_{i,:}\hat{\mathbf{W}}_{\mathbf{G}}\mathbf{\Lambda}_R\hat{\mathbf{W}}_{\mathbf{F}}[\mathbf{F}]_{:,i}s_i}_{r_i^{(i)}} + \sum_{j\neq i}\underbrace{[\mathbf{E}_{\mathbf{G}}]_{i,:}\hat{\mathbf{W}}_{\mathbf{G}}\mathbf{\Lambda}_R\hat{\mathbf{W}}_{\mathbf{F}}\hat{\mathbf{F}}_{:,j}s_j + \hat{\mathbf{G}}_{i,:}^T\hat{\mathbf{W}}_{\mathbf{G}}\mathbf{\Lambda}_R\hat{\mathbf{W}}_{\mathbf{F}}[\mathbf{E}_{\mathbf{F}}]_{:,j}s_j}_{r_i^{(j)}}$$
$$+ \underbrace{([\mathbf{E}_{\mathbf{G}}]_{i,:} + \hat{\mathbf{G}}_{i,:})\mathbf{W}\mathbf{n}}_{\hat{n}_i^{fw}} + \mathbf{z}. \tag{3.21}$$

where $r_i^{(i)}$ denotes the contribution of the $i$th source, $r_i^{(j)}$ represents the interference from the $j$th source, and $\hat{n}_i^{fw}$ denotes the forwarded noise.

### 3.3.2 The relation of destination interference and number of relay antennas

The inter-destination interference, resulting from the CSI error increasess the probability of outage. Next, we show that a larger number of relay antennas results in less interferences at the destinations. It is assumed that the channel coefficients of $\mathbf{F}$ and $\mathbf{G}$ are i.i.d., $\mathcal{CN}(0,1)$.

The average interference at the $i$th destination from $j$th source equals

$$\mathbb{E}|r_i^j|^2 = \mathbb{E}|\beta[\mathbf{E}_{\mathbf{G}}]_{i,:}\hat{\mathbf{W}}_{\mathbf{G}}\Lambda_R\hat{\mathbf{W}}_{\mathbf{F}}[\hat{\mathbf{F}}]_{:,j}s_j + \alpha[\hat{\mathbf{G}}^T]_{i,:}\hat{\mathbf{W}}_{\mathbf{G}}\Lambda_R\hat{\mathbf{W}}_{\mathbf{F}}[\mathbf{E}_{\mathbf{F}}]_{:,j}s_j|^2 \tag{3.22}$$
$$= \beta^2\rho_j^2P_j|[\mathbf{E}_{\mathbf{G}}]_{i,:}[\hat{\mathbf{W}}_{\mathbf{G}}]_{:,j}|^2 + \alpha^2\rho_i^2P_j|[\hat{\mathbf{W}}_{\mathbf{F}}]_{i,:}[\mathbf{E}_{\mathbf{F}}]_{:,j}|^2 \tag{3.23}$$
$$= \beta^2\rho_j^2P_j\hat{\sigma}_{\mathbf{g}_j}^2 + \alpha^2\rho_i^2P_j\hat{\sigma}_{\mathbf{f}_i}^2 \tag{3.24}$$
$$= \beta^2\frac{\gamma_j}{P_j - \gamma_j\hat{\sigma}_{\mathbf{f}_j}^2}P_j\hat{\sigma}_{\mathbf{g}_j}^2 + \alpha^2\frac{\gamma_i}{P_i - \gamma_i\hat{\sigma}_{\mathbf{f}_i}^2}P_j\hat{\sigma}_{\mathbf{f}_i}^2 \tag{3.25}$$

where $\hat{\sigma}_{\mathbf{f}_i}^2 \triangleq ||[\hat{\mathbf{W}}_{\mathbf{F}}]_{i,:}||^2$, $\hat{\sigma}_{\mathbf{g}_i}^2 \triangleq ||[\hat{\mathbf{W}}_{\mathbf{G}}]_{:,i}||^2$ capture the effective channel gains of the $i$th source to the relay and the relay to the $i$th destination, respectively. Note that the elements of the channel matrices $\hat{\mathbf{F}}$ and $\hat{\mathbf{G}}$ are i.i.d. complex Gaussian

random variables, with variance of real and imaginary parts, respectively, $\frac{1}{2}-\frac{1}{2}\alpha^2$ and $\frac{1}{2}-\frac{1}{2}\beta^2$. Thus, it holds that $(\hat{\sigma}^2_{\mathbf{g}_j})^{-1} \sim \chi^2(2(K-M+1), \frac{1}{2}-\frac{1}{2}\beta^2)$ and $(\hat{\sigma}^2_{\mathbf{f}_i})^{-1} \sim \chi^2(2(K-M+1), \frac{1}{2}-\frac{1}{2}\alpha^2)$. By increasing the number of antennas, $\hat{\sigma}^2_{\mathbf{f}_i}$ and $\hat{\sigma}^2_{\mathbf{g}_j}$ decrease so that the average interference at each destination decreases. Correspondingly, the outage probability performance improves. It can be argued that the useful signal power at each destination decreases when the channel gains of S-D pairs increases, because then the $|\rho_i|$s also decrease. The interference strength, however, decreases much faster (proportionally to $\rho_i^2\sigma^2_{\mathbf{f}_i}$ and $\rho_i^2\sigma^2_{\mathbf{g}_i}$) than the useful signal power (decreases proportionally to $\rho_i^2$).

### 3.3.3 Combating CSI errors via adaptive relay weight design

In this section, we propose to adjust $\rho_1, ..., \rho_M$, the diagonal elements of $\mathbf{\Lambda}_R$, to combat the negative effects of imperfect relay CSI. The idea is can be outlined as follows: 1) Using the statistics of the CSI errors, the relay determines the worst possible SINR of all S-D pairs corresponding to fixed set $\{\rho_i, i = 1, .., M\}$. 2) The relay increases each S-D pair's weight amplitude, $|\rho_i|$, to make the worst case SINR larger than the required threshold. 3) The increased $\|\rho_i|$ decreases the SINR of all the other $j = 1, ..., M, \neq i$ destinations. Thus the weight adjustment process has to be done iteratively until convergence, or until a maximum number of iterations is reached. The convergence is guaranteed when the worst case SINR constraints are feasible. The advantage of this method is that in each iteration the minimal required weights, $\rho_i, i = 1, ..., M$, can be directly computed. Note that each source is assumed to have the same transmit power $P_T$ for simplicity.

Based on (3.21), `SINR` at the $i$th destination can be expressed as

$$\texttt{SINR}_i = \frac{\mathbb{E}_{s_i}|r_i^{(i)}|^2}{\mathbb{E}_{s_j, j\neq i}|\sum_{j=1,...,M}^{j\neq i} r_i^{(j)}|^2 + \mathbb{E}_{\mathbf{n}}|\hat{n}_i^{fw}|^2 + 1}. \tag{3.26}$$

At the initial stage, the relay decides what levels of CSI errors it can accommodate based on two control parameters, $\mu_1, \mu_2$, as

$$|[\mathbf{E_F}]_{i,j}| \leq \mu_1; \quad |[\mathbf{E_G}]_{i,j}| \leq \mu_2 \tag{3.27}$$

The relay can then evaluate a lower bound of the SINR, which is here referred to as the worst case $\mathtt{SINR}_i^{wc}$, i.e.,:

$$\mathtt{SINR}_i^{wc} \triangleq \frac{\min\limits_{[\mathbf{E_F}]_{i,j}\leq\mu_1,[\mathbf{E_G}]_{i,j}\leq\mu_2} \mathbb{E}_{s_i}|r_i^{(i)}|^2}{\max\limits_{[\mathbf{E_F}]_{i,j}\leq\mu_1,[\mathbf{E_G}]_{i,j}\leq\mu_2} \mathbb{E}_{s_j,j\neq i}|\sum_{j=1,\ldots,M}^{j\neq i} r_i^{(j)}|^2 + \max\limits_{[\mathbf{E_F}]_{i,j}\leq\mu_1,[\mathbf{E_G}]_{i,j}\leq\mu_2} \mathbb{E}_{\mathbf{n}}|\hat{n}_i^{fw}|^2 + 1}. \tag{3.28}$$

Next, we compute the quantities $\min \mathbb{E}_{s_i}|r_i^{(i)}|^2$, $\max \mathbb{E}_{s_j,j\neq i}|\sum_{j=1,\ldots,M}^{j\neq i} r_i^{(j)}|^2$ and $\max \mathbb{E}_{\mathbf{n}}|\hat{n}_i^{fw}|^2$.

By ignoring the second order power of $\alpha$ and $\beta$, $r_i^{(i)}$ can be approximated as:

$$r_i^{(i)} \approx [\hat{\mathbf{G}}]_{i,:}\mathbf{W_G}\mathbf{\Lambda}_R\mathbf{W_F}[\hat{\mathbf{F}}]_{:,i}s_i + [\hat{\mathbf{G}}]_{i,:}\mathbf{W_G}\mathbf{\Lambda}_R\mathbf{W_F}[\mathbf{E_F}]_{:,i}s_i + [\mathbf{E_G}]_{i,:}\mathbf{W_G}\mathbf{\Lambda}_R\mathbf{W_F}[\hat{\mathbf{F}}]_{:,i}s_i \tag{3.29}$$

$$= (1 + [\mathbf{W_F}]_{i,:}[\mathbf{E_F}]_{:,i} + [\mathbf{E_G}]_{i,:}[\mathbf{W_G}]_{:,i})\rho_i s_i. \tag{3.30}$$

It holds that,

$$\min \mathbb{E}_{s_i}|r_i^{(i)}|^2 \geq (1 - \hat{\sigma}_{\mathbf{g}_i}\mu_2 - \hat{\sigma}_{\mathbf{f}_i}\mu_1)^2|\rho_i|^2 P_T \tag{3.31}$$

The minimal of (3.30) is achieved when $[\mathbf{E_F}]_{k,i} = -\mu_1\frac{[\hat{\mathbf{W}}_\mathbf{F}]^*_{i,:}}{|[\hat{\mathbf{W}}_\mathbf{F}]_{i,:}|}$ and $[\mathbf{E_G}]_{i,k} =$

$-\mu_2 \frac{[\hat{\mathbf{W}}_{\mathbf{G}}]^*_{k,i}}{|[\hat{\mathbf{W}}_{\mathbf{G}}]_{k,i}|}$. Via similar arguments, we obtain

$$\max \mathbb{E}_{s_j, j\neq i} |\sum_{j=1,\ldots,M}^{j\neq i} r_i^{(j)}|^2 \leq \sum_{j=1,\ldots,M}^{j\neq i} (|\rho_j|\mu_1 \hat{\sigma}_{\mathbf{g}_j} + |\rho_i|\alpha\mu_2 \hat{\sigma}_{\mathbf{f}_i})^2 P_T, \tag{3.32}$$

$$\max \mathbb{E}_{\mathbf{n}} |\hat{n}_i^{fw}|^2 \leq (|\rho_i|(\hat{\sigma}_{\mathbf{f}_i} + \mu_2 \hat{\sigma}_{\mathbf{g}_i}\hat{\sigma}_{\mathbf{f}_i}) + \mu_2 \sum_{j=1,\ldots,M}^{j\neq i} \hat{\sigma}_{\mathbf{g}_j}\hat{\sigma}_{\mathbf{f}_j}|\rho_j|)^2. \tag{3.33}$$

Applying (3.31), (3.32) and (3.33) into (3.28), we obtain

$$\mathtt{SINR}_i^{wc} \triangleq \frac{a_i|\rho_i|^2}{b_{i,1}|\rho_i|^2 + b_{i,2}|\rho_i| + b_{i,3}} \tag{3.34}$$

where

$$a_i = (1 - \hat{\sigma}_{\mathbf{g}_i}\mu_2 - \hat{\sigma}_{\mathbf{f}_i}\mu_1)^2 P_T \tag{3.35}$$

$$b_{i,1} = (M-1)\alpha^2\mu_2^2\hat{\sigma}_{\mathbf{f}_i}^2 P_T + (\hat{\sigma}_{\mathbf{f}_i} + \mu_2\hat{\sigma}_{\mathbf{g}_i}\hat{\sigma}_{\mathbf{f}_i})^2 \tag{3.36}$$

$$b_{i,2} = 2\mu_2(\mu_1\hat{\sigma}_{\mathbf{f}_i}P_T + \hat{\sigma}_{\mathbf{f}_i} + \mu_2\hat{\sigma}_{\mathbf{g}_i}\hat{\sigma}_{\mathbf{f}_i}) \sum_{j=1,\ldots,M}^{j\neq i} \hat{\sigma}_{\mathbf{g}_j}\hat{\sigma}_{\mathbf{f}_j}|\rho_j| \tag{3.37}$$

$$b_{i,3} = \sum_{j=1,\ldots,M}^{j\neq i} |\rho_j|^2\beta^2\mu_1^2\hat{\sigma}_{\mathbf{g}_j}^2 + \beta^2\mu_2^2 \left( \sum_{j=1,\ldots,M}^{j\neq i} \hat{\sigma}_{\mathbf{g}_j}\hat{\sigma}_{\mathbf{f}_j}|\rho_j| \right)^2 \tag{3.38}$$

The relay transmission power with CSI errors is written as

$$\begin{aligned} P_R^e &= \mathbb{E}_{\mathbf{E_F}} P_T \mathtt{Tr}\left(\hat{\mathbf{W}}(\hat{\mathbf{F}} + \mathbf{E_F})(\hat{\mathbf{F}} + \mathbf{E_F})^{\mathcal{H}}\hat{\mathbf{W}}^{\mathcal{H}}\right) + \mathtt{Tr}\left(\hat{\mathbf{W}}\hat{\mathbf{W}}^{\mathcal{H}}\right) \\ &= P_T \sum_{i=1}^{M} \hat{\sigma}_{\mathbf{g}_i}^2 |\rho_i|^2 + (1 + \alpha^2 P_T)\mathbf{x}^T\hat{\mathbf{\Gamma}}\mathbf{x} \end{aligned} \tag{3.39}$$

With the worst case SINR expressions, the relay power minimization problem

becomes:

$$\min_{|\rho_i|,i=1,...,M} P_T \sum_{i=1}^{M} \hat{\sigma}^2_{\mathbf{g}_i} |\rho_i|^2 + (1+\alpha^2 P_T)\mathbf{x}^{\mathcal{H}} \hat{\mathbf{\Gamma}} \mathbf{x}$$

$$s.t. \;\; \mathtt{SINR}_i^{wc} \geq \gamma_i, \;\; i = 1, ..., M \tag{3.40}$$

where $\mathbf{x} = [\rho_1, ..., \rho_M]^T$, $\hat{\mathbf{\Gamma}} = \sum_{i=1}^{K} \mathtt{diag}\{[\hat{\mathbf{W}}_{\mathbf{F}}]_{:,i}\}^{\mathcal{H}} \hat{\mathbf{W}}_{\mathbf{G}}^{\mathcal{H}} \hat{\mathbf{W}}_{\mathbf{G}} \mathtt{diag}\{[\hat{\mathbf{W}}_{\mathbf{F}}]_{:,i}\}$.

To achieve low computational complexity, we further simplify (3.40) into a feasibility problem (similar to the proposed suboptimal method of (3.11) for solving (3.8)), i.e., finding the smallest weights $\{\rho_1, ..., \rho_M\}$ to satisfy the worst case SINR constraints. This simplification is near optimal when the source transmit power is in the medium to high range ($P_T > 20dB$) and $\alpha^2 P_T \sim O(1)$. The resulting feasibility problem is written as follows:

$$\mathtt{SINR}_i^{wc} = \frac{a_i |\rho_i|^2}{b_{i,1}|\rho_i|^2 + b_{i,2}|\rho_i| + b_{i,3}} \geq \gamma_i, \;\; i = 1, ..., M \tag{3.41}$$

Note that in (3.41), only the amplitudes of $\rho_1, ..., \rho_M$ are involved. Based on (3.41), we can make two important observations: 1) If $|\rho_j|, \;\; j \neq i$ are fixed, then $\mathtt{SINR}_i^{wc}$ is a monotonically increasing function of $|\rho_i|$; 2) If $|\rho_i|$ is fixed then $\mathtt{SINR}_i^{wc}$ is a monotonically decreasing function of $|\rho_j|$ for $j \neq i$. Observation 1) is obtained by differentiating $\mathtt{SINR}_i^{wc}$ with respect to $|\rho_i|$, i.e.,

$$\frac{\partial \mathtt{SINR}_i^{wc}}{\partial |\rho_i|} = \frac{a_i (b_{i,2}|\rho_i|^2 + 2b_{i,3}|\rho_i|)}{(b_{i,1}|\rho_i|^2 + b_{i,2}|\rho_i| + b_{i,3})^2} > 0. \tag{3.42}$$

Observation 2) is obvious since the denominator of $\mathtt{SINR}_i^{wc}$ increases as $|\rho_j|, \;\; j \neq i$ increase and the numerator of $\mathtt{SINR}_i^{wc}$ does not change if $|\rho_i|$ is fixed. With fixed $|\rho_j|, \;\; j \neq i$, if there exists a minimal $|\rho_i^{min}|$ corresponding to that $\mathtt{SINR}_i^{wc} \geq \gamma_i$,

then $|\rho_i^{min}|$ is unique and equals the positive root of the equation

$$(a_i - b_{i,1}\gamma_i)|\rho_i|^2 - b_{i,2}\gamma_i|\rho_i| - b_{i,3}\gamma_i = 0, \tag{3.43}$$

which is obtained by setting $\texttt{SINR}_i^{wc} = \gamma_i$ in (3.41). Note that it must hold that $a_i > b_{i,1}$ in order to obtain a positive and finite root. Assuming that $\texttt{SINR}_i^{wc} = \gamma_i$ for a set of $\{|\rho_j|,\ j = 1, ..., M\}$, an increase in $\{|\rho_j|,\ j \neq i\}$ would cause the $\texttt{SINR}_i^{wc}$ to drop below the threshold $\gamma_i$. This suggests that an iterative method should be used to update $|\rho_i|,\ i = 1, ..., M$ so that $\texttt{SINR}_i^{wc} \geq \gamma_i$. We proposed the following iterative method.

In the initial step (step $k = 0$), the relay sets $|\rho|_i^{(0)} = 0,\ i = 1, ..., M$. Let $|\rho|_i^{(k)},\ k = 0, 1, ...$ be the weights generated by the relay in the $k$th step for the $i$th S-D pair. In the $k$th step, the relay updates $|\rho|_i^{(k-1)}, i = 1, ..., M$ and generates new weights $|\rho|_i^{(k)}, i = 1, ..., M$ in sequence. For the $i$th S-D pair, the relay first calculates $b_{2,i}^{(k)}, b_{3,i}^{(k)}$ (see (3.37) and (3.38)) by setting $|\rho|_j = |\rho|_j^{(k-1)},\ j \neq i$ in (3.37) and (3.38). Note that $a_i$ and $b_{1,i}$ are not updated because they are not functions of $\{|\rho|_j,\ j \neq i\}$. Then, $|\rho|_i^{(k)}$ is updated as

$$|\rho|_i^{(k)} = \frac{b_{i,2}^{(k)} + \sqrt{(b_{i,2}^{(k)})^2\gamma_i^2 + 4(a_i - b_{i,1}\gamma_i)b_{i,3}^{(k)}\gamma_i}}{2(a_i - b_{i,1}\gamma_i)} \tag{3.44}$$

The iteration ends when $|\rho_i|, i = 1, ..., M$ converge, or the iteration reaches the maximal allowed step number. The step-by-step algorithm is described in Algorithm 1.

**Theorem 3.1:** *The proposed iterative method converges when there exists a solution for (3.41).*

**Proof:** We prove this argument in two steps. Let $|\tilde{\rho}_1|, ..., |\tilde{\rho}_M|$ be any solution of (3.41). First, it is obvious that in every iteration of the proposed method, $\{|\rho_i^{(k)}|, i = 1, ..., M\}$ are increasing. Second, in every iteration, the $|\rho_i^{(k)}|$ cannot

**Algorithm 1** Calculate $|\rho|_i,\ i = 1, ..., M$ for combating CSI errors

**INITIAL**

Initiate $N, \epsilon$ {The maximal of iteration times and small convergence parameter};

Initiate $\mu_1$, $\mu_2$ {The maximal CSI errors in $\mathbf{F}$ and $\mathbf{G}$ the relay can tolerate};

**for** $i = 1$ to $M$ **do**

$|\rho_i^{(0)}| = 0$; $a_i = (1 - \hat{\sigma}_{\mathbf{g}_i}\mu_2 - \hat{\sigma}_{\mathbf{f}_i}\mu_1)^2 P_T$;

$b_{i,1} = (M-1)\alpha^2\mu_2^2\hat{\sigma}_{\mathbf{f}_i}^2 P_T + (\hat{\sigma}_{\mathbf{f}_i} + \mu_2\hat{\sigma}_{\mathbf{g}_i})^2$;

**end for**

**ITERATION**

**while** $n < N$ **do**

$n \leftarrow n + 1$;

**for** $i = 1$ to $M$ **do**

$b_{i,2}^{(n)} = 2\mu_2(\mu_1\hat{\sigma}_{\mathbf{f}_i}P_T + \hat{\sigma}_{\mathbf{f}_i} + \mu_2\hat{\sigma}_{\mathbf{g}_i}) \sum_{j=1,...,M}^{j\neq i} \hat{\sigma}_{\mathbf{g}_j}|\rho_j^{(n-1)}|$

$b_{i,3}^{(n)} = \sum_{j=1,...,M}^{j\neq i} |\rho_j|^2\beta^2\mu_1^2\hat{\sigma}_{\mathbf{g}_j}^2 + \beta^2\mu_2^2 \left(\sum_{j=1,...,M}^{j\neq i} \hat{\sigma}_{\mathbf{g}_j}|\rho_j^{(n-1)}|\right)^2$

$|\rho|_i^{(n)} = \frac{b_{i,2}^{(n)} + \sqrt{(b_{i,2}^{(n)})^2\gamma_i^2 + 4(a_i - b_{i,1}\gamma_i)b_{i,3}^{(n)}\gamma_i}}{2(a_i - b_{i,1}\gamma_i)}$

**end for**

**if** $\max_{i=1,...,M} ||\rho_i|^{(n)} - |\rho_i|^{(n-1)}| \leq \epsilon, i = 1, ..., M$ **then**

**End Iteration**

**end if**

**end while**

exceed $|\tilde{\rho}_i|$. This can be shown by contradiction. Let $k$ be the first iteration step in which the weight amplitude, e.g., $|\rho_i^{(k)}|$, exceeds $|\tilde{\rho}_i|$. At that point, all the other weight amplitudes are smaller than $|\tilde{\rho}_j|, j \neq i$. Therefore, it must hold that $\mathtt{SINR}_i^{wc,(k)} > \gamma_i$, where $\mathtt{SINR}_i^{wc,(k)}$ is calculated based on (3.34) with the weights obtained in the $k$th iteration. So, we can decrease slightly $|\rho_i^{(k)}|$ without violating the conditions of (3.41). This contradicts the fact that $|\rho_i^{(k)}|$ is the minimal solution of (3.41) in the $k$th step for calculating the weight for the $i$th weight. By combining these two observations, it can be seen that the sequence $\{|\rho_i^{(0)}|, |\rho_i^{(1)}|, ...\}$ in monotonically increasing and upper bounded by $\{|\tilde{\rho}_i|, i = 1, ..., M\}$. Therefore, the convergence is guaranteed when a solution for (3.41) exists. In the case in which (3.41) does not have a solution, we can either decrease $\mu_1$ and $\mu_2$, to allow for a solution, or stop the algorithm when the iteration reaches a preset number of steps.■

**Remark**: *Selection of $\mu_1$ and $\mu_2$ and convergency*

The parameters $\mu_1$ and $\mu_2$ should be selected so that equation (3.43) has a positive solution, i.e., $a_i > b_{i,1}\gamma_i$. $\mu_1$ and $\mu_2$ also depend on the SINR thresholds. When the SINR requirements are small, $\rho_i$ does not increase very fast in each iteration. In this case, the relay can use large $\mu_1$ and $\mu_2$ to cover a large range of CSI errors without increasing by too much the transmission power. However, the relay may find that $\rho_i$ increases much faster in the case of large SINR requirements according to (3.44). To reduce power consumption, the relay may select smaller values for $\mu_1$ and $\mu_2$ in the case of large SINR thresholds. Channel conditions also affect the way that the relay selects $\mu_1$ and $\mu_2$. For example, if the $i$th S-D pair's channel is weak, i.e., $\sigma_{\mathbf{f}_i}$ and $\sigma_{\mathbf{g}_i}$ are small, the corresponding $\rho_i$ must be increased to satisfy the SINR requirement. However, while the increased weight improves the SINR at the $i$th destination, it hurts all other destinations' SINR. Therefore, selecting small $\mu_1$ and $\mu_2$ for the S-D pairs with weak channels provides a good protection for all other S-D pairs. In case of large interference, or large $\mu_1, \mu_2$,

$|\rho_i|$ has to increase fast in one iteration which put even larger interference to the other destinations in next iteration. This can cause continuously fast increment of $|\rho_i|, i = 1, .., M$. So the convergency speed is slower than in the case of small interference and small $\mu_1, \mu_2$.

### 3.3.4 Relay antenna selection for improving the outage performance

In Section III.A, it is shown that deploying more relay active antennas can reduce the destination interference and outage probability. However, the increased cost of RF modules and the larger size and complexity associated with more antennas at the relay can be of concern. Since the most expensive component of an antenna is the RF front, one way to overcome the cost issue is to introduce antenna selection at the relay, so that optimally selected antennas are connected to a small number of RF modules. The relay is assumed to have $M$ RF modules (which is the smallest to satisfy the ZF condition) and in each receive/transmit period, each RF module will use a distinct antenna. The relay uses the same antenna subset to receive in the first hop and forward in the second hop. The first method proposed in this chapter is directly based on minimizing the outage probability of all destinations.

#### Exhaustive search based on outage probability minimization

Define $p_{outage}(N, \mathcal{S}, \hat{\mathbf{F}}_{\mathcal{S}}, \hat{\mathbf{G}}_{\mathcal{S}})$ to be outage probability under the channels $\hat{\mathbf{F}}_{\mathcal{S}}, \hat{\mathbf{G}}_{\mathcal{S}}$, which are based on a selected active antenna set, $\mathcal{S}, |\mathcal{S}| = M$. $N$ indicates that this outage probability is obtained via simulations, based on $N$ independent CSI error realizations according to the distribution of the channel errors. Here, an "outage" occurs when one destination's SINR drops below the SINR requirement.

The optimal selection is as follows:

$$\mathcal{S}^* = \arg \min_{|\mathcal{S}|=M \ \mathcal{S}\subseteq\{1,\ldots,K\}} p_{outage}(N, \mathcal{S}, \hat{\mathbf{F}}_{\mathcal{S}}, \hat{\mathbf{G}}_{\mathcal{S}}) \tag{3.45}$$

The search is over all possible active antennas in set $\mathcal{S}$ . $N$ is chosen to be large to ensure the accuracy of the simulated outage probability. In all antenna selection methods, the optimal selection based on outage probability has the smallest outage probability, because it directly searches over all possible active sets and chooses the one that has the smallest number of outage events. To determine whether any destinations are in outage in a given trial of the CSI error realization, the relay must first compute $\mathbf{\Lambda}_R$. The computational complexity is proportional to the product of $N$ and the number of possible active antenna sets $\binom{K}{M}$.

**Exhaustive search based on average interference minimization**

Although the antenna selection based on outage probability is optimal, the computational load of this method is rather high. To avoid direct minimization of the outage probability, a natural choice is to reduce the destination interference. Note that minimization of the interference is not necessarily equivalent to minimization the outage probability. However, the minimization of outage probability and the minimization of the interference are highly correlated problems, because the interference is the main reason behind an outage.

From (3.25), one can see that when $\hat{\sigma}^2_{\mathbf{g}_j}$ and $\hat{\sigma}^2_{\mathbf{f}_j}$, $j = 1, \ldots M$ are small, i.e., when the effective channel of the first, or second hop of one S-D pair is strong, the inter-S-D-pair interference is reduced. Since $\hat{\sigma}^2_{\mathbf{g}_j}$ and $\hat{\sigma}^2_{\mathbf{f}_j}$ capture the channel quality, one can select the subset of active antennas which has the best channel conditions for relay receiving and forwarding, where the optimality criterion is

the minimization of the sum-interference at all destinations, i.e.,

$$\min_{\mathcal{S}} \mathbb{E} \sum_{i=1}^{M} \sum_{j \neq i} |r_i^j|^2 \tag{3.46}$$

$$s.t.\ |\mathcal{S}| = M;\ \mathcal{S} \subseteq \{1, ..., K\}. \tag{3.47}$$

where $\mathcal{S}$ is the selected subset of active antennas. One way to obtain the antenna set which minimizes the destination interference is to do an exhaustive search over all possible subsets $\mathcal{S} \subseteq \{1, ..., K\}$ as follows:

$$\mathcal{S}^* = \arg \min_{|\mathcal{S}|=M} \min_{\mathcal{S} \subseteq \{1,...,K\}} \sum_{i=1}^{M} \sum_{j \neq i} \beta^2 |\rho_{j,\mathcal{S}}|^2 P_j \hat{\sigma}^2_{\mathcal{S},\mathbf{g}_j} + \alpha^2 |\rho_{i,\mathcal{S}}|^2 P_j \hat{\sigma}^2_{\mathcal{S},\mathbf{f}_i} \tag{3.48}$$

where the subscript $\mathcal{S}$ denotes the parameters which are computed according to the trial subset of antennas, i.e., $\sigma^2_{\mathcal{S},\mathbf{f}_i} = ||[\hat{\mathbf{W}}_{\mathbf{F}_\mathcal{S}}]_{i,:}||^2$ and $\sigma^2_{\mathcal{S},\mathbf{g}_i} = ||[\hat{\mathbf{W}}_{\mathbf{G}_\mathcal{S}}]_{:,i}||^2$. $|\rho_{i,\mathcal{S}}|^2, i = 1, ...M$ are computed based on the trial selection set $\mathcal{S}$, and the adaptive design proposed in Section III.b. $\hat{\mathbf{W}}_{\mathbf{F}_\mathcal{S}}$ and $\hat{\mathbf{W}}_{\mathbf{G}_\mathcal{S}}$ are the pseudo inverses of the sources-relay and relay-destinations channel matrices when the antenna set $\mathcal{S}$ is activated. In each trial of the exhaustive search, the relay needs to recalculate the pseudo inverses of the channel matrices. The total number of trials can be very large. A simpler but suboptimal approach would be a greedy search, which is proposed next.

**Greedy search**

In each step of the greedy search, one antenna from the active antenna set of the previous step is removed. The antenna to be removed is selected based on the minimization of the average destination interference. The greedy search proceeds as follows:

- Greedy Search

Step 0:

$\mathcal{S}_0 = \{1, ..., K\}$; $\mathbf{F}_{\mathcal{S}_0} = \mathbf{F}$ and $\mathbf{G}_{\mathcal{S}_0} = \mathbf{G}$

Step i:

If $i == K - M + 1$, search ends.

Else Do the following:

For every $j \in \{1, ..., |\mathcal{S}_{i-1}|\}$, $\mathcal{S}_{tmp}^{(j)} = \mathcal{S}_{i-1} - [\mathcal{S}_{i-1}]_j$

Generate $\mathbf{F}_{\mathcal{S}_{tmp}^{(j)}}$ and $\mathbf{G}_{\mathcal{S}_{tmp}^{(j)}}$ by removing the $j$th column and row from $\mathbf{F}_{\mathcal{S}_{i-1}}$ and $\mathbf{G}_{\mathcal{S}_{i-1}}$. Choose $j^*$ as

$$j^* = \arg \min_{j \in \mathcal{S}_{i-1}} \sum_{i=1}^{M} \sum_{k \neq i} \beta^2 |\rho_{k, \mathcal{S}_{tmp}^{(j)}}|^2 P_k \hat{\sigma}^2_{\mathcal{S}_{tmp}^{(j)}, \mathbf{g}_k} + \alpha^2 |\rho_{i, \mathcal{S}_{tmp}^{(j)}}|^2 P_k \hat{\sigma}^2_{\mathcal{S}_{tmp}^{(j)}, \mathbf{f}_k} \quad (3.49)$$

$\mathcal{S}_i = \mathcal{S}_{i-1} - [\mathcal{S}_{i-1}]_{j^*}$.■

where $\mathcal{S}_i$ is the active antenna set selected in the $i$th step and $[]_i$ denotes the $i$th element of a set. $|\rho_{i, \mathcal{S}_{tmp}^{(j)}}|^2, i = 1, ..., M$ are computed based on the trial selection set $\mathcal{S}_{tmp}^{(j)}$ and the adaptive design proposed in Section III.b. In the above iteration, we need to calculate the pseudo inverse of the channel matrices to be used for computing $\hat{\sigma}^2_{\mathcal{S}_{tmp}^{(j)}, \mathbf{f}_i}$ and $\hat{\sigma}^2_{\mathcal{S}_{tmp}^{(j)}, \mathbf{g}_i}$ for trial $j$. Since each time we only remove one antenna, the channel matrices are only changed by one column or row. The matrix inversion lemma [71] can be used to update the pseudo-inverse at lower complexity. Since $\hat{\sigma}^2_{\mathcal{S}_{tmp}^{(j)}, \hat{\mathbf{F}}_i} = [(\hat{\mathbf{F}}^{\mathcal{H}}_{\mathcal{S}_{tmp}^{(j)}} \hat{\mathbf{F}}_{\mathcal{S}_{tmp}^{(j)}})^{-1}]^{-1}_{i,i}$ and $\hat{\sigma}^2_{\mathcal{S}_{tmp}^{(j)}, \hat{\mathbf{G}}_i} = [(\hat{\mathbf{G}}_{\mathcal{S}_{tmp}^{(j)}} \hat{\mathbf{G}}^{\mathcal{H}}_{\mathcal{S}_{tmp}^{(j)}})^{-1}]^{-1}_{i,i}$, in each trial, we only need to calculate $(\hat{\mathbf{F}}^{\mathcal{H}}_{\mathcal{S}_{tmp}^{(j)}} \hat{\mathbf{F}}_{\mathcal{S}_{tmp}^{(j)}})^{-1}$ and $(\hat{\mathbf{G}}_{\mathcal{S}_{tmp}^{(j)}} \hat{\mathbf{G}}^{\mathcal{H}}_{\mathcal{S}_{tmp}^{(j)}})^{-1}$. Without loosing generality, suppose that in the $i$th step, the last column $\mathbf{g}$ is removed from $\hat{\mathbf{G}}_{\mathcal{S}_i}$, i.e., $\hat{\mathbf{G}}_{\mathcal{S}_i} = [\hat{\mathbf{G}}_{\mathcal{S}_{tmp}^{(j)}}, \mathbf{g}]$. Based on the matrix inversion lemma, it holds that

$$(\hat{\mathbf{G}}_{\mathcal{S}_{tmp}^{(j)}} \hat{\mathbf{G}}^{\mathcal{H}}_{\mathcal{S}_{tmp}^{(j)}})^{-1} = (\hat{\mathbf{G}}_{\mathcal{S}_i} \hat{\mathbf{G}}^{\mathcal{H}}_{\mathcal{S}_i} - \mathbf{g}\mathbf{g}^{\mathcal{H}})^{-1} \quad (3.50)$$

$$= (\hat{\mathbf{G}}_{\mathcal{S}_i} \hat{\mathbf{G}}^{\mathcal{H}}_{\mathcal{S}_i})^{-1} + \frac{(\hat{\mathbf{G}}_{\mathcal{S}_i} \hat{\mathbf{G}}^{\mathcal{H}}_{\mathcal{S}_i})^{-1} \mathbf{g}\mathbf{g}^{\mathcal{H}} (\hat{\mathbf{G}}_{\mathcal{S}_i} \hat{\mathbf{G}}^{\mathcal{H}}_{\mathcal{S}_i})^{-1}}{1 - \mathbf{g}^{\mathcal{H}} (\hat{\mathbf{G}}_{\mathcal{S}_i} \hat{\mathbf{G}}^{\mathcal{H}}_{\mathcal{S}_i})^{-1} \mathbf{g}}. \quad (3.51)$$

Since $(\hat{\mathbf{G}}_{\mathcal{S}_i}\hat{\mathbf{G}}_{\mathcal{S}_i}^{\mathcal{H}})^{-1}$, needed at step $i$, has been already calculated at step $i-1$, computing the inverse matrices is a simple update and does not involve any matrix inversion. $(\hat{\mathbf{F}}_{\mathcal{S}_{tmp}^{(j)}}^{\mathcal{H}}\hat{\mathbf{F}}_{\mathcal{S}_{tmp}^{(j)}})^{-1}$ can be computed in a similar fashion.

By enforcing ZFBF structure, SINR requirements of destinations are decoupled so that low-dimensional and low-complexity approaches are enabled to compute the BF matrix. On the other hand, the numerical optimization over gBF matrices is not favorable because of the high dimensional problem involved and the significantly larger delay. ZFBF and the proposed adaptive design are also more suitable for antenna selection in case of imperfect relay CSI. Indeed, the implementation of antenna selection using optimization over gBF matrices would be difficult as numerical optimization would needed in every trial removal of one antenna. Further, the computational cost would increase with the number of antennas. The proposed greedy selection method with ZFBF is particularly well suited because each time one antenna is deselected, the new ZFBF matrix can be calculated based on the matrix inversion lemma. Generally, using a suboptimal BF matrix may result in worse performance that using gBF [61]. However, our simulations indicate that the performance penalty is very small. Moreover, when the antenna selection methods are used in conjunction with the proposed adaptive design, both the outage and power efficiency are shown to be superior to the gBF with numerical optimization.

### 3.3.5 Simulation Results

As in the case of perfect CSI, three distinct S-D pairs are simulated in this section. One relay with $K = 3$ antennas assists the data transmission. The targeted SINR is between 2dB and 10dB, which is a moderate SINR range and good for coded QPSK. The source transmit power is fixed at 20dB. Each point on the curves is obtained based on averaging over $5,000$ independent channel realizations, or CSI error realizations.

Next we consider the case in which the CSI at the relay is not accurate. First, we compare the proposed adaptive weight design method to the method of [61]. In [61], in order to accommodate the CSI errors, the relay executes a numerical optimization to find the generally structured BF matrix based on the enlarged SINR requirements at the destination Hereafter, we refer to the Optimization over general BF matrices in [61] with *gBF under imperfect CSI*.

We first follow the parameter setup of [61], i.e., the relay's the estimated CSI about $\mathbf{F}$ and $\mathbf{G}$ are set to

$$\hat{\mathbf{F}} = \begin{bmatrix} 0.64 + 0.52i & 0.048 - 0.52i & -0.057 - 0.021i \\ -1.57 + 0.67i & -1.42 - 0.63i & -1.39 + 0.43i \\ -0.169 + 1.36i & -0.25 - 2.30i & 0.55 + 0.73i \end{bmatrix}$$

$$\hat{\mathbf{G}} = \begin{bmatrix} -0.57 - 0.78i & -1.07 - 0.49i & 0.91 + 0.49i \\ 0.14 - 1.55i & 0.063 + 0.27i & 0.99 - 1.63i \\ -0.68 + 0.11i & -0.34 - 0.29i & 1.11 + 1.29i \end{bmatrix}$$

The channel uncertainty parameters used are set to $\alpha = \beta = 0.045$ and $\mu_1 = \mu_2 = 1.6$. Since the relay has only 3 antennas, there is no need to run the antenna selection. In this case, $P_T > \gamma_i |\sigma_{\mathbf{f}_i}|^2, i = 1, ..., M$ is always guaranteed so that we only need to consider the outage caused by the CSI errors at the relay. Fig. 3.6 shows the overall outage probability and Fig. 3.7 illustrates the power efficiency. The proposed adaptive weight design method with a ZFBF structure has the same outage performance as gBF with imperfect CSI, while the required transmit power at the relay is only slightly higher (by 1dB) than the power cost of gBF with imperfect CSI. This is because gBF with imperfect CSI in [61] is based on optimization over arbitrary beamforming matrices, while the proposed weight design method imposes to the beamforming matrix a ZF structure. However,

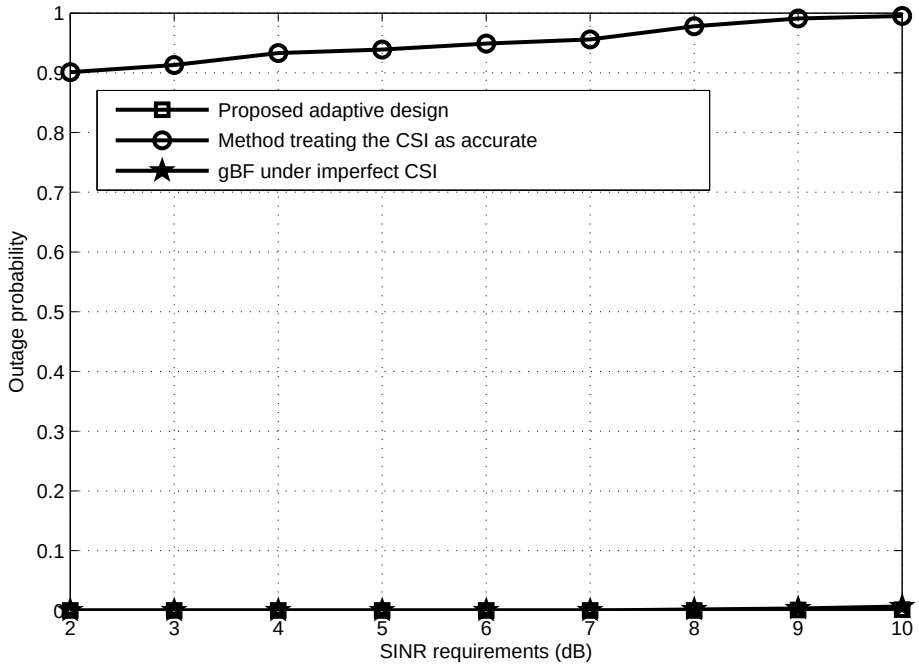


Figure 3.6: Outage probability of the iterative weight design under relay CSI errors and a particular $\mathbf{F}$ and $\mathbf{G}$

the proposed method is significantly less complex than [61], as it does not need any complicated numerical optimization. The detailed complexity comparison will be further discussed in the case of random channels. The outage probability curve of the proposed method with only one iteration is also included in Fig.3.6. After only one iteration, the outage performance is very close to the convergent performance.

Next, we test the proposed weight design method under fading channels. The target SINR range is adjusted to $[1dB, 8dB]$ because the outage probability in higher range is well above 0.1 which is not useful in a practical system. The relay is equipped with 5 antennas, or 3 antennas. The channel coefficients are assumed to be i.i.d., $\mathcal{CN}(0, 1)$. The following four cases are considered: 1) the relay has 3 antennas and does not run the proposed adaptive weight design method, 2) the relay has 3 antennas and runs the proposed adaptive weight design method

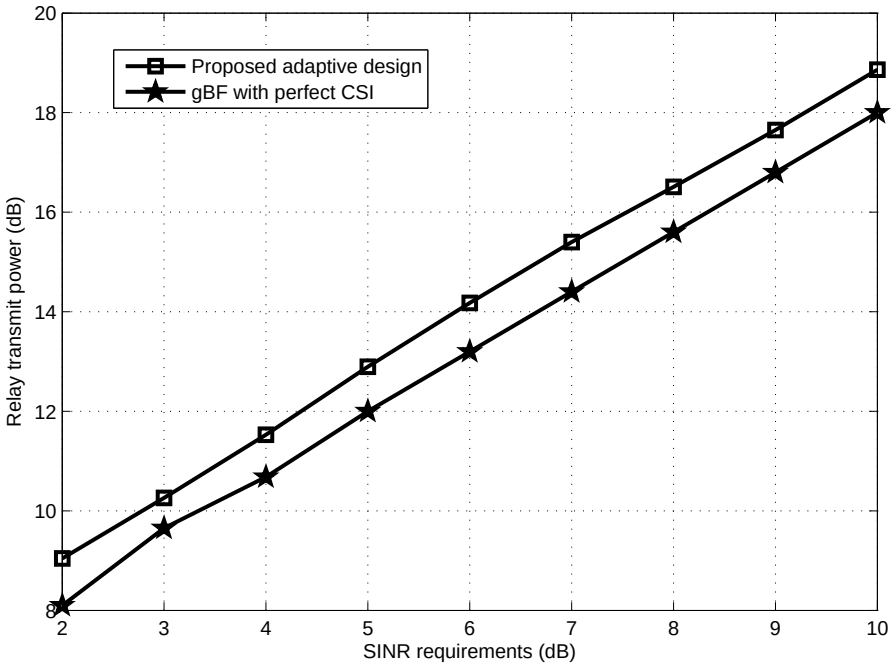


Figure 3.7: Relay transmit power of the iterative weight design under relay CSI errors and a particular **F** and **G**

and 2) the relay has 5 antennas and runs the proposed adaptive weight design method but does not implement the proposed antenna selection methods, and 4) the relay has 5 antennas, runs the proposed adaptive weight design method and also the proposed antenna selection methods. We should note that that we consider the outage caused by the CSI errors only, rather than that caused by the poor channel conditions, i.e., we do not count the outage if it occurs when there are no CSI errors.

The comparison of cases 1), 2) and 4) is shown in Figs. 3.8 and 3.9. It can be seen that the proposed adaptive weight design method greatly reduces the outage probability with the added expense of around 3dB relay transmission power compared to the case in which the relay CSI is treated as accurate. We also include comparison of the proposed adaptive weight design method to gBF under imperfect CSI [61]. In the fading channel case, when the channel conditions

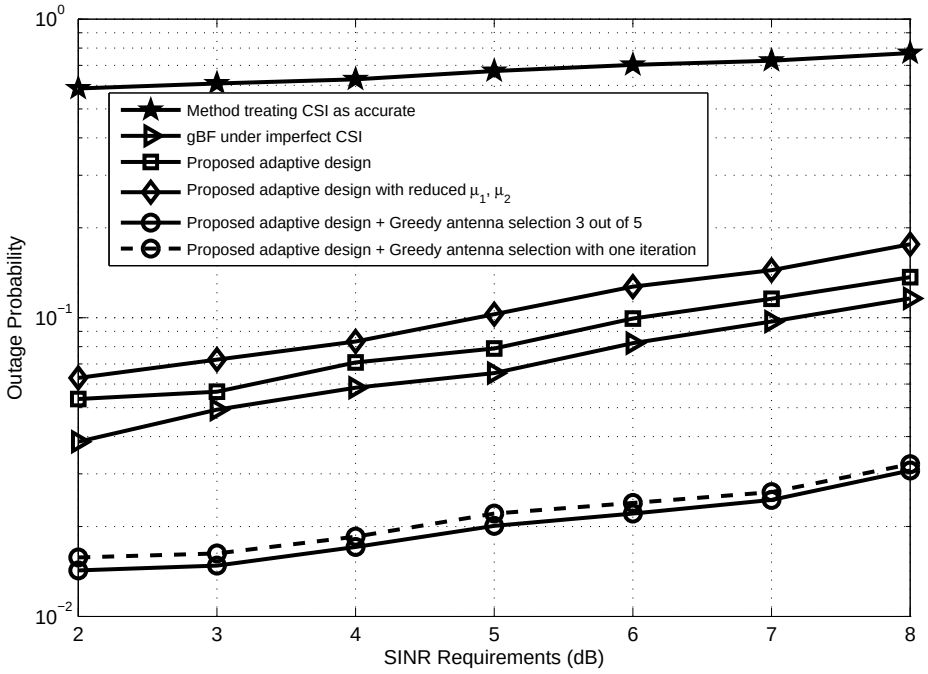


Figure 3.8: Outage probability of the iterative weight design under relay CSI errors and Rayleigh channels

for an S-D pair are bad, the constraint of (3.41) may not be always satisfied. In this situation, we decrease the CSI error bounds $\mu_1$ and $\mu_2$ for this specific S-D pair in the simulations to make the worst case problem feasible. Note that the same infeasibility issue occurs in the gBF under imperfect CSI. We also apply the $\mu_1$ and $\mu_2$ decreasing techniques in order to solve the infeasibility issue when testing the gBF under imperfect CSI. It can be seen that the proposed weight design method and gBF under imperfect CSI have very similar outage probability performance. In terms of relay transmission power, the proposed method costs an additional 1dB of relay power. When the proposed greedy antenna selection and the adaptive method are combined, both the outage probability and power efficiency are much smaller than in the method of gBF under imperfect CSI.

The complexity comparison in terms of MATLAB runtime is shown in Table.3.1. The proposed method for weight calculation with maximum number of iterations

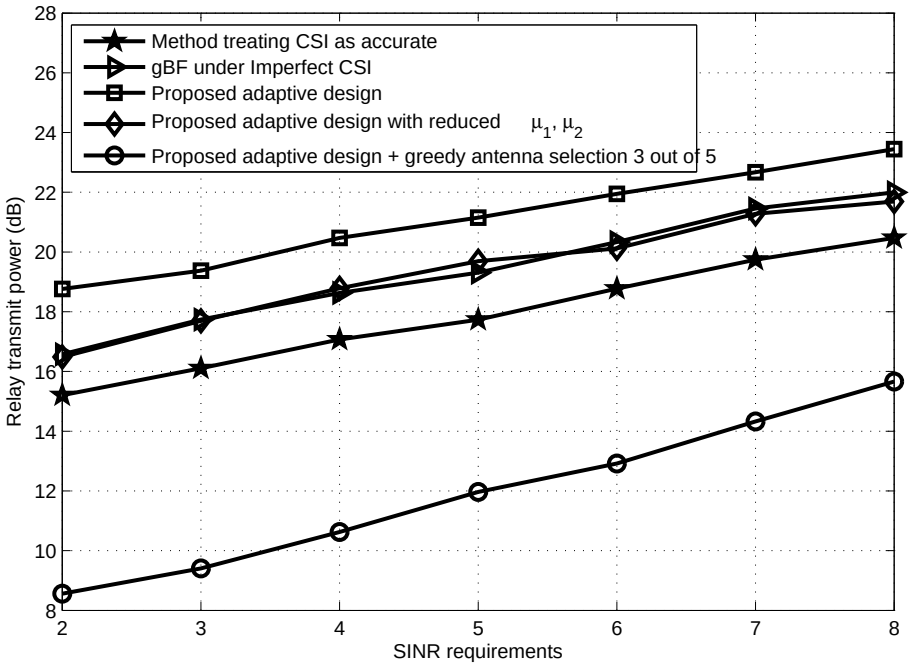


Figure 3.9: Relay transmit power of the iterative weight design under relay CSI errors and Rayleigh channels

set to 4, took 0.016s, while the optimization over general matrices took 1.09s. The greedy selection with two iterations per trial took $9 * 0.005 * 2s = 0.09s$, where 9 is the number of trials. For the test case with $K = 5$ and $M = 3$, the adaptive weight design combined with greedy selection took about 0.1s for one time channel/error realization. This still yields significantly lower time to generate weights than the optimization method over general matrices. Therefore, the proposed adaptive method with antenna selection has advantages over optimization based on general matrices in the aspects of outage probability, transmit power and computational complexity.

Next we move to cases 3) and 4) for testing the effectiveness of the proposed antenna selection methods. Here, the CSI error indicators are assumed to be $\alpha^2 = \beta^2 = 0.005$. The comparison results are shown in Fig.3.10. It can be seen that case 3), in which all five antennas are activated, has overall the best outage

Table 3.1: Complexity Comparison

| | Adaptive method (1 iteration) | Greedy selection (3 out of 5 antennas) | Matrix pseudo inversion ($5 \times 3$) |
|---|---|---|---|
| RunTime | 0.005s | 0.004s | 0.004s |
| | Adaptive method + Greedy selection (2 iteration) | gBF with perfect CSI | |
| RunTime | 0.11s | 1.09s | |

performance. This is because the extra active antennas at the relay give the best channel gains and the average lowest destination interference. The proposed antenna selection methods (optimal search based on outage, exhaustive search and greedy selection based on the minimization of average destination interference) combined with the adaptive weight design method have the second best outage performance. It is noted that the three selection methods have very close outage performance. The proposed greedy search performs especially well, considering it is the simplest and has almost identical outage probability as that of the optimal search based on outage, which has the minimal possible outage probability. In Fig.3.11, it can be seen that the power efficiency results of the three antenna selection methods are also very close. This means that in a practical system, the proposed greedy search method is preferable, because of its low computational load. The outage performance of the three proposed antenna selection methods all significantly outperform the case in which 3 relay antennas are randomly selected. This confirms the advantage of the antenna selection methods. Note that if the proposed adaptive weight design weight/antenna selection designs are not used, the outage probability will be almost 1 for every target SINR point as shown in Fig.3.10.

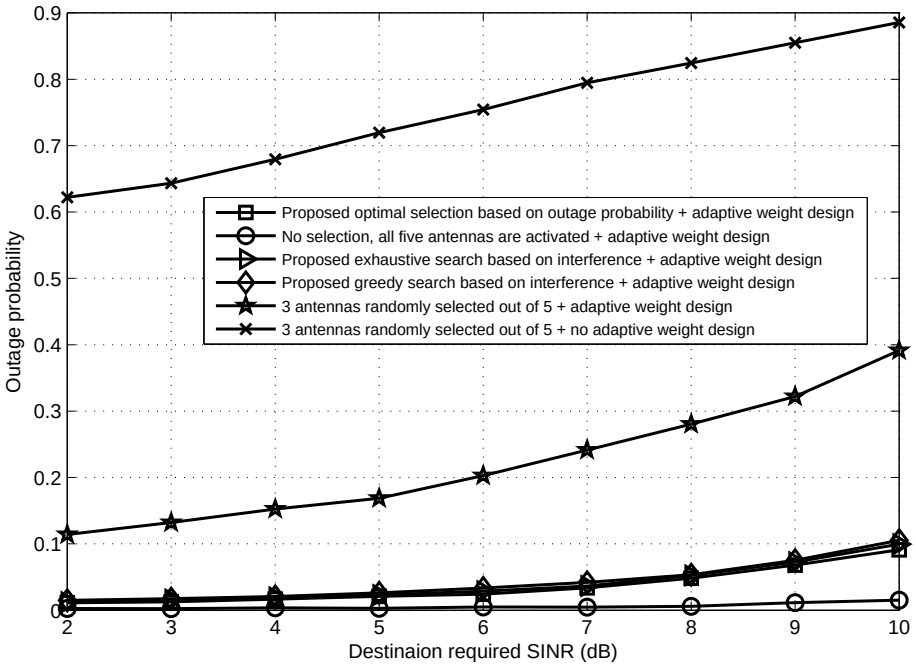


Figure 3.10: Outage probability of relay antenna selections with iterative weight design under relay CSI errors and Rayleigh channels

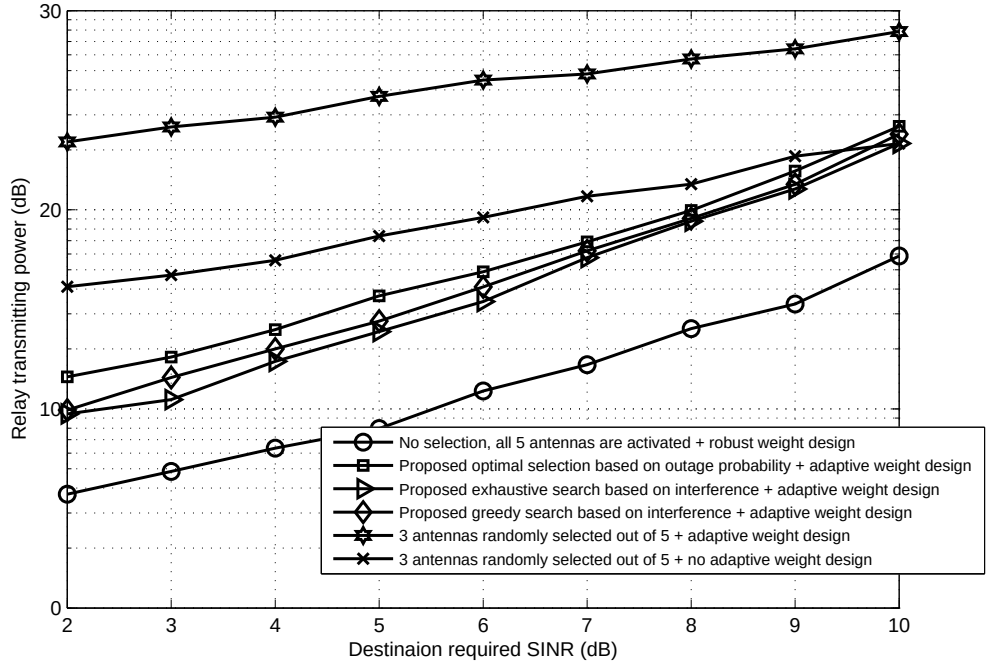


Figure 3.11: Relay transmit power of relay antenna selections with iterative weight design under relay CSI errors and Rayleigh channels

## 3.4 Summary

We have investigated the QoS guarantee problem in relay network that supports multiple source destination pairs. One AF relay with multiple antennas is deployed and uses a ZFBF beamforming matrix to process the received data streams. The target problem is to minimize the transmit power at the relay while satisfying the SINR requirement of each S-D pair. There is the need for CSI of both the S-R and R-D channels to accomplish this goal. When the CSI is perfect, both the optimal and a sub-optimal but simple methods have been proposed for solving this problem. When the CSI at the relay is imperfect, a low complexity adaptive weight design method has been presented for combating inter-S-D-pair interferences by iteratively increasing the weights for all S-D pairs. Relay antenna selection methods have been also proposed to further improve the outage performance. Simulation results have shown that combined use of the proposed adaptive weight design and antenna selection methods can achieve lower outage probability with less power and computational complexity than existing methods.

Using multiple distributed relays to support multiple source destination pairs is also investigated in the case of perfect CSI at a fusion center. With a enough large number of relays, the SINR requirements at all destination can be satisfied simultaneously. Compared with the scheme of one relay equipped with multiple antennas, the distributed relays are preferred when relay's size is limited to deploy multiple antennas. However, extra relay transmit power is required in the distributed case due to the less freedom to design the BF matrix.

# Chapter 4

# Joint Decode-and-forward and Jamming for Wireless Physical Layer Security with Destination Assistance

In wireless communications, the wireless channel makes the transmitted signal available to unauthorized users as well as the intended receiver. Cryptographic approaches, inspired by Shannon's pioneering work [72], aim at making it difficult for unauthorized users to decode the received signal. Physical layer security approaches are concerned with whether a positive secrecy rate can be supported, independent of the type of the decoding approach the unauthorized users might employ. Physical layer security has received considerable attention [73, 74, 75], following the pioneering works of [18] and [19]. In [18], it is shown that a positive secrecy data rate can be achieved when the channel between the source and the unauthorized user, referred to here as the eavesdropper, is a degraded version of the source-destination channel. The secrecy rate of orthogonal relay eavesdropper channels is investigated in [73]. For the Gaussian channel, the secrecy rate equals the difference of the capacities of the source-destination channel and the source-eavesdropper channel, again provided that the former link is stronger than the latter link [19]. Employing MIMO techniques [76, 77] in physical layer security systems can improve the secrecy rate because of the ability of MIMO systems to steer the desired signal away from the eavesdropper, provided the eavesdropper channel state information (CSI) is known.

Employing multiple antennas at a node is usually costly and limited by the size of the node. Alternatively, improved secrecy rate can be achieved by employing

cooperating relays [23, 22, 78, 79, 80]. Relays can either forward the signal to the destination, or jam the eavesdropper. Recently, multiple decode-and-forward (DF) relays were employed in [24, 81] to cooperatively beamform the signal to the destination. The transmission takes two slots; in the first slot, the source transmits, and in the second slot, the relays cooperatively beamform the decoded source signal to the destination. However, since in the first slot the eavesdropper can hear the source signal, the system cannot take full advantage of a total power increase. The same holds for [82], in which one relay is selected to forward the useful signal and another relay is chosen for jamming the eavesdropper in the second slot. Another issue associated to multiple DF relays is that each forwarding relay must decode the source data correctly and securely. This may decrease the overall secrecy rate due to the tighter first hop secrecy constraint. So, selecting a proper relay subset for signal forwarding is necessary. Destination jamming schemes are also studied in [39, 40] when the source-destination link is ignored. In this Chapter, however, we answer the question that the destination should listen or transmit in the first slot when the source is connected to the destination.

In this chapter, we consider the same model of secrecy relay network as in [24, 81, 82] with one source, one destination, one eavesdropper, and one or multiple friendly half-duplex relays running DF protocol. Unlike [24, 81, 82], we propose to use the destination as a jammer instead of a receiver in the first slot. The proposed work can be summarized as follows:

- *Transmitter assisted jamming via cooperative beamforming* - A two-slot transmission scheme is proposed. First, the source transmits a weighted combination of data and noise. During that time, the destination does not listen, but rather cooperates with the source in transmitting noise along the null space of the source-relay channel. The goal of the jamming is to degrade the eavesdropper Signal-to-Interference-plus-Noise-Ratio (SINR) ratio, while creating no interference at a preselected relay. This step

does not require any eavesdropper channel information. In the second slot, one preselected relay retransmits the decoded source signal, and at the same time, cooperates with the source to jam the eavesdropper without creating interference at the destination. Again, in this step, no eavesdropper channel information is required.

The benefit of jamming can be understood via the following arguments. In the absence of any jamming towards the eavesdropper in the first slot, the relay may not be able to achieve high enough secrecy rate, thus limiting the overall system secrecy rate. Further, when the destination listens, the eavesdropper listens too. Thus, in the absence of jamming, the secrecy rate cannot benefit from a total power increase. As it will be shown in this chapter, the secrecy rate of the proposed scheme always increases with the total power budget increase. The benefit of using the destination, as opposed to any other relay, as a jammer, stems from the fact that if the destination was far away from the source, its received signal in the first hop would be weak. It, therefore, makes sense to let the destination serve another more useful purpose, during the first slot, i.e., jam the eavesdropper. Moreover, as it will become clearer in the following, using one or more relays instead of the destination for jamming would require inter-relay channel information at the relays. On the contrary, the destination assisted jamming does not require inter-relay CSI.

- *Optimal power allocation and relay selection* - The power of the source, relay, and destination transmitted signals is allocated in an optimal fashion, in order to maximize the system secrecy rate subject to a total transmit power budget. The optimization problem is generally non-convex, however, we show that the problem can be converted into an one dimensional line search plus a bi-sectional search problem. When the number of active relays that participate in the second slot transmission increases, the source-relay

link with the smallest secrecy rate limits the system overall secrecy rate. Therefore, we propose to select only one relay, the "best" one, to decode-and-forward the signal in the second slot. In this way, the first slot constraint is no longer the system bottleneck. We propose two relay selection schemes for choosing the best relay, i.e., an optimal and a suboptimal method, with vastly different computational complexities. The optimal method is based on a exhaustive search over all relays, while the suboptimal is based on the CSI of each relay. We also propose a distributed approach for relay selection, in which CSI and beamforming vectors are communicated between the nodes through limited rate feedback channels.

Optimal power allocation and relay selection require global CSI, including that of the eavesdropper. We also study the case in which only the statistics of the eavesdropper CSI are known, and propose power allocation and relay selection based on approximate expressions of the secrecy rate.

Relay selection methods have been researched in [83, 84, 85]. However, these selection methods do not account for an eavesdropper, therefore, do not apply to the proposed jamming scheme. Relay selection in the presence of eavesdroppers are proposed in [82]. However, the achieved secrecy rate suffers from high eavesdropper SINR when the total power budget increases, which does not allow the secrecy rate to increase as the power increases. Imperfect CSI

- *Secrecy rate scaling law* - We show that the proposed scheme can take advantage of both the power budget ($P_0$) increase and the number of available relays ($K$), according to the secrecy rate scaling law $\frac{1}{2}\log_2(1+\frac{P_0}{8}\log K)-1.6$.

## 4.1 System model and motivation

We consider a distributed wireless network configuration as depicted in Fig.4.1, with one source, one destination, one eavesdropper and $K$ friendly relays . $h_{SD}$, $h_{SR_i}$, $h_{SE}$, $h_{R_iE}$, $h_{R_iD}$, $h_{DE}$ represent respectively the channel gains between the source and the destination, the source and the $i$th relay, the source and the eavesdropper, the $i$th relay and the eavesdropper, the $i$th relay and the destination, and the destination and the eavesdropper. The additive noise at each node is assume to be i.i.d. complex Gaussian with unit variance. All transmission nodes (source, relay, destination) share a total transmission power budget $P_0$. The goal of this chapter is to design a cooperative transmission strategy to improve the secrecy rate.

The relays operate in half duplex DF protocol, i.e., each relay must hear and decode the signal correctly in the first slot, before transmitting it in the second slot. Therefore, the system secrecy rate is constrained by the minimal secrecy between the source and all the relays, i.e.,

$$R_s \leq \frac{1}{2}C_{1s} = \min_{i=1,\ldots,K} \frac{1}{2}(\log_2(1+|h_{SR_i}|^2 P_s^U) - \frac{1}{2}\log_2(1+|h_{R_iE}|^2 P_s^U)).$$

where $P_s^U$ is the source transmission power for the data signal. Note that the factor $\frac{1}{2}$ is due to the fact that the communications is divided into two slots. With an increasing number of the relays, the constraint becomes tighter and decreases the overall secrecy rate. In this chapter, we will select only one relay to decode-and-forward the signal. The selection algorithm is introduced in the next section. Since only one relay is used, we will drop the relay index $i$ in the channel gain notation, i.e., will use $h_{SR}$, $h_{RE}$ and $h_{RD}$ to denote the channels gains between the source and the active relay, the active relay and the eavesdropper, and the active relay and the destination, respectively (see Fig.4.1).

Let us consider the throughput between the source and the eavesdropper.

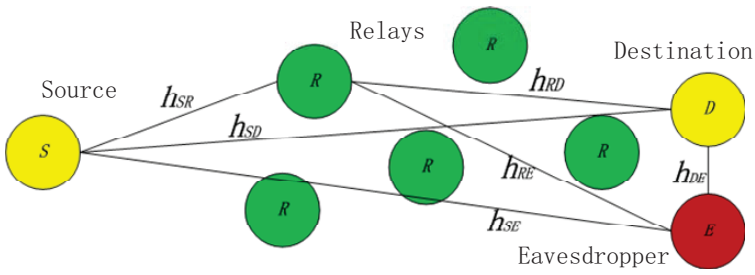


Figure 4.1: The wireless physical layer security system with multiple relays

When the destination only listens, the overall capacity at the eavesdropper after a two-slot reception is lower bounded by

$$C_E \geq \log_2(1 + P_s^U |h_{SE}|^2) \tag{4.1}$$

The above holds with equality when the eavesdropper ignores the signal it received during the second slot. It is noted that $P_s$ should increase proportionally to $P_0$, otherwise, the overall secrecy rate will be limited by the first slot secrecy capacity constraint. So, the eavesdropper capacity increases with a scaling law $\log P_0$. Considering that the destination capacity can increase at most as fast as $\log P_0$ with $P_0$ increasing, and that the system secrecy rate equals the difference of the capacities of the destination and eavesdropper, the system without first slot jamming may have a limited secrecy rate, and thus cannot take full advantage of a total power increase. To address this issue, in this chapter, we will design a transmission scheme in which the destination transmits a jamming signal in the first slot instead of listening. Note that this scheme requires that the destination has the ability to transmit, and its channel to the eavesdropper is known.

## 4.2 The proposed transmission scheme with destination assisted jamming

In this section, the transmission scheme is first outlined under the assumption that a single relay has been selected. Second, the optimal power allocation among the first and second slot jamming and data signals is discussed. Third, the method for selecting the best relay is presented. Finally, the case of statistical eavesdropper CSI is studied.

### 4.2.1 The proposed transmission scheme

Let us assume that the forwarding relay for the second slot has been selected, and that each node involved has CSI between itself and the relay, and between itself and the destination.

- In the first slot, the source transmits a weighted combination of (i) the information bearing signal, with power $P_S^U$, and (ii) jamming noise. At the same time, the destination cooperates with the source to transmit a jamming signal with power $P_{SD}^J$ over a beamformer $\mathbf{w}_{SD-E}$, which is along the null space of $[h_{SR}, h_{DR}]$, where $||\mathbf{w}_{SD-E}||^2 = 1$. This jamming beamformer results in no interference at the selected relay. Based on the source-destination transmission strategy, the first slot source and destination transmitted signals are written as

$$x_{1,S} = \sqrt{P_S^U}u + \sqrt{P_{SD}^J}[\mathbf{w}_{SD-E}]_1 v_1 \tag{4.2}$$

$$x_D = \sqrt{P_{SD}^J}[\mathbf{w}_{SD-E}]_2 v_1. \tag{4.3}$$

  where $u$ and $v_1$ are the data and first slot jamming signal, which are assumed to be i.i.d. complex Gaussian with unit variance. In (4.2) $[\mathbf{a}]_i$ denotes the $i$th element of a vector $\mathbf{a}$.

The first slot SNR at the relay can be expressed as

$$SNR_1^R = |h_{SR}|^2 P_S^U. \tag{4.4}$$

and the SINR at the eavesdropper as

$$SINR_1^E = \frac{|h_{SE}|^2 P_s^U}{1 + P_{SD}^J |[h_{SE}, h_{DE}]\mathbf{w}_{SD-E}|^2}. \tag{4.5}$$

- In the second slot, the selected relay forwards the data with power $P_R^U$, using the same codebook as the source, along with jamming noise. During the same time, the source cooperates with the relay to transmit a jamming signal with power $P_{SR}^J$ over a beamformer $\mathbf{w}_{SR-E}$, which is along the null space of $[h_{SD}, h_{RD}]$, where $||\mathbf{w}_{SR-E}||^2 = 1$. This jamming beamformer results in no interference at the destination.

  Based on the source-relay transmission strategy, the first slot source and destination transmission signals are written as

$$x_{2,S} = \sqrt{P_{SR}^J}[\mathbf{w}_{SD-E}]_1 v_2 \tag{4.6}$$

$$x_R = \sqrt{P_R^U} u + \sqrt{P_{SR}^J}[\mathbf{w}_{SR-E}]_2 v_2, \tag{4.7}$$

  where $v_2$ is the second slot jamming signal, which is complex Gaussian with unit variance.

  Therefore, in the second slot the SNR at the destination equals

$$SNR_2^D = |h_{RD}|^2 P_R^U. \tag{4.8}$$

In the second slot, the SINR at the eavesdropper becomes

$$SINR_2^E = \frac{|h_{RE}|^2 P_R^U}{1 + P_{SR}^J |[h_{SD}, h_{RD}]\mathbf{w}_{SR-E}|^2}. \tag{4.9}$$

Based on above SNR expressions, the secrecy rate at the destination can be written as:

$$\begin{aligned} R_s &= \min \frac{1}{2}([C_{1s}]^+, [C_{2s}]^+) && (4.10)\\ &= \min \frac{1}{2} \Big( \left(\log_2(1 + SNR_1^R) - \log_2(1 + SINR_1^E)\right)^+, \\ &\quad \left(\log_2(1 + SNR_2^D) - \log_2(1 + SINR_1^E + SINR_2^E)\right)^+ \Big) && (4.11) \end{aligned}$$

where $(x)^+ \triangleq \max(x, 0)$. Based on (4.11), it can be seen that if $P_{SD}^J$ is comparable to $P_S^U$, and $P_{SR}^J$ is comparable with $P_R^U$, the eavesdropper's SINR in both slots is of the order of 1. Also, the destination's SNR in the second slot increases as the transmission power increases. So, in the proposed transmission scheme, the overall secrecy rate can benefit from increasing the total power.

### 4.2.2 Optimal Power Allocation

In this section, we assume that each node involved has global CSI, including the eavesdropper CSI. The source adjusts the power allocation among $P_S^U$, $P_R^U$, $P_{SD}^J$ and $P_{SR}^J$ to maximize (4.11) based on a sum power constraint $P_0$, i.e.,

$$\max_{P_S^U, P_R^U, P_{SD}^J, P_{SR}^J} \min([C_{1s}]^+, [C_{2s}]^+) \tag{4.12}$$

$$s.t. \;\; P_S^U + P_R^U + P_{SD}^J + P_{SR}^J = P_0 \tag{4.13}$$

We next show that the optimal power allocation can be reduced to a one-dimensional line search problem.

Let the first slot transmission power be fixed, i.e., $P_S^U + P_{SD}^J = P_1$. Under this

condition, the optimization problem becomes

$$\max_{P_S^U+P_{SD}^J=P_1;P_R^U+P_{SR}^J=P_0-P_1} \min \left( \underbrace{\log_2 \frac{1+|h_{SR}|^2 P_S^U}{1+\frac{|h_{SE}|^2 P_s^U}{1+P_{SD}^J|[h_{SE},h_{DE}]\mathbf{w}_{SD-E}|^2}}}_{C_{1s}}, \underbrace{\log_2 \frac{1+|h_{RD}|^2 P_R^U}{1+\frac{|h_{SE}|^2 P_s^U}{1+P_{SD}^J|[h_{SE},h_{DE}]\mathbf{w}_{SD-E}|^2}+\frac{|h_{RE}|^2 P_R^U}{1+P_{SR}^J|[h_{SE},h_{RE}]\mathbf{w}_{SR-E}|^2}}}_{C_{2s}} \right)$$

Note that generally, $C_{1s}$ and $C_{2s}$ are both not concave functions of $\{P_S^U, P_R^U, P_{SD}^J, P_{SR}^J\}$, so direct use of convex optimization methods is not applicable. It is easy to see that $C_{2s}$ decreases monotonically with $P_S^U$ increasing. It can also be shown that $C_{1s}$ has one of three possible behaviors over $P_S^U \leq P_1$, i.e., 1) $C_{1s}$ monotonically increases, 2) $C_{1s}$ monotonically increases when $P_S^U \leq P_S^{U,*1}$ and monotonically decreases when $P_S^U \geq P_S^{U,*1}$ and 3) $C_{1s} \leq 0$. Apparently, we need to deal with only the first two cases. In either of these two cases, $\min(C_{1s}, C_{2s})$ has a unique maximum at $P_S^{U,*2}$, and the function $\min(C_{1s}, C_{2s})$ monotonically increases when $P_S^U \leq P_S^{U,*2}$, and monotonically decreases when $P_S^U \geq P_S^{U,*2}$. Note that the maximum may be achieved on the boundaries, i.e., $P_S^{U,*2} = 0$ or $P_S^{U,*2} = P_1$.

Therefore, the optimization over $P_S^U + P_{SD}^J = P_1$ and $P_R^U + P_{SR}^J = P_0 - P_1$ can be decoupled when $P_1$ is fixed. A bi-sectional search over $[0, P_1]$ can be conducted to find the optimal solution is $P_S^{U,*2}$ and in each trial of $P_S^U$ the optimal $P_R^U$ and $P_{SR}^J$ which maximize $C_{2s}$ should be determined. The latter task has a fairly simple solution. By setting the partial differentiation of $C_{2s}$ with respect to $P_R^U$ equal to zero we get

$$a\left(P_R^U\right)^2 + bP_R^U + c = 0. \tag{4.14}$$

where $a = c_1 g_2 (g_2 - g_1)$, $b = -2a_1 g_2 [1 + g_2(P_0 - P_1)]$, $c = [c_1 + c_1 g_2 (P_0 - P_1) - g_1][1 + g_2(P_0 - P_1)]$ with $c_1 = |h_{RD}|^2$, $g_1 = \frac{|h_{RE}|^2}{1+\frac{|h_{SE}|^2 P_s^U}{1+P_{SD}^J |[h_{SE}, h_{DE}]\mathbf{w}_{SD-E}|^2}}$ and $g_2 = |[h_{SD}, h_{RD}]\mathbf{w}_{SR-E}|^2$. It can be shown that when $c \leq 0$, the optimal $P_R^{U,*} = 0$. When $c \geq 0$ and (4.14) has a root $\theta$ within $[0, P0 - P1]$, then $P_R^{U,*} = \theta$. Otherwise, $P_R^{U,*} = P_0 - P_1$.

Through the bi-sectional search for $P_S^U$ and $P_{SD}^J$, and solving (4.14) for $P_R^U$ and $P_{SR}^J$, we can obtain the optimal power allocation when $P_1$ is fixed. The optimal first slot transmission power $P_1$ can be obtained by a line search. The algorithm to find the optimal power allocation is summarized as follows:

- Perform a one-dimensional line search on $P_1$ to find the optimal first slot power.
- For every trial of $P_1$, perform a bi-sectional search for $P_S^U \in [0, P_1]$ to find the optimal first slot data power $P_s^U$.
- For every trial of $P_S^U$ with a fixed $P_1$, perform (4.14) to find the optimal $P_R^U$ and $P_{SR}^J$.

### 4.2.3 Relay selection

#### Optimal Selection

Based on the optimal power allocation proposed in the previous section, the source can calculate the secrecy rate $R_s^{(i)}$ for any relay $i$, $i = 1, ..., K$. Therefore, the source can select the optimal relay that maximizes the secrecy, via exhaustive search as follows,

$$i_{opt} = \arg \max_{i=1,...,K} R_s^{(i)} \tag{4.15}$$

where $R_s^{(i)}$ is the secrecy rate achieved with the $i$th relay being selected and using the proposed optimal power allocation. Note that the computation of the beamforming vector, the power allocation and the relay selection, can be done at any single node who has the full CSI on the source, destination and relays. These tasks can also be carried out in a distributed way as follows. The source destination CSI is broadcasted to all relays. Then, each relay computes the secrecy rate corresponding its own optimal power allocation. All relays secrecy rates are then fedback to the source, one by one, to be used in the selection of the relay with the largest secrecy rate. Each relay needs the CSI to the source, destination and the eavesdropper plus the CSI from the source to the destination to perform the optimal power allocation.

**Sub-optimal Selection**

Although the exhaustive search based on the optimal power allocation can achieve the maximal secrecy rate, it involves high complexity. In the following, we describe a simpler selection scheme, which, according to simulations has comparable performance to the optimal one.

To make $R_S$ large, the selected relay $R$ should exhibit the following characteristics:

1. $|h_{SR}|$ and $|h_{RD}|$ should be both large, to make both $C_{1s}$ and $C_{2s}$ large.

2. The difference between $|h_{SR}|$ and $|h_{RD}|$ should not be too large, because a weak source-relay, or relay-destination link can become the bottleneck of the system.

3. The channel $\mathbf{h}_{SD-E} \triangleq [h_{SE}, h_{DE}]^T$ should have high correlation with $\mathbf{w}_{SD-E}$, to make the the interference of the first slot large.

4. The channel $\mathbf{h}_{SR-E} \triangleq [h_{SE}, h_{RE}]^T$ should have high correlation with $\mathbf{w}_{SR-E}$, to make the interference of the second slot large.

Based on (3) and (4), two parameters $0 < \alpha, \beta < 1$ can be used by the source to prescreen all the relays before they enter the selection process, i.e., $\left|\frac{\mathbf{h}_{SD-E}\mathbf{h}_{SD-R_i}^{\mathcal{H}}}{|\mathbf{h}_{SD-E}||\mathbf{h}_{SD-R_i}|}\right| \leq \alpha$ and $\left|\frac{\mathbf{h}_{SR_i-E}^{\mathcal{H}}\mathbf{h}_{SR_i-D}}{|\mathbf{h}_{SR_i-E}||\mathbf{h}_{SR_i-D}|}\right| \leq \beta$, where $\mathbf{h}_{SR_i-D} \triangleq [h_{SD}, h_{R_iD}]^T$ and $\mathbf{h}_{SD-E} \triangleq [h_{SE}, h_{DE}]^T$. Assuming that $\tilde{K}$ relays pass the prescreening, then the following relay selection scheme can be carried out to guarantee the characteristics (1) and (2) in the above list.

Based on the above, the source should select the relays according to the Algorithm 2.

**Algorithm 2** Relay selection based on the S-R and R-D CSI

1. Sort the channel gains of source-relay channels of all relays into $Seq_{SR}$ in decreasing order.
2. Sort the channel gains of relay-destination channels of all relays into $Seq_{RD}$ in decreasing order.
3. Let $X_i^h$ and $X_i^g$ denote the locations of the $i$th relay in $Seq_{SR}$ and $Seq_{RD}$.
4. The "best" relay $i^*$ is selected according to $i^* = \arg\min_{i=1,\ldots,\tilde{K}} X_i^h + X_i^g$.
5. If there are multiple relays satisfying the above selection criterion, the one with the smallest $|X_i^h - X_i^g|$ is chosen.

**Distributed relay selection with limited feedback channels**

In this section we consider a distributed relay selection scheme, in which, instead of requiring the source to maintain information on all relays' CSI, the relays participate in determining the optimal power allocation by informing the source on their secrecy rate. For a more realistic scenario, we consider the case in which this communication occurs via a limited feedback channel. The scheme proceeds as in Algorithm 3.

Via Algorithm 3, the computation load for relay selection can be evenly distributed to all relays. This is particularly important in a system without a powerful fusion center.

**Algorithm 3** Distributed relay selection

1. The source and destination broadcast training signals to the relays. Based on the training symbols, each relay recovers the source-relay and destination-relay CSI and the source estimates $h_{SD}$. It is assumed that the recovery is perfectly and that the destination-relay and rely-destination channels are identical.
2. The source broadcasts a quantized version of $h_{SD}$ to the relays.
3. The $i$th relay ($i = 1, ..., K$) calculates (4.11) based on its local CSI, $h_{S-R_i}$, and $h_{R_i-D}$, the CSI of the S-D link that was sent by the source in step 2.
4. The relays feedback the quantized secrecy rate to the source one by one.
5. The source selects the relay $i^*$ with the largest secrecy rate and broadcasts the index.
6. The relay $i^*$ computes $\mathbf{w}_{SD-E}$ and $\mathbf{w}_{SR-E}$ and broadcasts the quantized weight vector to the source and destination.
7. The transmission begins with the assigned weights and equal power allocation.

## 4.3 The scaling law of the secrecy rate

In this section, we will show that the ergodic secrecy rate of the proposed scheme satisfies

$$\mathbb{E}C_s \geq \frac{1}{2}\log_2(1 + \frac{P_0}{8}\log K) - 1.6252. \tag{4.16}$$

where the expectation is taken with respect to the distribution of all channel. We assume that the channels between any two nodes are independent identical Gaussian distributed with unit variance. The proof is shown as follows:

$$\mathbb{E}C_s \geq \mathbb{E}\min(\log_2(1 + |h_{SR}|^2\frac{P_0}{4}), \log_2(1 + |h_{RD}|^2\frac{P_0}{4})) \tag{4.17}$$

$$- \mathbb{E}\log_2\left(1 + \frac{|h_{SE}|^2\frac{P_0}{4}}{1 + \frac{P_0}{4}|[h_{SE}, h_{DE}]\mathbf{w}_{SD-E}|^2} + \frac{|h_{RE}|^2\frac{P_0}{4}}{1 + \frac{P_0}{4}|[h_{SE}, h_{RE}]\mathbf{w}_{SR-E}|^2})\right) \tag{4.18}$$

$$\triangleq \mathbb{E}\min(\log_2(1 + |h_{SR}|^2\frac{P_0}{4}), \log_2(1 + |h_{RD}|^2\frac{P_0}{4})) \tag{4.19}$$

$$- \mathbb{E}\log_2\left(1 + \frac{\chi_1^2}{\frac{4}{P_0} + \chi_2^2} + \frac{\chi_3^2}{\frac{4}{P_0} + \chi_4^2}\right). \tag{4.20}$$

where $\chi_1^2$, $\chi_2^2$, $\chi_3^2$ and $\chi_4^2$ are i.i.d. chi-square with freedom degree of 2. We first show that (4.19) $\geq \frac{1}{2}\log_2(1+\frac{P_0}{8}\log K)$. First note that

$$(4.19) = \mathbb{E}\log_2\left(1+\frac{P_0}{4}\min(|h_{SR}|^2,|h_{RD}|^2)\right). \tag{4.21}$$

Then, we construct a relay selection method to let $\min(|h_{SR}|^2,|h_{RD}|^2) > \log\sqrt{K}$ with probability 1. The relay selection method is outlined as follows:

- Divide randomly the total $K$ relays into $\sqrt{K}$ groups with $\sqrt{K}$ relays in each group.
- Within each group, the one relay with the largest $|h_{SR}|^2$ is selected. So totally $\sqrt{K}$ relays are selected.
- Form these $\sqrt{K}$ selected relays into a new group.
- The relay with the largest $|h_{RD}|^2$ within the new group is selected for jamming and signal forwarding.

Based on the above selection process, the selected relay's channel gain $|h_{SR}|^2$ and $|h_{RD}|^2$ are both the largest one out of two independent sets of $\sqrt{K}$ chi-square random variables. According to order statistics, if $K$ is very large, $|h_{SR}|^2 \geq \log\sqrt{K}$ and $|h_{RD}|^2 \geq \log\sqrt{K}$ both happen with probability larger than $1-\frac{1}{\log\sqrt{K}}$. Therefore, the event $\min(|h_{SR}|^2,|h_{RD}|^2) > \log\sqrt{K}$ occurs with probability larger than $1-\frac{1}{\log\sqrt{K}}$ [86]. Therefore, with large $K$, the RHS of (4.19) $\geq \frac{1}{2}\log_2(1+\frac{P_0}{8}\log K)$ holds.

Then we show that $\mathbb{E}\log_2\left(1+\frac{\chi_1^2}{\frac{4}{P_0}+\chi_2^2}+\frac{\chi_3^2}{\frac{4}{P_0}+\chi_4^2}\right)<1.6$. We have

$$\mathbb{E}\log_2\left(1+\frac{\chi_1^2}{\frac{4}{P_0}+\chi_2^2}+\frac{\chi_3^2}{\frac{4}{P_0}+\chi_4^2}\right) \tag{4.22}$$

$$\leq \mathbb{E}\log_2\left(1+\frac{\chi_1^2}{\chi_2^2}+\frac{\chi_3^2}{\chi_4^2}\right) \tag{4.23}$$

$$= \mathbb{E}\log_2(\chi_2^2\chi_4^2+\chi_1^2\chi_4^2+\chi_3^2\chi_2^2)-\mathbb{E}\log_2(\chi_3^2)-\mathbb{E}\log_2(\chi_4^2) \tag{4.24}$$

$$\leq \log_2(3)-2\mathbb{E}\log_2(\chi_3^2) \tag{4.25}$$

$$\leq \log_2(3)-2*1.4427\gamma. \tag{4.26}$$

where (4.25) is based on the Jensen inequality and the facts that log is a concave function and $\chi_i^2, i=1,...,4$ are i.i.d. with $\mathbb{E}\chi_i^2=1$; $\gamma$ is the Euler constant and (4.26) is based on [55].

By combining (4.16) and (4.26), Theorem 1 is proven.

### 4.3.1 Relay selection under incomplete eavesdropper CSI

Assuming perfect eavesdropper CSI knowledge might not be feasible in a real scenario. In this section we consider the case in which only statistical information on eavesdropper CSI is available. As the beamforming step does not require any eavesdropper CSI, only the effect on relay selection and power allocation need to be considered. The channels $\mathbf{h}_{SD-R}$ and $\mathbf{h}_{SR-D}$ are still assumed to be fully available.

Let us assume that $h_{SE}$,$h_{DE}$ and $h_{RE}$ are i.i.d. Gaussian distributed with zero mean and unit variance. In this case, a closed form expression, or the bound of $\min\{C_{1s},C_{2s}\}$, are difficult to obtain. Therefore, we proposed to use a modified secrecy rate expression by substituting $|[h_{SE},h_{DE}]\mathbf{w}_{SD-E}|^2$, $|[h_{SE},h_{DE}]\mathbf{w}_{SD-E}|^2$ and $|[h_{SE},h_{RE}]\mathbf{w}_{SR-E}|^2$ by their expected value [87], i.e., 1, to approximate the

secrecy rate. The modified secrecy rate becomes

$$R_s^{modified} \triangleq \min \left( \underbrace{\log_2 \frac{1+|h_{SR}|^2 P_S^U}{1+\frac{2P_s^U}{1+P_{SD}^J}}}_{C_{1s}}, \underbrace{\log_2 \frac{1+|h_{RD}|^2 P_R^U}{1+\frac{2P_s^U}{1+P_{SD}^J}+\frac{2P_R^U}{1+P_{SR}^J}}}_{C_{2s}} \right) \tag{4.27}$$

The above expression of the secrecy rate has exactly the same form as the secrecy rate in case of perfect eavesdropper CSI, thus the proposed optimal power allocation method should still apply.

Since the eavesdropper CSI is unknown, the relay selection is based solely on the source-relay and relay-destination channels, i.e.,

$$i_{opt} = \arg \max_{i=1,\ldots,K} \min \left( \log_2(1+|h_{SR_i}|^2 P_S^U), \log_2(1+|h_{R_iD}|^2 P_{R_i}^U) \right) \tag{4.28}$$

## 4.4 Simulation Results

### 4.4.1 Performance under perfect CSI

The simulation setting is as follows. The channels among each pair of nodes are assumed to be i.i.d., complex Gaussian with unit variance. Every secrecy rate point is based on averaging over 5000 independent channel realizations. The number of relays is specified in the discussion of the different experiments. The eavesdropper CSI is first assumed perfectly known. In each transmission period, first, the active relay is selected and then, the secrecy rate is calculated based on the proposed optimal power allocation. For benchmarking purposes, the result of the equal power allocation is also shown. In the equal power allocation scheme the total power $P_0$ is divide equally among the first slot data power from the source, the first slot jamming power from the source and destination, the second slot data power from the relay and the second slot jamming power from the source

and relay.

We first compare the proposed scheme with the methods in [82, 81]. Fig.4.2 shows that the proposed scheme with optimal power allocation and exhaustive relay selection outperforms the two comparison methods over the entire transmission power range. We should note that there are ten relays in the system ($K = 10$); the proposed method employs the best of them, while the comparison methods employ all ten. The method of [82] selects two relays to do jamming and signal forwarding in the second hop respectively. It exhibits a secrecy rate floor because of the high SNR at the eavesdropper as the power increases. The method of [81] increases much slower than the proposed method because all ten relays are used, thus the weakest one becomes the bottleneck in terms of secrecy rate.

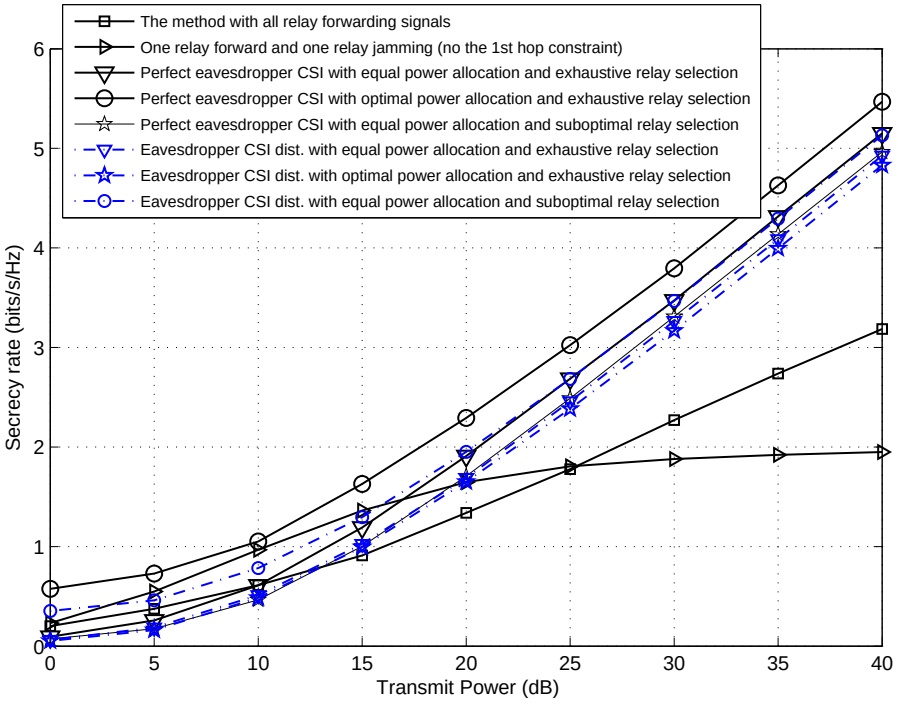


Figure 4.2: Secrecy rate versus total power ($P_0 = 0dB \sim 40dB$) for a system with 10 relays.

The proposed scheme with equal power allocation and either exhaustive relay

selection, or suboptimal selection (with orthogonality prescreening) are also plotted in Fig. 4.2. For the suboptimal selection with orthogonality prescreening, it was set $\alpha = \beta = 0.85$. One can see that both relay selection methods with equal power allocation result in high secrecy rate, which is smaller than that of the optimal power allocation. Further, the suboptimal relay selection with orthogonality prescreening achieves a comparable secrecy rate as the exhaustive search.

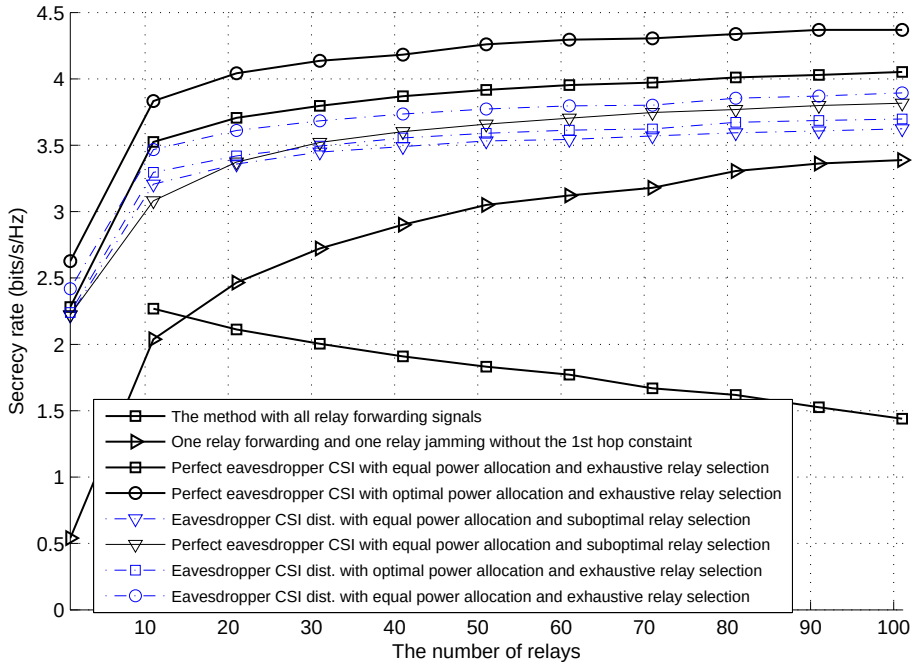


Figure 4.3: Secrecy rate versus number of relays ($1 \sim 100$ relays) with total power $P_0 = 30dB$).

Fig.4.3 shows the secrecy rate versus the number of relays for the proposed scheme for the same scenarios as in Fig.4.2). Compared to the methods of [82, 81], the proposed scheme provides significantly higher secrecy rate. Also, the secrecy rate of the proposed scheme increases with the number of relays. Figs.4.4 and 4.5 illustrate the relation between the secrecy rate of the proposed scheme, the total transmission power and the number of relays.

Next we show the impact of parameters $\alpha$ and $\beta$ used in the orthogonality

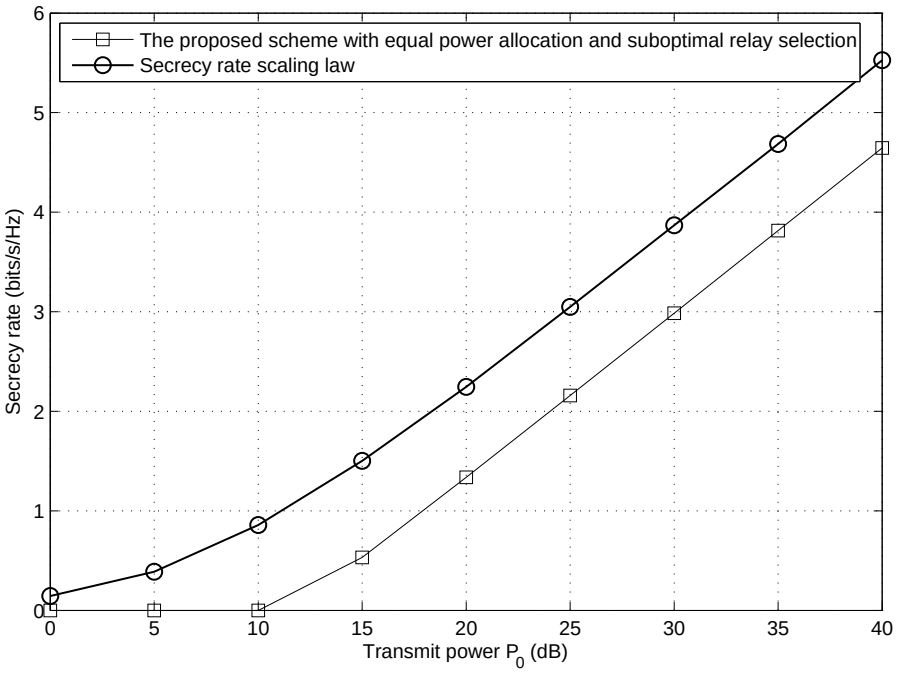


Figure 4.4: The scaling law of secrecy rate versus power ($P_0 = 0dB \sim 40dB$) for a system with 10 relays.

prescreening. The secrecy rate versus the value of $\alpha = \beta$ is shown in Fig.4.6. The total transmission power is $30dB$. The figure shows the tradeoff between the channel gains of the desired signal and the jamming signal strength. On one hand, if $\alpha, \beta$ are too small, there is only a small number of relays that qualify to forward the signal, which limits the selection of the S-R and R-D channel gains. On the other hand, if the $\alpha, \beta$ are too large, the generated jamming signal beam $\mathbf{w}_{SD-E}$ and $\mathbf{w}_{SR-E}$ may not have high correlation with $\mathbf{h}_{SD-E}$ and $\mathbf{h}_{SR-E}$, respectively. So, the jamming signal to the eavesdropper may not be strong enough, which reduces the impact of the jamming. The optimal $\alpha$ and $\beta$ occur in the range $[0, 1]$. It can be seen that with the increase of the number of the relay, the optimal $\alpha, \beta$ decrease.

Figs.4.4 and 4.5 show the secrecy rate of the proposed scheme against the scaling law of (4.16), for different levels of transmit power (Fig.4.4) and different

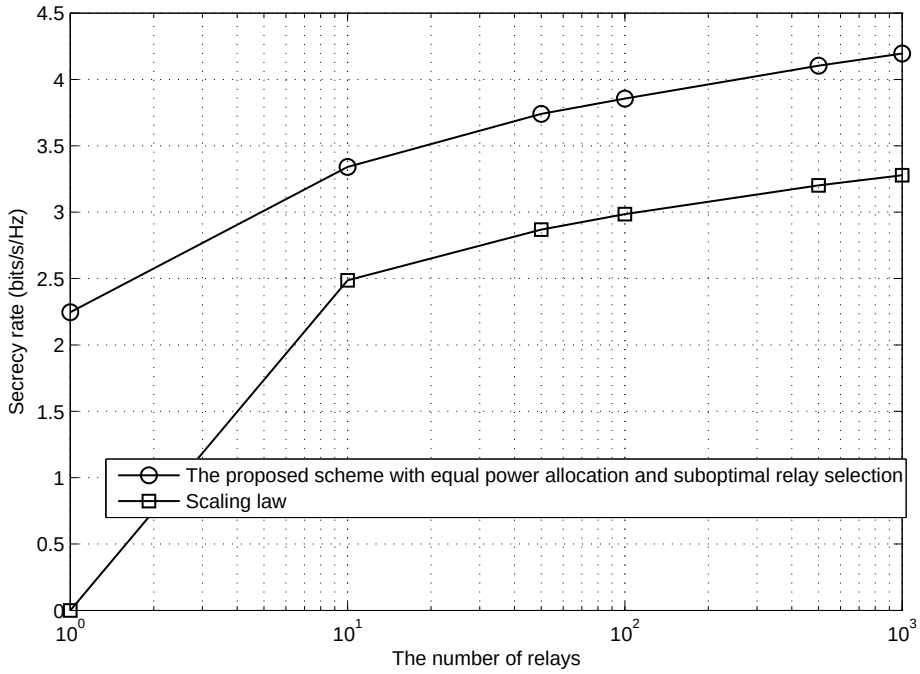


Figure 4.5: The scaling law of secrecy rate versus number of relays ($1 \sim 1000$ relays) with total power $P_0 = 30dB$.

number of relays (Fig. 4.5). The scaling law serves as a lower bound for the secrecy rate of the proposed scheme in both cases. Further, the curves corresponding to the proposed scheme are parallel to the curves of the scaling law in the region of high transmit power and large number of relays. So, the multiple relay diversity of $\log K$ is achieved.

### 4.4.2 Performance under incomplete eavesdropper CSI

In this subsection we present some simulations results to quantify the performance loss when full CSI is not available, and relay selection and power allocation are performed based on the approximate secrecy rate of (4.27). Note that the beamformers are based on $\mathbf{h}_{SD-R}$ and $\mathbf{h}_{SR-D}$, which are still assumed to be perfect in this subsection.

The secrecy rate curves corresponding to the case of known distribution of

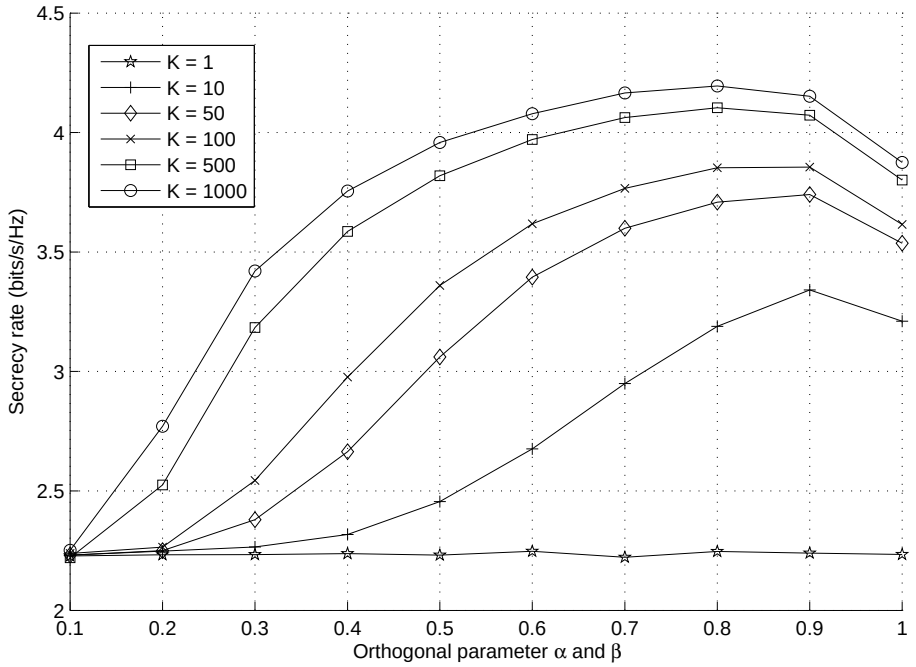


Figure 4.6: The relation between secrecy rate and orthogonality prescreening parameter, $0 \geq \alpha = \beta \leq 1$

eavesdropper CSI for the scenario of Fig. 4.2, are plotted in Fig.4.2. Since the eavesdropper CSI is unknown, the relay selection is based solely on the source-relay and relay-destination channels, i.e., (4.28). It can be seen that the optimal power allocation based on the rate approximation, combined with the simple exhaustive search provides a secrecy rate which is only 0.3 bits/s/Hz smaller that the secrecy rate in the case of perfect eavesdropper CSI.

### 4.4.3 Performance under limited feedback

In this section we evaluate the distributed relay selection scheme described in Algorithm 3.

We first simulate Step 1 of Algorithm 3. Fig.4.7 shows the secrecy rate v.s. transmission power for $K = 50$ relays. We consider two cases: 1) the number of the feedback bits broadcasting to all relays for $h_{S-D}$ increases with power,

i.e., $B_{h_{S-D}} = \lfloor(\frac{P_0(dB)}{4}) + 2$ bits; 2) the number of the feedback bits is fixed at 3bits (other fixed number of feedback has similar impact on the secrecy rate). Each relay uses reconstructed $\hat{h}_{S-D}$ to calculate the power allocation and the beamforming vectors. The secrecy rate is computed with these beamforming vectors based on the inaccurate CSI $\hat{h}_{S-D}$. For case 1, it is shown in Fig.4.7 that the secrecy rate increases as fast as with perfect relay CSI. However, in case 2, the secrecy rate hits a floor at high transmit power.

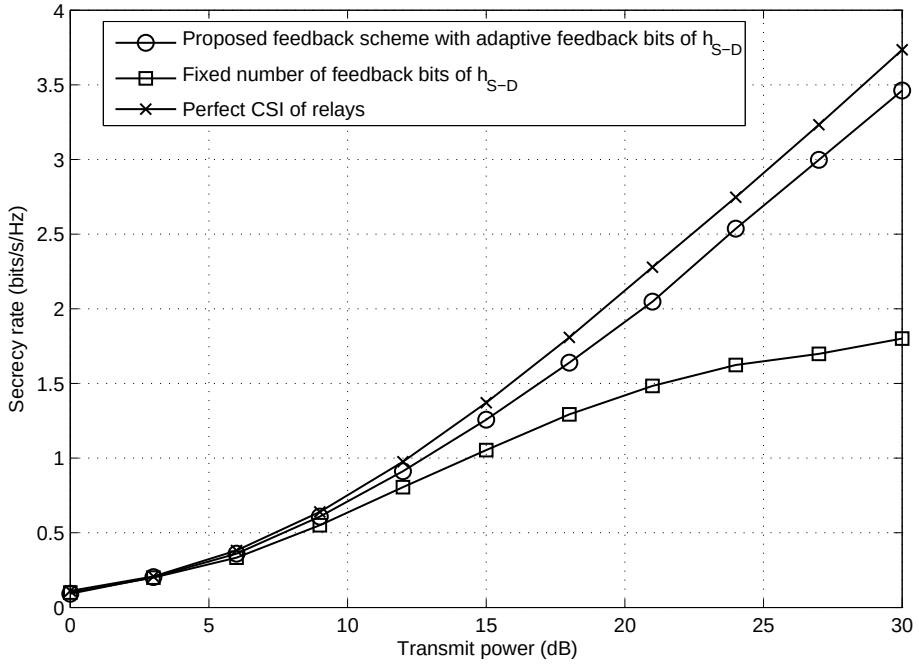


Figure 4.7: Secrecy rate versus power ($P_0 = 0dB \sim 30dB$) for the distributed relay selection scheme with limited feedback.

Next, we investigate the impact of limited feedback in step 6. The secrecy rate versus the number of relays is shown in Fig.4.8 with total transmission power 30dB. Again, two cases are considered: 1) the number of feedback bits of the weight vector $\mathbf{w}_{SD-E}$ and $\mathbf{w}_{SR-E}$ increases with the number of relays, i.e., $B_{\mathbf{w}_{SD-E}} = B_{\mathbf{w}_{SR-E}} = \log_2 \log K + 6$ bits, and 2) the number of feedback bits is

fixed at 6 bits. Random vector quantization (RVQ) [88] is used for the quantization. For the former case, the secrecy rate maintains the same trend in the perfect feedback case. However, for the latter case, the secrecy rate stops increasing as the number of relays increases. Note that in these two figures, the throughput feedback from the relays is assigned $\log_2 K$ bits.

From the above two simulations on limited feedback, one can see that to preserve the increasing trends of the secrecy rate with perfect feedback, the number of feedback bits of CSI should be increased with with power and number of relays.

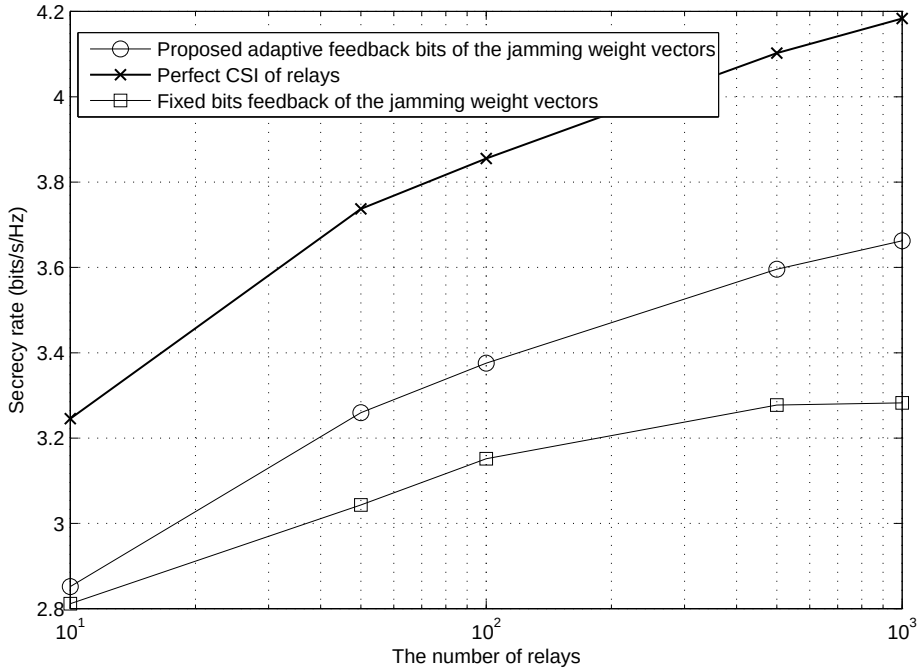


Figure 4.8: Secrecy rate versus total number of relays ($10 \sim 1000$ relays) for the distributed relay selection scheme with limited feedback.

## 4.5 Summary

We have investigated the transmission strategy in a distributed relay networks for physical layer security. Unlike conventional methods, the proposed scheme

requires the destination to transmit a jamming signal to confound the eavesdropper, thus significantly decreasing the eavesdropper SINR and improving the secrecy rate. This destination assisted scheme allows the system to benefit from an increase in the total transmission power. Relay selection methods has been proposed to overcome the tighter secrecy constraint in the first slot when the number of relays increases under perfectly known eavesdropper CSI and unknown eavesdropper CSI. With relay selection, the secrecy rate improves with an increasing number of relays. Optimal power allocation among the first/second slot and jamming/data signals has been proposed to further improve the secrecy rate. The increase of the secrecy rate with the power and the number of relays is confirmed by the derived scaling law of the secrecy rate. The proposed scheme is also investigated under imperfect relay CSI. A distributed limited feedback scheme has been proposed to reduce the feedback payload. It has been shown that the system can avoid hitting a secrecy rate floor, as long as the number of feedback bits increases at a specific rate as the power and number of relays increases.

# Chapter 5
# Conclusions and Future Directions

## 5.1 Conclusions

The thesis has considered challenges associated with achieving high data rates, reliability and secrecy in wireless communications. In particular, utilization of relay(s) have been proposed in a system with multiple sources and destinations to improve the data rate and reliability. Relay assisted multi-user system has been investigated to prevent information leakage to the untrusted nodes.

A relay scheme has been proposed in which a relay node with multiple antennas is inserted between the sources and destinations to assist data transmission. Via a ZFBF matrix at the relay, all sources can transmit simultaneously and all destinations can receive interference-free signals with the help of a relay with multiple antennas. To pursue high sumrate, an optimal power allocation across all source-destination pairs has been proposed by implementing semi-definite-programming. Analysis on the throughput has been conducted showing that the proposed design can achieve the full multiplexing gain of $M/2$, where $M$ is the number of source-destination pairs. However, the beamforming design under investigation depends on the source and destination CSI at the relay, which is used to compute the ZFBF matrix. Subsequently, the impact of imperfect relay CSI on the system throughput has been analyzed. It has been shown that the throughput can keep the increasing trend of $\frac{M}{2}\log(SNR)$ as long as the CSI error is inversely proportional to the total transmit power. On the contrary, if the CSI errors at the relay is fixed when the transmitted power increases, the throughput

presents a floor at high power region. The results obtained in Chapter 2 confirm that simultaneous data transmission can be enabled by the relay assistance in a system with multiple source-destination pairs to achieve high data rate.

The QoS meeting problem under the model of multiple source-destination pairs has been investigated in Chapter 3. The designs of relay beamforming matrix have been addressed to meet the destination SINR requirements simultaneously with minimized relay transmitted power. In the case of perfect CSI at the relay, the problem has been relaxed into a semi-definite-programming problem which can be solved by using the standard convex optimization techniques. The case of imperfect relay CSI has also been studied. It has been been shown that if the relay chooses the beamforming matrix as if the CSI is accurate, the outage probability is high; this is due to the interference which cannot be completely canceled by the ZFBF matrix not matching the channels perfectly. A relay BF design method has been designed in Chapter 3 by iteratively increasing the relay amplifying factors for all S-D pairs. The iteration process makes sure that the worst case SINRs are larger than the targeted thresholds. The convergency has been guaranteed as long that the set of worst case SINR constraints has a solution. The iterative amplifying factor design can significantly improve the performance of outage probability while requiring slightly higher relay transmitted power. The results obtained in Chapter 3 confirm that a proper designed relay can provide the system high reliability in terms of SINR with small outage probability and reasonable power consumption. The most remarkable aspect of these results is practicality; the simultaneous QoS guarantee is achievable in both ideal and practical environment with perfect and imperfect relay CSI, respectively. Also the iterative design does not involve any numerical optimization and has low complexity.

The physical layer secrecy has been investigated in a model with one source, one destination and one eavesdropper with the assistance of one or more relays. In

this two-slot transmission system, the destination has been designed to transmit jamming signal to confound the eavesdropper, instead of listening to the signal from the source in the first slot. This design avoids the high first hop signal power at the eavesdropper which resulted in the low secrecy rate ceiling when the source power is high. Based on this key idea, a two-slot destination jamming scheme has been proposed. The total power budget has been proposed to be optimally allocated among first and second hop's data and jamming signals to maximize the secrecy rate. When there are multiple relays, a relay selection algorithm has been designed to further improve the secrecy rate by taking advantage of the multi-relay diversity. A distributed algorithm has been proposed that the computational load of optimal power allocation and relay selection can be distributed to all relays. The most interesting result in Chapter 4 is that, though we sacrifice the first slot received signal power, the system secrecy rate still benefits significantly. Also, the computational complexity of proposed power allocation and relay selection can be shared at all relays so that super fusion center is not necessary.

## 5.2 Future Directions

A few future directions are discussed below.

### 5.2.1 Distributed processing and synchronization among cooperative nodes

A distributed algorithm has been designed in Chapter 4 to let all cooperative node share the computation load for power allocation and relay selection. For a more complicated problem, e.g., the distributed beamforming in Chapter 3, a fusion center with all CSI information is needed for handling the beamforming computation. This require the the fusion center to have powerful computation capability. To avoid the high cost or long delay caused by the large amount

of computation, the computational load should be distributed to all cooperative nodes. The distributed solution would require the development of distributed algorithm based on exchange of low rate backhaul information (e.g., CSI and the intermediate variables of the optimization algorithms) among cooperative nodes. The beamforming from the distributed nodes also require synchronized transmission from the cooperative nodes. The synchronizations includes timing, frequency and phase synchronization. Without synchronization, the signals from cooperative nodes will not be added up or canceled in the desired way at the receivers. Synchronization research will be key in pushing the distributed beamforming to the stage of implementation. No matter how advanced a synchronization algorithm is, there will still be residual synchronization errors. So investigation of the impact of synchronization errors on the system performance is necessary to confirm that the distributed beamforming can work in a real world setting.

### 5.2.2 More general beamforming structures

The proposed BF structures in the systems with multiple source-destination pairs are based on ZF. In general ZF is not optimal because of the possible amplified noise when doing the matrix inversion. So using a BF matrix with a more general form, e.g., MMSE-BF, is possibly a way to further improve the system performances in terms of sumrate, outage probability and relay transmitted power. However, a more general beamforming matrix may not result in a manageable problem. For instance, the sumrate expression will be much more complicated if an arbitrary beamforming matrix is used at the relay. The other difficulty is that the complexity may be much higher if using a general beamforming matrix. For instance, the QoS constraints cannot be separated with an arbitrary beamforming matrix at the relay under imperfect CSI. This problem will require numerical optimization to solve. To implement a more general beamforming relay schemes and thus achieve higher performance, methods to simplify formulation and decrease

the complexity need to be investigated.

### 5.2.3 User subset selection and scheduling

When the number of relay antennas is less than the number of source-destination pairs, the simultaneous data streams from all sources cannot be supported in one transmission period. In this case, the relay needs to select a subset of source-destination pairs in every transmission period. The subset selection should be based on the channel conditions of the sources so that multiple user diversity can be exploited. The subset selection should also take the QoS requirements into account to activate source-destination pairs with higher priority. The selection should also consider the fairness of all S-D pairs to make sure all source-destination pairs can share the wireless resource fairly.

### 5.2.4 Reactive untrusted nodes in physical layer secrecy

In the study of physical layer secrecy, non-reactive eavesdroppers are usually considered. However, the untrusted nodes may also act intelligently. For instance, 1) multiple untrusted nodes can cooperatively process the received signals and filter out the jamming signal and 2) the untrusted nodes may derive the signal structures through wiretapping the signaling exchange. Future physical layer secrecy algorithms should be designed to adapt to a wide range of behaviors of the untrusted nodes.

In summary, relay assistance approaches are strong candidates for solving the challenges of high data rate, reliability and secrecy in current wireless systems and even future wireless evolution. The proposed designs in this thesis address the practicality of relay approaches by considering low complexity algorithms, imperfect CSI and distributed beamforming and processing.

# References


[1] E. Telatar, "Capacity of multi-antenna gaussian channels," *Euro. Trans. on Telecommun.*, vol. 10, no. 6, pp. 585–596, June 1999.

[2] G. J. Foschini, "Layered space-time architecture for wireless communication in a fading environment when using multiple antennas," *Euro. Trans. on Telecommun.*, vol. 1, no. 2, pp. 41–59, Feb. 1996.

[3] O. Goldreich, *Foundations of Cryptography: Volume II, Basic Applications*, Cambridge Univ Pr, 2009.

[4] H. Delfs and H. Knebl, *Introduction to cryptography: principles and applications*, Springer-Verlag New York Inc, 2007.

[5] G.S. Vernam, "Cipher printing telegraph systems for secret wire and radio telegraphic communications," *J. Amer. Inst. Elect. Eng.*, vol. 55, pp. 109–115, 1926.

[6] *Ssl 3.0 specification*, 1996.

[7] "Medium access control (mac) and physical layer (phy) specifications, ieee standard 802.11 edtion 1999," *Computer Society LAN MAN Standards Committee working group.*, 2000.

[8] X. Wang, D. Feng, X. Lai, and H. Yu, "Collisions for hash functions md4, md5, haval-128 and ripemd," in *The 24rd Annual International Cryptology Conference (CRYPTO 2004)*, 2004.

[9] C. E. Shannon, "A mathematical theory of communication," *Bell System Technical Journal*, vol. 27, pp. 379–423, 1948.

[10] S. Vishwanath, N. Jindal, and A. Goldsmith, "Duality, achievable rates, and sum-rate capacity of gaussian mimo broadcast channels," *IEEE Trans. on Info. Theory*, vol. 49, no. 10, pp. 2658–2668, Oct. 2003.

[11] R.H. Etkin, D.N.C. Tse, and W. Hua, "Gaussian interference channel capacity to within one bit," *IEEE Trans. on Info. Theory*, vol. 54, no. 12, pp. 5534–5562, Dec. 2008.

[12] A. Carleial, "A case where interference does not reduce capacity," *IEEE Trans. on Info. Theory*, vol. 21, no. 5, pp. 569–570, sep 1975.

[13] T. Han and K. Kobayashi, "A new achievable rate region for the interference channel," *IEEE Trans. on Info. Theory*, vol. 27, no. 1, pp. 49–60, jan 1981.

[14] H. Sato, "The capacity of the gaussian interference channel under strong interference (corresp.)," *IEEE Trans. on Info. Theory*, vol. 27, no. 6, pp. 786–788, Nov 1981.

[15] A.J. Viterbi, *CDMA: Principles of spread spectrum communication*, Prentice Hall PTR., 1995.

[16] A. Host-Madsen and A. Nosratinia, "The multiplexing gain of wireless networks," in *Proc. International Symposium on Info. Theory, 2005 (ISIT 2005)*, Sep. 2005, pp. 2065–2069.

[17] V.R. Cadambe and S.A. Jafar, "Interference alignment and degrees of freedom of the user interference channel," *IEEE Trans. on Info. Theory*, vol. 54, no. 8, pp. 3425–3441, Aug. 2008.

[18] A.D. Wyner, "The wire-tap channel," *Bell System Technical Journal*, vol. 54, no. 8, pp. 1355–1387, 1975.

[19] S.K. Leung-Yan-Cheong and M.E. Hellman, "The gaussian wire-tap channel," *IEEE Trans. on Info. Theory*, vol. 24, no. 4, pp. 451–456, 1978.

[20] P.K. Gopala, L. Lai, and H.E. Gamal, "On the secrecy capacity of fading channels," *IEEE Trans. on Inf. Theory*, vol. 54, no. 10, pp. 4687–4698, Oct. 2008.

[21] I. Csiszar and J. Korner, "Broadcast channels with confidential messages," *IEEE Trans. on Info. Theory*, vol. 24, no. 3, pp. 339–348, 1978.

[22] V. Aggarwal, L. Sankar, A.R. Calderbank, and H.V. Poor, "Secrecy capacity of a class of orthogonal relay eavesdropper channels," *EURASIP Journal on Wireless Communications and Networking*, , no. 7, 2009.

[23] L. Lai and H. El Gamal, "The relay-eavesdropper channel: Cooperation for secrecy," *IEEE Trans. on Info. Theory*, vol. 54, no. 9, pp. 4005–4019, 2008.

[24] L. Dong, Z. Han, A.P. Petropulu, and H. V. Poor, "Improving wireless physical layer security via cooperating relays," *IEEE Trans. on Wireless Comm.*, vol. 5, no. 8, pp. 1875–1888, Aug. 2010.

[25] T. Cover, "Capacity theorems for the relay channel," *IEEE Trans. on Info. Theory*, vol. 25, no. 5, pp. 572–584, Sep. 1979.

[26] A. Sendonaris, E. Erkip, and B. Aazhang, "User cooperation diversitypart i: system description," *IEEE Trans. on Info. Theory*, vol. 51, no. 11, pp. 1927–1938, 2003.

[27] A. Sendonaris, E. Erkip, and B. Aazhang, "User cooperation diversity. part ii. implementation aspects and performance analysis," *IEEE Trans. on Info. Theory*, vol. 51, no. 11, pp. 1939–1948, 2003.

[28] A. Host-Madsen and J. Zhang, "Capacity bounds and power allocation for wireless relay channels," *IEEE Trans. on Info. Theory*, vol. 51, no. 6, pp. 2020–2040, June 2005.

[29] G. Kramerand M. Gastpar and P. Gupta, "Cooperative strategies and capacity theorem for relay networks," *IEEE Trans. on Info. Theory*, vol. 51, no. 9, pp. 3037–3063, Sep. 2005.

[30] R.U. Nabar, F.W. Kneubuhler, and H. Bolcskei, "Performance limits of amplify-and-forward based fading relay channels," 2005, vol. 51, pp. 2020–2040.

[31] J. Laneman and G. Wornell, "Distributed space-time coded protocols for exploiting cooperative diversity in wireless networks," *IEEE Trans. on Info. Theory*, vol. 49, no. 10, pp. 2415–2425, Oct. 2003.

[32] D. Tse N. Laneman and G. Wornell, "Cooperative diversity in wireless networks: efficient protocols and outage behavior," *IEEE Trans. on Info. Theory*, vol. 50, no. 11, pp. 3062–3080, Nov 2004.

[33] S. Jin, M.R. McKay, C. Zhong, and K.K. Wong, "Ergodic capacity analysis of amplify-and-forward mimo dual-hop systems," *IEEE Trans. on Info. Theory*, vol. 56, no. 5, pp. 2204–2224, May 2010.

[34] C. Chae, T. Tang, R.W. Heath, and S. Cho, "Mimo relaying with linear processing for multiuser transmission in fixed relay networks," *IEEE Trans. on Signal Proc.*, vol. 56, no. 2, pp. 727–738, 2008.

[35] Rui Zhang, Chin Choy Chai, and Ying-Chang Liang, "Joint beamforming and power control for multiantenna relay broadcast channel with qos constraints," *IEEE Trans. on Signal Proc.*, vol. 57, no. 2, pp. 726–737, Feb. 2009.

[36] H. Bolcskei, R.U. Nabar, O. Oyman, and A.J. Paulraj, "Capacity scaling laws in mimo relay networks," *IEEE Trans. on Wireless Comm*, vol. 5, no. 6, pp. 1433–1444, June 2006.

[37] L. Dong, A.P. Petropulu, and H.V. Poor, "Weighted cross-layer cooperative beamforming for wireless networks," *IEEE Trans. on Signal Proc*, vol. 57, no. 8, pp. 3240–3252, Aug. 2009.

[38] Y. Liu and A.P. Petropulu, "Cooperative beamforming in multi-source multi-destination relay systems with sinr constraints," in *2010 IEEE International Conference on Acoustics Speech and Signal Processing (ICASSP 2010)*, march 2010, pp. 2870–2873.

[39] J. Huang and A.L. Swindlehurst, "Cooperative jamming for secure communications in mimo relay networks," *IEEE Trans. on Signal Process*, vol. 59, no. 10, pp. 4871–4884, Oct. 2011.

[40] Z. Ding, K.K. Leung, D.L. Goeckel, and D. Towsley, "Opportunistic relaying for secrecy communications: Cooperative jamming vs. relay chatting," *IEEE Trans. on Wireless Comm.*, vol. 10, no. 6, pp. 1725–1729, Jun. 2011.

[41] B. Wang, J. Zhang, and A. Host-Madsen, "On the capacity of mimo relay channels," *IEEE Trans. on Info. Theory*, vol. 51, no. 1, pp. 29–43, Jan. 2005.

[42] X. Tang and Y. Hua, "Optimal design of non-regenerative mimo wireless relays," *IEEE Trans. on Wireless Comm.*, vol. 6, no. 4, pp. 1398–1407, Apr. 2007.

[43] K. J. Lee, K.W. Lee, H. Sung, and I. Lee, "Sum-rate maximization for two-way mimo amplify-and-forward relaying systems," in *IEEE 69th Vehicular Technology Conference (VTC 2009)*, April 2009.

[44] S.A. Jafar, K.S. Gomadam, and C. Huang, "Duality and rate optimization for multiple access and broadcast channels with amplify-and-forward relays," *IEEE Trans. on Info. Theory*, vol. 53, no. 10, pp. 3350–3371, Oct. 2007.

[45] J. Joung and Ali H. Sayed, "Multiuser two-way amplify-and-forward relay processing and power control methods for beamforming systems," *IEEE Trans. on Signal Proc*, vol. 58, no. 3, pp. 1833–1846, Mar. 2010.

[46] R.U. Nabar, O. Oyman, H. Bolcskei, and A.J. Paulraj, "Capacity scaling laws in mimo wireless networks," in *Annual Allerton Conference on Communication, Control, and Computing*, 2003.

[47] S. Hui, T. Abe, T. Asai, and H. Yoshino, "Relaying schemes using matrix triangularization for mimo wireless networks," *IEEE Trans. on Comm.*, vol. 55, no. 9, pp. 1683–1688, Sep. 2007.

[48] Q.H. Spencer, A.L. Swindlehurst, and M. Haardt, "Zeroforcing methods for downlink spatial multiplexing in multiuser mimo channels," *IEEE Trans. on Signal Proc*, vol. 52, no. 2, pp. 461–471, Feb. 2004.

[49] T. Yoo and A. Goldsmith, "Optimality of zero-forcing beamforming with multiuser diversity," in *IEEE International Conference on Communications (Globecom 2005)*, May 2005, pp. 542–546.

[50] T.M. Cover and J.A. Thomas, *Elements of information theory*, Wiley Press, 2006.

[51] Y. Liu and A.P. Petropulu, "On amplify-and-forward relay networks with multiple source-destination pairs," in *IEEE International Conference on Communications (Globecom 2010)*, Nov 2010.

[52] J.F. Sturm, "Using sedumi 1.02, a matlab toolbox for optimization over symmetric cones," *Optimization Methods and Software*, vol. 11, no. 1, pp. 625–653, Jan. 1999.

[53] N.D. Sidiropoulos, T.N. Davidson, and Z. Luo, "Transmit beamforming for physical-layer multicasting," *IEEE Trans. on Signal Proc*, vol. 54, no. 6, pp. 2239–2251, June 2006.

[54] G. Caire and S. Shamai, "On the achievable throughput of a multiantenna gaussian broadcast channel," *IEEE Trans. on Info. Theory*, vol. 49, no. 7, pp. 1691–1706, July 2003.

[55] I. S. Gradshteyn and I. M. Ryzhik, *Table of Integrals, Series and Products, 6th edition*, Academic Press, 2000.

[56] D. Tse and P. Viswanath, *Fundamental of Wireless Communication*, Cambridge Univ Press, 2005.

[57] J. Lee and N. Jindal, "High snr analysis for mimo broadcast channels: Dirty paper coding versus linear precoding," *IEEE Trans. on Info. Theory*, vol. 53, no. 12, pp. 4787–4792, Dec. 2007.

[58] G. Caire, N. Jindal, M. Kobayashi, and N. Ravindran, "Multiuser mimo achievable rates with downlink training and channel state feedback," *IEEE Trans. on Info. Theory*, vol. 56, no. 6, pp. 2845–2866, June 2010.

[59] M. Grant and S. Boyd, "cvx users guide," .

[60] B.K. Chalise, L. Vandendorpe, and J. Louveaux, "Mimo relaying for multi-point to multi-point communication in wireless networks," in *2nd IEEE CAMSAP07*, Dec. 2007, pp. 217–220.

[61] B.K. Chalise and L. Vandendorpe, "Mimo relay design for multipoint-to-multipoint communications with imperfect channel state information," *IEEE Trans. on Signal Proc.*, vol. 57, no. 7, pp. 2785–2796, July 2009.

[62] S.A. Vorobyov, A.B. Gershman, and Z. Luo, "Robust adaptive beamforming using worst-case performance optimization: A solution to the signal mismatch problem," *IEEE Trans. on Sig. Proc.*, vol. 51, no. 2, pp. 2257–2269, Feb. 2003.

[63] S. Shahbazpanahi, A.B. Gershman, and Z. Luo, "Robust adaptive beamforming for general-rank signal models," *IEEE Trans. on Sig. Proc.*, vol. 51, no. 9, pp. 2257–2269, Sep. 2003.

[64] A. Pascual-Iserte, D.P. Palomar, and A.I. Perez-Neira, "A robust maximin approach for mimo communications with imperfect channel state information based on convex optimization," *IEEE Trans. on Sig. Proc.*, vol. 54, no. 1, pp. 346–360, Jan 2006.

[65] Y. Liu and A.P. Petropulu, "On the sumrate of amplify-and-forward relay networks with multiple source-destination pairs," *IEEE Trans. on Wireless Comm.*, vol. 10, no. 11, pp. 3732–3742, Oct, 2011.

[66] V. Havary-Nassab, S. Shahbazpanahi, A. Grami, and Z. Luo, "Distributed beamforming for relay networks based on second-order statistics of the channel state information," *IEEE Trans. on Signal Proc*, vol. 56, no. 9, pp. 4306–4316, Sep. 2008.

[67] Y. Liu and A.P. Petropulu, "Qos guarantees in relay networks with multiple source-destination pairs and imperfect csi," in *IEEE 7th Sensor Array and Multichannel Signal Processing Workshop (SAM)*, June 2012.

[68] A. Wittneben and B. Rankov, "Distributed antenna systems and linear relaying for gigabit mimo wireless," in *IEEE 60th, VTC2004-Fall*, Sep. 2004, vol. 5, pp. 3624–3630.

[69] T.L. Marzetta and B.M. Hochwald, "Fast transfer of channel state information in wireless systems," *IEEE Trans. on Sig. Proc.*, vol. 54, no. 4, pp. 1268–1278, Apl. 2006.

[70] M. Kobayashi and G. Caire, "Joint beamforming and scheduling for a multi-antenna downlink with imperfect transmitter channel knowledge," *IEEE J. Select. Areas Commun.*, vol. 25, no. 7, pp. 1468–1477, July 2007.

[71] W.W. Hager, "Updating the inverse of a matrix," *SIAM Review*, vol. 31, no. 2, pp. 221–239, June 1989.

[72] C.E. Shannon, "Communication theory of secrecy systems," *The Bell System Technical Journal*, vol. 28, pp. 656–715, 1949.

[73] Y. Liang, H. V. Poor, and S. Shamai (Shitz), "Secure communication over fading channels," *IEEE Trans. on Inf. Theory*, vol. 54, no. 6, pp. 2470–2492, June 2008.

[74] Y. Liang, H. V. Poor, and S. Shamai (Shitz), "Physical layer security in broadcast networks," *Security and Communication Networks*, vol. 2, pp. 227–238, 2009.

[75] R. Liu, T. Liu, H. V. Poor, and S. Shamai (Shitz), "Mimo gaussian broadcast channels with confidential messages," in *Int. Symp. Inf. Theory (ISIT)*, June-July 2009.

[76] A. Khisti and G. Wornell, "The mimome channel," in *Proceedings of the 45th Annu. Allerton Conf. Commun., Control, Comput.*, Sep. 2007.

[77] F. Oggier and B. Hassibi, "The secrecy capacity of the mimo wiretap channel," in *Proc. IEEE Int. Symp. Inf. Theory (ISIT)*, July 2008, pp. 524–528.

[78] M. Yuksel and E. Erkip, "Secure communication with a relay helping the wiretapper," in *IEEE Inf. Theory Workshop*, Sep. 2009.

[79] V. Aggarwal, L. Sankar, A. R. Calderbank, and H. V. Poor, "Secrecy capacity of a class of orthogonal relay eavesdropper channels," *EURASIP Journal Wireless Commun. Netw., Special Issue on Wireless Physical Layer Security*, , no. 3, Mar 2009.

[80] E. Tekin and A. Yener, "The general gaussian multiple access and two-way wire-tap channels: achievable rates and cooperative jamming," *IEEE Trans. on Inf. Theory*, vol. 54, no. 6, pp. 2735–2751, June 2008.

[81] J. Li, A. P. Petropulu, and S. Weber, "On cooperative relaying schemes for wireless physical layer security," *IEEE Trans. on Signal Proc.*, vol. 59, no. 10, pp. 4985–4997, Oct. 2011.

[82] I. Krikidis, J.S. Thompson, and S. McLaughlin, "Relay selection for secure cooperative networks with jamming," *IEEE Trans. on Wireless Comm.*, vol. 59, no. 10, pp. 5003–5011, Oct. 2009.

[83] R. Madan, N. B. Mehta, A. F. Molisch, and J. Zhang, "Energy-efficient cooperative relaying over fading channels with simple relay selection," in *Proc. IEEE Globecom*, Nov.-Dec. 2006.

[84] A. Bletsas, D.P. Reed, and A. Lippman, "A simple cooperative diversity method based on network path selection," *IEEE J. Select. Areas Comm.*, vol. 24, no. 3, pp. 659–672, Mar. 2006.

[85] Y. Jing and H. Jafarkhani, "Single and multiple relay selection schemes and their achievable diversity orders," *IEEE Trans. on Wireless Comm.*, vol. 8, no. 3, pp. 1414–1423, Mar. 2009.

[86] T. Yoo, N. Jindal, and A.Goldsmith, "Multi-antenna downlink channels with limited feedback and user selection," *IEEE Journal on Selected Areas in Comm.*, vol. 25, no. 7, pp. 1478–1491, July 2007.

[87] A.L. Moustakas and S.H. Simon, "Optimizing multiple-input single-output (miso) communication systems with general gaussian channels: Nontrivial covariance and nonzero mean," *IEEE Trans. on Inf. Theory*, vol. 49, no. 10, pp. 2770–2780, Oct. 2003.

[88] C.K. Au-Yeung and D.J. Love, "On the performance of random vector quantization limited feedback beamforming in a miso system," *IEEE Trans. on Wireless Comm.*, vol. 6, no. 2, pp. 458–462, Feb. 2007.